Performance Analysis of Direct Sequence CDMA Power Line Communication Systems over the Frequency Selective Channel
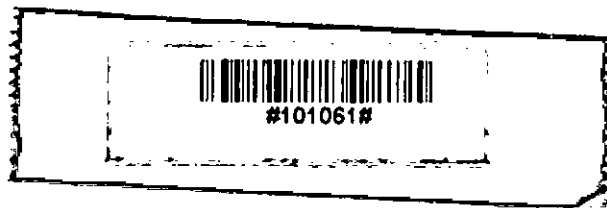
by

Md. Mahmud Hasan

A thesis submitted to the department of Electrical and Electronic Engineering of
Bangladesh University of Engineering and Technology
In partial fulfillment of the requirements for the degree of

MASTER OF SCIENCE IN ELECTRICAL AND ELECTRONIC ENGINEERING

BANGLADESH UNIVERSITY OF ENGINEERING AND TECHNOLOGY

2005

APPROVAL CERTIFICATE

The thesis titled "**Performance Analysis of Direct Sequence CDMA Power Line Communication Systems over the Frequency Selective Channel**" submitted by Md. Mahmud Hasan, Student No. 040306103F, Session 2003-04 has been accepted as satisfactory in partial fulfillment of the requirement for the degree of Master of Science in Electrical and Electronic Engineering on November 20, 2005.

BOARD OF EXAMINERS

1.

Dr. Md. Saifur Rahman

Professor
Department of Electrical and Electronic Engineering
BUET, Dhaka-1000, Bangladesh

Chairman

2.

Dr. S. Shahnawaz Ahmed

Professor & Head
Department of Electrical and Electronic Engineering
BUET, Dhaka-1000, Bangladesh

Member
(Ex-Officio)

3. _20.11.2005_

Dr. Md. Abdul Matin

Professor
Department of Electrical and Electronic Engineering
BUET, Dhaka-1000, Bangladesh

Member

4. 20.11.05

Md. Abdul Moqaddem

Deputy General Manager
Teletalk Bangladesh Limited
House No. 41, Block A, Road No. 27
Banani, Dhaka-1213, Bangladesh

Member
(External)

CANDIDATE'S DECLARATION

It is hereby declared that this thesis or any part of it has not been submitted elsewhere for the award of any degree or diploma.

Signature of the Candidate

Md. Mahmud Hasan 24.11.2005

Md. Mahmud Hasan

In Memory of

My Mother

CONTENTS

CHAPTER 1: INTRODUCTION

CHAPTER 2: DIRECT SEQUENCE CODE DIVISION MULTIPLE ACCESS

CHAPTER 3: POWER LINE CHANNEL

CHAPTER 4: RESIDENTIAL POWER LINE NOISE CHARACTERISTICS

CHAPTER 5: DEVELOPMENT OF AN ANALYTICAL MODEL FOR THE DS-CDMA PLC SYSTEM

CHAPTER 6: PERFORMANCE ANALYSIS AND DISCUSSIONS

CHAPTER 7: CONCLUSIONS AND SUGGESTIONS

REFERENCES   104

LIST OF FIGURES

LIST OF TABLES

LIST OF TECHNICAL SYMBOLS

N	Length of serial bit stream
$C_{CA}(t)$	Continuous time autocorrelation
$c(t)$	Pseudo noise sequence
T_b	Bit duration
T_c	Chip duration
$m(t)$	Data signal
$s(t)$	Modulated signal
F_s	Spreading factor
$r(t)$	Received signal
$r_m(t)$	Received signal after demodulation
G_p	Processing gain
$C_{CX}(t)$	Continuous time cross correlation
Y	Admittance
Z	Impedance
R	Resistance
G	Conductance
C	Capacitance
L	Inductance
ω	Angular velocity
γ	Propagation constant
Z_0	Characteristic impedance
α	Attenuation constant
β	Phase constant
g_i	Weighting factor
μ	Permeability
ε	Permittivity
$n(t)$	Noise

N_{PL}	Power line noise power
f	Frequency
t_w	Impulse width
t_{IAT}	Interarrival time of impulse
$m_k(t)$	Data signal of kth user
$s_k(t)$	Transmitted signal of kth user
K_u	Number of simultaneous user
L	Number of available path
a	Path gain
σ^2	Variance of path gain
$Z(t)$	Correlator output
R_b	Bit rate
E_b	Energy per bit
$h_k(t)$	Impulse response of channel for k^{th} user
P_k	Transmitted signal power for k^{th} user
τ_k	Delay of signal for k^{th} user
Γ	Average signal to interference ratio

LIST OF ABBREVIATIONS OF TECHNICAL TERMS

PLC	Power Line Communication
PVC	Polyvinyl Chloride
CENELEC	European Committee for Electro-technical Standardization
FCC	Federal Communications Commission
DS	Direct Sequence
CDMA	Code Division Multiple Access
SSMA	Spread Spectrum Multiple Access
PN	Pseudo-random Noise
CT	Continuous Time
DSSS	Direct Sequence Spread Spectrum
DS-CDMA	Direct Sequence CDMA
MC-CDMA	Multi Carrier CDMA
BPSK	Binary Phase Shift Keying
QPSK	Quadrature Phase Shift Keying
OFDM	Orthogonal Frequency Division Modulation
FHSS	Frequency Hopping Spread Spectrum
AWGN	Additive White Gaussian Noise
AWCN	Additive White Class A Noise
PVC	Polyvinyl Chloride
PSD	Power Spectral Density
SNR	Signal to Noise Ratio
SIR	Signal to Interference Ratio
BW	Bandwidth
AC	Alternating Current
DC	Direct Current
LV	Low Voltage
BER	Bit Error Rate
EMC	Electro Magnetic Compatability
MAI	Multiple Access Interference
DPSK	Differential Phase Shift keying

DQPSK	Differential QPSK
PSK	Phase Shift Keying
QAM	Quadrature Amplitude Modulation
PAM	Pulse Amplitude Modulation
FH CDMA	Frequency Hopping CDMA
IEEE	Institute of Electrical and Electronic Engineers
LAN	Local Area Network
WLAN	Wireless Local Area Network
MAC	Multiple Access Control
CSMA	Carrier Sense Multiple Access
DBPSK	Differential BPSK
IP	Internet Protocol
DSL	Digital Subscriber Line
EMI	Electromagnetic Interference
MRC	Maximum Ratio Combining
CMOE	Constrained Minimum Output Energy
PDF	Probability Density Function
SCR	Silicon Controlled rectifier
TEM	Transverse Electromagnetic

ACKNOWLEDGEMENTS

ABSTRACT

Outdoor power line communications (PLC) systems represent an additional and alternative for classical and communications. In this dissertation an analytical model of Direct Sequence CDMA power line communications systems has been developed for frequency-selective fading channel based on the concepts of wireless communication. Binary phase shift keying (BPSK) modulation scheme is considered. The fading in power line is considered to follow Rayleigh distribution. During the analysis it is considered that power line channel can carry frequencies from 1 to 21.48 MHz (bandwidth occupation 20.48 MHz) and the chip rate would be 10.24 Mchips/s for DS-CDMA. The current research of power line channel modeling has been concentrated on home automation, broadband indoor communications and broadband data transfer in a low voltage distribution network between home and transformer station. A frequency selective multipath channel is modeled whose path gain is found to be Rayleigh distributed. A noise term has been introduced in the developed model, which consists of all type of noises in power line. To estimate impulse noises the statistical probability density functions have been used.

On the basis of the analytical model, the performance of the DS-CDMA technique has been evaluated. The impact of power line noise and multipath propagation on signal to interference ratio (SIR) and bit error rate (BER) are then analyzed under various conditions. The performance parameters are evaluated as a function of number of simultaneous users. PLC with DS-CDMA is found to be a promising option for future telecommunication in a LAN and MAN.

CHAPTER 1

INTRODUCTION
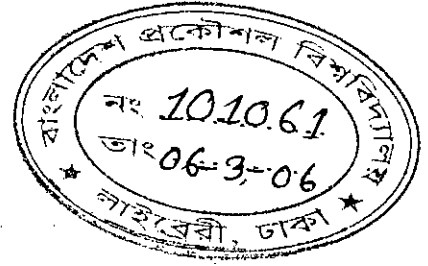
Power Line Communications or PLC is not new to the realm of the telecommunication industry. In its most basic definition, PLC is a type of "Carrier Current System" as defined by the FCC and is the transmission of information along the existing electric utility infrastructure. The industry uses this as a medium to connect computer network, or other telecommunications devices to standard AC outlets within homes and businesses [1]. Power line frequency is 50 Hz in European standard and 60 Hz in the United States of America (USA). However, the power line cables can carry additional frequencies, which has been utilized in achieving power line communications (PLC).

1.1 Brief History of PLC

Digital communications over power lines is an old idea that dates back to the early 1920s. For some decades, the omnipresent power grid has been used for data communications. Many standardized or proprietary systems have been used for the transmission of control and management signals by power supply companies.

It has been used since the 1950s by power companies to send control messages (the "Ripple Control"), using low frequencies (100-00 Hz), this one way communication technology was also used in the management of street lights. In the mid 1980s experiments on higher frequencies were carried out (5 to 500 kHz) and a bi-directional communication technology was developed by the end of the decade.

Since then, several solutions have been experimented and even commercialized for use in the home as a networking medium for internal LAN's. While utility companies have long used narrowband, the low-voltage spectrum, PLC to monitor and control devices on the power grid, broadband PLC started to develop [1].

Since the 1997 experiment in a school of Manchester (UK), utility companies continued to experiment with higher bandwidth data transfer across the electric grids in Europe, South America, and the United States. Recent advances in power line Communications technology now allow for high speed, broadband communications over medium-and low-voltage media yielding unprecedented market opportunities. A recent analysis on the group velocity of signals in power line cables indicate that high-speed data communication is possible over a bandwidth 0-30 MHz through a PVC insulated power line cable [2].

1.2 Modern PLC Systems

Early PLC systems were designed for relatively lower frequencies. The modern approach uses a much higher frequency (1.6 to 30 MHz), that permits transmissions rate higher than 1 Mbps. This application is particularly interesting for power utilities enabling them to enter in this way into the telecommunications market.

PLC SYSTEM			
HF Wide-band	Access		1.6 to 30 MHz
	In house		12 to 30 MHz
LF Narrow-band	USA		0 to 500 kHz (100 kHz reserved for Navigation systems)
	Europe	Access	3 to 95 kHz
		In house	95 to 148.5 kHz

Table 1.1: Frequency band of power line communications.

It can also have a big economic impact, permitting to stop the monopoly of the telecommunication companies over the "last mile" to the customer. Table 1.1 shows the frequency band of various power line communication systems [1].

1.2.1 Broadband PLC

The concept of power line communication is based on the 50/60 Hz power transmission line; using another higher frequency as the carrier for signal transmission. This kind of concept is also used in DSL (telephone line) and cable (cable TV) communication. The PLC has the largest coverage and almost all families make use of it. PLC can work in every kind of power line from outdoor to indoor. Due to that the communication carrier signal cannot pass through transformer, most PLC system is based in the same voltage area [3]. The usage of frequency is limited below 30 MHz due to the attenuation characteristic of power line.

The applications for broadband PLC systems fall into two broad categories: In-house applications and last-mile applications.

1.2.1.1   In-house Applications

These applications occur within a single building with both ends of the communications link within the same building. The building might be a house, an apartment, block or an office building. The path over which the transfer of data occurs within these building is relatively short- typically it is less than 100m between devices.

Broadband power line communications systems are the attractive means of retrofitting of data services to existing buildings because no additional wiring is necessary. The networking of computers, printers and other telecommunications services by simply plugging into the existing AC supply wiring is attractive for both home use and small office systems.

1.2.1.2 Last-mile Applications

These applications typically include the distribution to the home or office Internet and other services by broadband service suppliers. In addition to broadband Internet connections, these broadband distribution systems are intended to also provide voice

(IP telephony), video (VHS video quality), surveillance systems, entertainment (gaming) and utilities metering (electricity/water/gas) services.

A significant proportion of the cost of providing broadband services to the public is associated with the so called last-mile connection between the network and the individual user. The provision of cabling to and into each building represents a significant cost and inconvenience due to the differences between buildings and the lack of an existing infrastructure within the building.

The technology for this category of application is less well developed, mainly due to the need for higher signal levels for the longest last-mile paths. Higher signal levels mean higher levels of emissions, and these have not been possible to contain within existing EMC requirements in most case [4].

1.2.2 PLC Standards & Regulations

Lack of centralized standardization has been one of the major factors behind the late deployment of power line networks. This section highlights the standards and regulations pertaining to the PLC [5].

1.2.2.1 European Committee for Electro-technical Standardization (CENELEC)

For Western Europe (i.e. the countries forming European Union plus Iceland, Norway and Switzerland) the regulations concerning residential powerline described in CENELEC standard EN50065 entitled "Signaling on low-voltage electrical installations in the frequency range 3 KHz to 148.5 KHz". In part I of this EN-standardization paper, entitled "General requirements, frequency bands and electromagnetic disturbances", the allowed frequency band and output voltage for communications are indicated. According to this standards transmitter voltage should not exceed 116 dB (μV) and the maximum allowed peak voltage is 134 dB (μV). Table 1.2 shows the CENELEC frequency range.

Band	Frequency range	Usage
	3 kHz- 9 kHz	Limited to energy providers; However with their approval it may also be used by other parties inside the customer premises. (No "letter" description exists, due to the fact that this band was defined at a later stage)
A-band	9 kHz- 95 kHz	Limited to energy providers and their concession-holders.
B-band	95 kHz- 125 kHz	Limited to energy provider's customers; No access protocol is defined for this frequency band.
C-band	125 kHz- 140 kHz	Limited to energy provider's customers; In order to make simultaneous operation of several systems within this frequency band possible, a carrier-sense multiple access protocol using a center frequency of 132.5 kHz was defined.
D-band	140 kHz- 148.5 kHz	Limited to energy provider's customers; No access protocol is defined for this frequency band.

Table 1.2: CENELEC frequency range.

1.2.2.2 Federal Communications Commission (FCC)

PLC systems have developed in the USA under part 15 of the FCC Rules and Regulations. This part of the FCC Rules and Regulations relates to requirements for unlicensed low power radio communications digital devices and emissions from non-radio communications digital equipment that might otherwise cause electromagnetic interference (EMI) to radio communications services.

PLC systems are treated in part 15 as non-radio communications digital equipment. They are referred to in this part as current carrier systems specific arrangements. The FCC Rules and Regulations specify limits for both conducted and radiated emissions for current carrier systems [4]. Table 1.3 shows the FCC specified limits for conducted current carrier systems.

Limits for the all devices except class A (operating frequency below 30 MHz)		
Frequency (MHz)	Quasi Peak (dBmV)	Average (dBmV)
0.15-0.5	66 to 56	56 to 46
0.5-5	56	46
5-30	60	50
Limits for class A digital devices (operating frequency below 30 MHz)		
Frequency (MHz)	Quasi Peak (dBmV)	Average (dBmV)
0.15-0.5	79	66
0.5-30	73	60

Table 1.3: FCC specified limits for conducted current carrier systems.

1.2.2.3   HomePlug Powerline Alliance

The mission HomePlug Powerline alliance is to enable and promote rapid availability, adoption and implementation of cost effective interoperable and standard based home power line networks and products. HomePlug 1.0 specification was announced in June 2001. HomePlug 1.0 uses a physical layer (PHY) protocol based on equally spaced, 128 carriers orthogonal frequency division multiplexing (OFDM) from 0 Hz to 25 MHz, in conjunction with concatenated Viterbi and Reed Solomon coding with interleaving for payload data and turbo product codes for control data. 84 carriers are used to transmit data. BPSK, DBPSK, DQPSK or ROBO (a robust form of DBPSK) modulation is used for data, with a cyclic prefix for synchronization. The presence of large attenuation prevents detection of collisions, so HomePlug 1.0 uses CSMA/CA for its MAC protocol.

The HomePlug PHY occupies the band form about 4.5 to 21 MHz. The PHY includes reduced transmitter power spectral density in the amateur radio bands to minimize the risk of radiated energy from the power line interfering with these systems. The raw bit rate using DQPSK modulation with all carriers active is 20 Mbps. The bit rate delivered to the MAC by the PHY layer is about 14 Mbps.

1.2.2.4   PLC Forum

PLC forum is an international industry association representing the interests of manufacturers, energy utilities and research organizations active in the field of last-mile and in-house power line type systems. PLC forum was established in early 2000 through the merger of two existing associations to lobby for satisfactory regulatory frameworks for PLC, to pursue coexistence and interoperability standardization and support the marketing and financial models of its members. The forum organized a world summit of PLC Associations in Brussels in June 2003 to discuss aspects of international standardization and the need to lobby for a common regulatory approach by regulators.

Beyond these standards The Institute of Electrical and Electronic Engineers (IEEE) has also a set of recommendations and standards pertaining to the Power Line Communications.

1.3   Requirements for PLC systems

The power line channel is very hostile, because many concepts work partly. The choice of the communication method must take the requirements to be met by the system and the transmission channel into consideration. The transmission channel is characterized by the transfer function. Between transmitter and receiver and the interference the receiver sees.

Since the distribution line network was not designed for communication the wave impedances are not matched and reflections, multipath propagation and frequency-selective channels may occur. As every branch is already a point of reflection, termination at the end points would bring only little improvement. The terminators draw power from the network and there by increase the fundamental attenuation and reduce the possible range.

Therefore it is much more reasonable to choose a communication method, which can use the multipath propagation efficiently. Due to the many possible transmit paths and the time varying channel pulse response it is not possible to measure the channel at the beginning and provide channel estimation for data transmission.

The growing number of Internet users requires more and more bandwidth efficient technology for accessing the World Wide Web, establishing video conference connections, using conventional telephony services or controlling the household machines from far away. To reduce the enormous costs, attached to laying down wide band optical fiber to every user's door, providers are looking for reasonable, so-called "last-mile" solutions, such as wireless technologies like Wireless Local Area Networks (WLAN) or mobile ad-hoc networks. However, all this denotes even huge expenditures, so it is worthy employing a media that is already accessible at every electric machine used in a home: the electrical wiring. Power line seems to be a faithful medium for bridging the last mile and what's more, for creating Local Area Networks without laying down coaxial cables. The goal is to have the chance for each computer to access the Internet without installing new cables. The only problem is

that this wiring was not designed for data transmission, just for supplying electric power. Our task is to make this media capable for transmitting high data rates.

There are different multiplexing techniques that are applicable for PLC. Within Code Division Multiple Access (CDMA), two techniques are appropriate: one is Multi Carrier (MC) CDMA, that uses more carriers and thus more frequency channels for multiple access purpose, and the other is Direct Sequence (DS) CDMA, where only one carrier is used, and the different users are separated by orthogonal codes. Another very common applied technique used for PLC is Orthogonal Frequency Division Multiplexing (OFDM) that employs inverse Fourier Transformation to spread the transmitted signal spectrum to cope with frequency selective fading and impulse noises.

1.4   Background of this Study

PLC channel is extremely challenging and claims for highly sophisticated communication techniques. Generally, communication is supported to occur in channel characterized by frequency selective phenomena, presence of echoes, impulsive and colored noise with the superposition of narrow-band interference [6], [7]. All of these negative features push to consider communication techniques that can effectively face a hostile environment.

Now, spread spectrum technologies have drawn the interest of PLC developers [8]. Between different Spread Spectrum Multiple Access (SSMA) techniques, direct sequence (DS) is known as an efficient scheme for communication systems due to its characteristics such as remarkable capacity, narrow-band interference suppression, and anti- multipath capabilities.

Direct sequence pseudonoise (PN) modulation for single user PLC was studied at 9.6 Kbps in [9]. This data rate is very low with respect to modern PLC. In another work performance of a DS-SS transceiver was simulated with 128 Kbps [10]. However, it did not consider the multiple accessibility of the technique over power line channel.

Performance of three types of Spread Spectrum Multiple Access (SSMA) techniques DS-CDMA, MC-CDMA, and OFDM were compared in [11]. In that simulation work DQPSK was used with DS-CDMA and BPSK was used with MC-CDMA system. A special type of receiver named Constrained Minimum Output Energy (CMOE) was considered for the DS-CDMA system.

Performances of MC-CDMA PLC systems under various conditions were simulated in [12]. In that study, a high-speed data communication systems were considered for applying advance signal processing techniques at the receiver end, for achieving good performance.

In [13] a fair comparison was provided between DS-CDMA and OFDM systems for broadband down-stream PLC. In that simulation work, the transmission is performed according to point to multi-point situation. Over all transmitted data was separated into many parallel substreams. A Maximum Ratio Combine (MRC) RAKE receiver was considered for DS-CDMA system.

In [9], [13] the power line channel was taken as the AWGN (Additive White Gaussuian Noise) channel. However this is not the practical scenario. Impulsive noises are more prevalent. In [11] MC-CDMA technique is considered with impulsive noise.

In [14] power line was considered as a frequency non-selective (flat) Rayleigh fading channel with additive white class A noise (AWCN). In that simulation work, 4-PAM modulation technique was considered and multiple access was not considered. In another work, higher order QAM and PSK was considered with OFDM multiple access technique [15]. They also considered power line as a frequency non-selective Rayleigh fading channel.

All the performance curves in [9-15] were drawn as BER versus SNR (Signal to Noise Ratio). Table 1.4 shows a brief overview for previous researches in this area.

Referene No.	Communication Techniques	Power line channel descriptions
[9]	Direct sequence pseudonoise (PN) modulation for multiuser environment.	AWGN channel, multipath propagation was not considered.
[10]	Direct sequence spread spectrum followed by BPSK modulation for single user.	Typical values for noise and attenuation were assumed, multipath propagation was not considered.
[11]	DS-CDMA with DQPSK modulation scheme, CMOE receiver.	Typical values for noise and path gain parameters were assumed, multipath propagation was considered.
[12]	MC-CDMA with RAKE receiver.	Impulsive noises were considered, typical values for path gain parameters were assumed, multipath propagation was considered.
[13]	DS-CDMA with BPSK modulation scheme, RAKE receiver.	Impulsive noise was not considered, AWGN with multipath propagation was considered.
[14]	4-PAM modulation scheme. Multiple accessibility was not mentioned.	AWCN and flat Rayleigh distributed path gain was considered.
[15]	OFDM with modulation schemes: 64-QAM, 32-QAM, 16-QAM, 8-PSK, and 4-PSK.	An equivalent term of AWGN was introduced, frequency non-selective (flat) Rayleigh distributed path gain was considered.

Table 1.4: A brief overview of previous researches.

None to the best of our knowledge, has included the frequency selective Rayleigh distributed path gain (fading) parameters along with the power line impulse noises for DS-CDMA systems in their analysis.

1.5   Objective of This Study

The objective of this research is to study the performance of a direct sequence CDMA PLC system for frequency selective fading. In this work, BPSK modulation and Rayleigh distributed frequency selective fading will be considered. All type of noises will be considered and an average noise level will be estimated. An analytical model will be formulated from a similar model, which was first developed for wireless communication. The modified model will be used to analyze PLC.

Direct sequence code division multiple access (DS-CDMA) is considered in the current study because of its robustness to hostile environment. Power line is considered as a hostile communication media. Moreover, DS-CDMA is known as an efficient multiple access technique for communication systems due to its characteristics such as higher capacity, multiple access interference suppression, and anti- multipath capabilities.

In power line network, signal propagation does not only take place along a direct line-of-sight path between transmitter and receiver, but additional paths (echoes) also exist. The connected loads and the joints of the cables with different characteristic impedance cause numerous reflections. The number of connected loads varies randomly within power line network.

The presence of reflecting objects and scatterers in the channel creates a constantly changing environment that dissipates the signal energy, in amplitude, phase, and time. These effects result in multiple versions of the transmitted signal that arrive at the receiver. Multipath delay spread leads to time dispersion and frequency selective fading [16]. In a frequency selective fading channel path gain is different for different frequency components. Different transmitted signals will undergo different values of path gain components. The delay-spread function may be modeled as a zero-mean complex valued Gaussian random process; thus the signal envelope is Rayleigh distributed [17]. From [15] we see histogram of transfer function of power line

network is well approximated by Rayleigh distribution. The Rayleigh distribution is commonly used to describe the statistical time-varying nature of the envelope of an individual multipath component.

In the light of above discussions, the power line channel may be considered as a frequency selective Rayleigh fading channel. Since we are going to study the performance of a multiple access technique, our attention will be to increase the number of users with a reasonable Bit Error Rate (BER). Impact of power line noise under various conditions will also be analyzed. Impact of number of path, processing gain, and bit rate will be analyzed too. Then a comparative study will be shown between correlation and RAKE receiver under the same scenario.

1.6 Thesis Outline

Chapter 1 (the current chapter) gives the introduction of Power Line Communication with some basic features, the knowledge of which will be needed through out this report. Then the background and the objective of this research are mentioned.

Chapter 2 describes the theoretical background and working principle of the Direct Sequence CDMA technique.

Chapter 3 describes the power line channel characteristics.

Chapter 4 describes the power line noises. The modeling of impulsive noise and the estimation of average power line noise from statistics are explained.

Chapter 5 describes the analytical model for DS-CDMA systems. The equations for signal to interference ratio (SIR) and bit error rate (BER) of the system are derived.

Chapter 6 shows the impact of various parameters under different operating conditions. The system performance of correlation and RAKE receiver is compared also.

Chapter 7 gives the conclusions and the suggestions for future work.

CHAPTER 2

DIRECT SEQUENCE CODE DIVISION MULTIPLE ACCESS

2.1 Spread Spectrum

Spread spectrum communication refers to modulating a signal for the purpose of spreading its energy across a frequency range that is wider than its original unmodulated bandwidth. The two most common methods of performing this modulation are direct sequence (DS) and frequency hopping (FH). In DSSS, a high-frequency PN sequence is used to modulate the signal directly yielding a wide bandwidth baseband signal (refer to Figure 2.1a). In FH spread spectrum (FHSS), a modulating frequency is varied according to a PN sequence so that the signal occupies a frequency slot for a short time before hopping to another slot in a pseudo-random order (refer to Figure 2.1b). The random nature of the PN sequence makes the DSSS modulated spectrum "white" or spectrally flat and in the case of FHSS [18], it evenly distributes the hopped frequency band across the expanded spectrum.
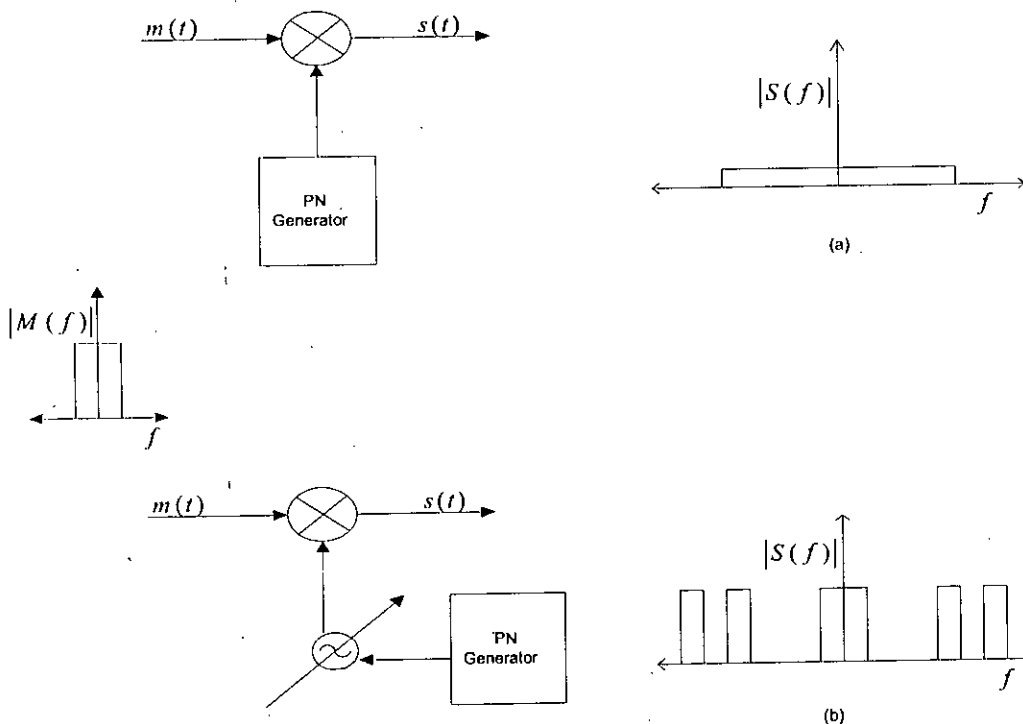
Figure 2.1 Spectrum expansions for (a) DSSS modulation and (b) FHSS modulation.

Expanding the bandwidth with either method will achieve the following benefits as the signal passes through the communication channel: immunity to spectrum fades, immunity from jamming signals (external interference and multipath distortion), reusability of spectrum, and simultaneous multi-user access of the same spectrum.

Narrow-band fades, jamming signals, or interferers can only corrupt a small portion of the spread spectrum signal only slightly degrading its signal-to-noise ratio (SNR). For DSSS, multipath signals looks like noise to a direct-path signal causing only a slight degradation in its SNR. The DSSS signal looks like background noise to other users communicating in the same frequency band and for FHSS, orthogonal hopping avoids interference with other users in the same band. Thus in either modulation, multiple pairs of users with unique random codes will be able to communicate simultaneously over the same spectrum permitting reusability. For these reasons spread spectrum modulation is often a popular choice for data and voice communications today.

The main advantages of DSSS are: tolerance to interference, secure communication and jamming resistance, several users on the same band of frequency, resistance to multipath fading [19]. Only impairment is near-far problem. Power control is used to solve near-far problem.

2.2 Pseudo-random Noise (PN) Code Sequences

The unique characteristics of PN sequences make them useful in spectral whitening, random test-data generation, data scrambling and spectral expansion (as in SS). It is their close-to-ideal randomness and ease of generation that makes them so useful. These sequences are easily generated by using an M-bit shift register with the appropriate feedback taps, as shown in Figure 2.2 for $M = 5$. With the appropriate taps, the length (N) of the serial bit stream at the output will be a maximum (L_{max}).

$$N = L_{max} = 2^M - 1 \tag{2.1}$$

The meaning of bit-stream length in this context is the maximum length of the bit sequence before it starts repeating itself. PN sequences of maximum length are called maximal linear code sequences, but because non-maximal PN sequences are rarely used in SS systems, "PN sequences" will be used to denote maximal linear code sequences.

mod-2 add
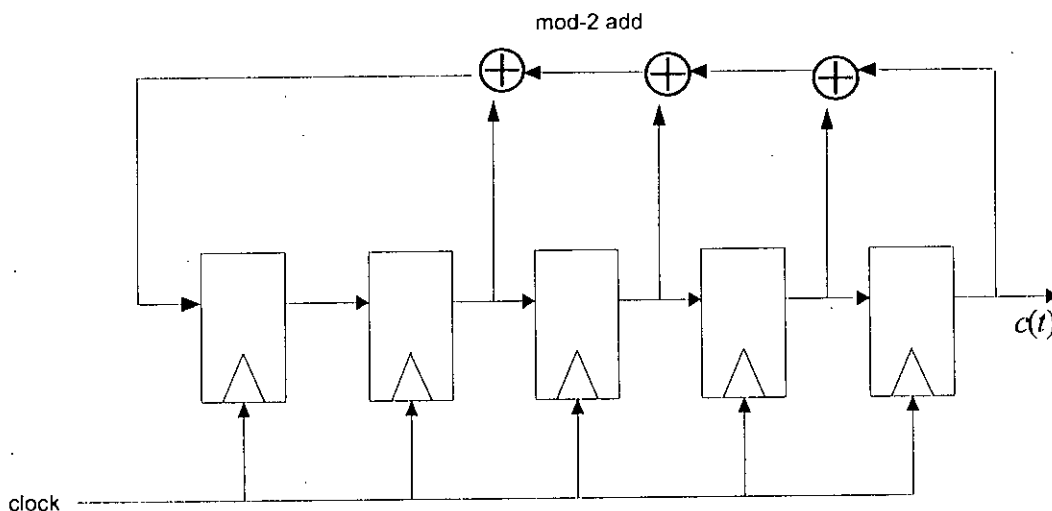
Figure 2.2 Maximal length PN sequence generator ($M=5$, $N=31$).

Also "PN codes" or "PN code sequences" will be used synonymously with "PN sequences". The feedback taps are added modulo-2 (exclusive ORed) and fed to the input of the initial shift register. Only particular tap connections will yield a maximum length for a given shift register length. These maximal length PN codes have the following properties:

1. Code balance: The number of ones and the number of zeros differ by only 1, i.e., there is 1 more one than the number of zeros. This is particularly useful when the channel is AC coupled (no DC transmission).

2. Run-length distribution: The run-lengths of ones, i.e., the number of ones in a row, and zeros are distributed in a deterministic and somewhat statistically balanced way. Table 2-1 illustrates this distribution for $M = 7$. In words, there is exactly 1 run of M ones, 1 run of $M-1$ zeros, 1 each of runs of $M-2$ ones and zeros, 2 each of runs of $M-3$ ones and zeros, 4 each of runs of $M-4$ ones and zeros, 2^3 each of runs of

$M-5$ ones and zeros,..., 2^K each of runs of $M-2-K$ ones and zeros, ... and 2^{M-3} each of runs of 1 ones and zeros.

Run-length	Runs of Ones	Runs of Zeros	Bit Total
7	1	0	7
6	0	1	6
5	1	1	10
4	2	2	16
3	4	4	24
2	8	8	32
1	16	16	32
All Runs			127

Table 2.1 Run-length distribution ($M = 7$).

3. Autocorrelation: Using signaling values of ±1, the autocorrelation of a PN sequence has a value of -1 for all phase shifts of more than one bit time. For no phase shift (perfect alignment with itself), the autocorrelation has a value of N, the sequence length (Figure 2.3).

4. Modulo-2 addition: Modulo-2 addition of a PN sequence with a shifted version of itself results in a differently-shifted version of itself.

5. Shift Register States: The binary number represented by the M bits in the shift register randomly cycle through all 2^M values, except for 0, in successive $2^M - 1$ clock. If the value of 0 (all shift register bits are 0) is ever present in the shift register, it will stay in that state until reloaded with a nonzero value.

The second and third properties are the most important PN sequence properties for use in SS systems. The run-length distribution property is responsible for the randomness and for the spectral "whiteness" of the PN sequence. The randomness is

ideal for generating pseudo-random data for testing purposes while its whitening characteristic makes it useful as a scrambling modulator to flatten the spectral content of a signal prior to transmission or as a spreading modulator to expand as well as flatten a signal [18].

The continuous-time (CT) autocorrelation of a PN sequence is defined as:

$$C_{CA}(\tau) = \frac{N}{N.T_c} \int_{NT_c} c(t).c(t+\tau)dt \qquad (2.2a)$$

$$= \frac{1}{T_c} \int_{NT_c} c(t).c(t+\tau)dt \qquad (2.2b)$$

where $c(t)$ is the PN sequence as a function of time with value ± 1, N is the number of PN sequence bits, T_c is a PN bit-time and is its length. Figure 2.3 is a plot of the CT autocorrelation function, $C_{CA}(\tau)$. This plot assumes that $c(t)$ wraps around when computing the integral. Timing synchronization in a DSSS receiver takes advantage of unique shape of $C_{CA}(t)$ by searching for the peak autocorrelation value which signals perfect alignment ($\tau = 0$) of the incoming received signal to the DSSS receivers' internally generated PN sequence. The longer the PN code length, N, the larger the correlation peak and hence the more resistant to false synchronization from noise and interference.
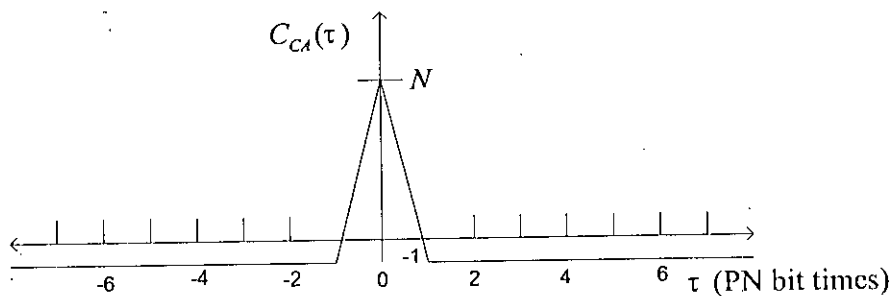
Figure 2.3: Continuous time autocorrelation function.

2.3 Single User DSSS modulation

Now we consider the simplest case of DSSS modulation; that of transmission and reception of a single (user) data stream. In this case, a PN code directly modulates the binary data signal, $m(t)$. The bandwidth expansion of signal's spectrum (Fig. 2.1) is a result of the higher bit rate of the PN code. The expansion or spread factor (FS) is the ratio of the PN code bit rate to the data signal bit rate. The modulation process is illustrated in Figure 2.4. The modulated output $s(t)$ has the same bit rate as the PN code. To avoid confusion with the data bits ($m(t)$), the PN code bits and modulated data bits ($s(t)$) are commonly referred to as chips.
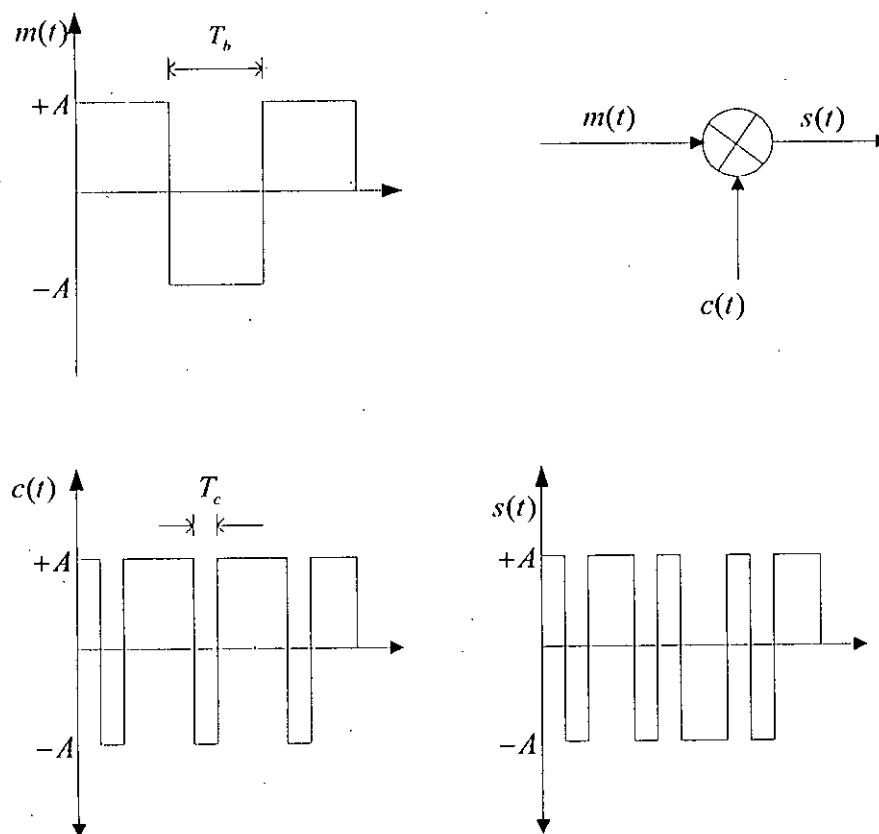
Figure 2.4: DSSS modulation representation ($N.T_c > T_b$).

Thus bit time (T_b) will refer to the duration of one unmodulated data bit and chip time (T_c) to that of a PN code or modulated data bit time. With this convention, an alternative definition for spread factor is:

$$F_S = \frac{T_b}{T_c}$$

(2.3)

Normally the PN code length $N.T_c$ is greater that or equal to the data bit time, T_b.

2.4 Demodulation of a single DSSS user

Recovering the original data stream requires timing alignment of the receiver's internal PN code ($c(t)$) to the embedded PN code in the baseband received signal ($r_m(t)$), then demodulation, or despreading, of the received signal and finally detection of the data bits. Timing alignment, or *synchronization*, will be covered at the end of the chapter so until that section we will assume perfect PN code alignment during demodulation.

Demodulation of the DS signal converts the wide-band modulated signal back to a narrow-band signal indicating some type of decimation or filtering function. Correlation, or more specifically cross-correlation, of the received signal ($r_m(t)$) with the desired PN code ($c(t)$) accomplishes this decimation. Figure 2.5 shows a simplified block diagram of a DSSS receiver where a correlator is used as the baseband demodulator. Continuous time cross-correlation for data demodulation is defined as:

$$C_{CX}(\tau) = \frac{1}{T_b} \int_{T_b} r_m(t).c(t+\tau)dt$$

(2.4)

where the extent of the integration in this case is restricted to the duration of one data bit (T_b) as opposed to the PN sequence length.

Since noise and interference processing will be covered in the next section, we will restrict ourselves to an ideal noiseless transmission and reception of a single user's data signal to make the demodulation picture clearer. In this case the baseband receive signal would be:

$$r_m(t) = A.s(t) = A.m(t).c(t) \tag{2.5}$$
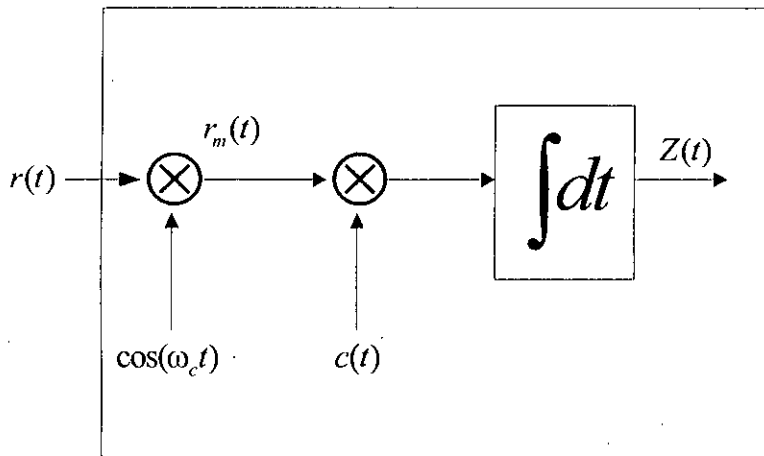
Figure 2.5: A simplified DSSS correlation receiver

where A represents the signal amplitude, $s(t)$ is the PN modulated baseband binary signal, and $m(t)$ is the original unmodulated binary data signal. For simplicity also assume that $A = 1$, so $r_m(t)$ looks exactly like the baseband modulated data signal, $s(t)$. Then the continuous time cross-correlation with perfect synchronization ($\tau = 0$) is:

$$C_{CX}(0) = \frac{1}{T_c} \int_{T_b} r_m(t).c(t+0)dt \tag{2.6a}$$

$$= \frac{1}{T_c} \int_{T_b} m(t).c(t).c(t+0)dt \tag{2.6b}$$

$$= m\big|_{T_b} \cdot \frac{T_b}{T_c} = m\big|_{T_b} \cdot F_S \qquad\qquad (2.6c)$$

$$= m\big|_{T_b} \cdot \frac{1}{T_c} \int_{T_b} c^2(t)dt \qquad\qquad (2.6d)$$

Therefore the correlator output is equal to the original data bits evaluated at T_b intervals and scaled by the spread factor. Figure 2.6 shows input and output waveforms for this example, when $Fs=8$ and $N=31$. From the output waveform it is clear that the final data recovery is simply sign detection of the correlator output at T_b intervals. The output magnitude contains no data information itself but does represent the strength of the signal, which can be used in calculating the post-demodulation signal-to-noise ratio (SNR) to give an indication of the correlation bit-error rate performance.

In a more realistic example, the received signal could be corrupted by interference and noise signals as well as distorted by the RF channel characteristics. This effect will randomly vary $r_m(t)$ such that the product will be ±1 with some variance. Integrating this variance over the interval T_b results in an averaging effect, which reduces the variance, or noise power, while not affecting signal power. This reduction in the noise power is called the processing gain (G_p) of an SS system.
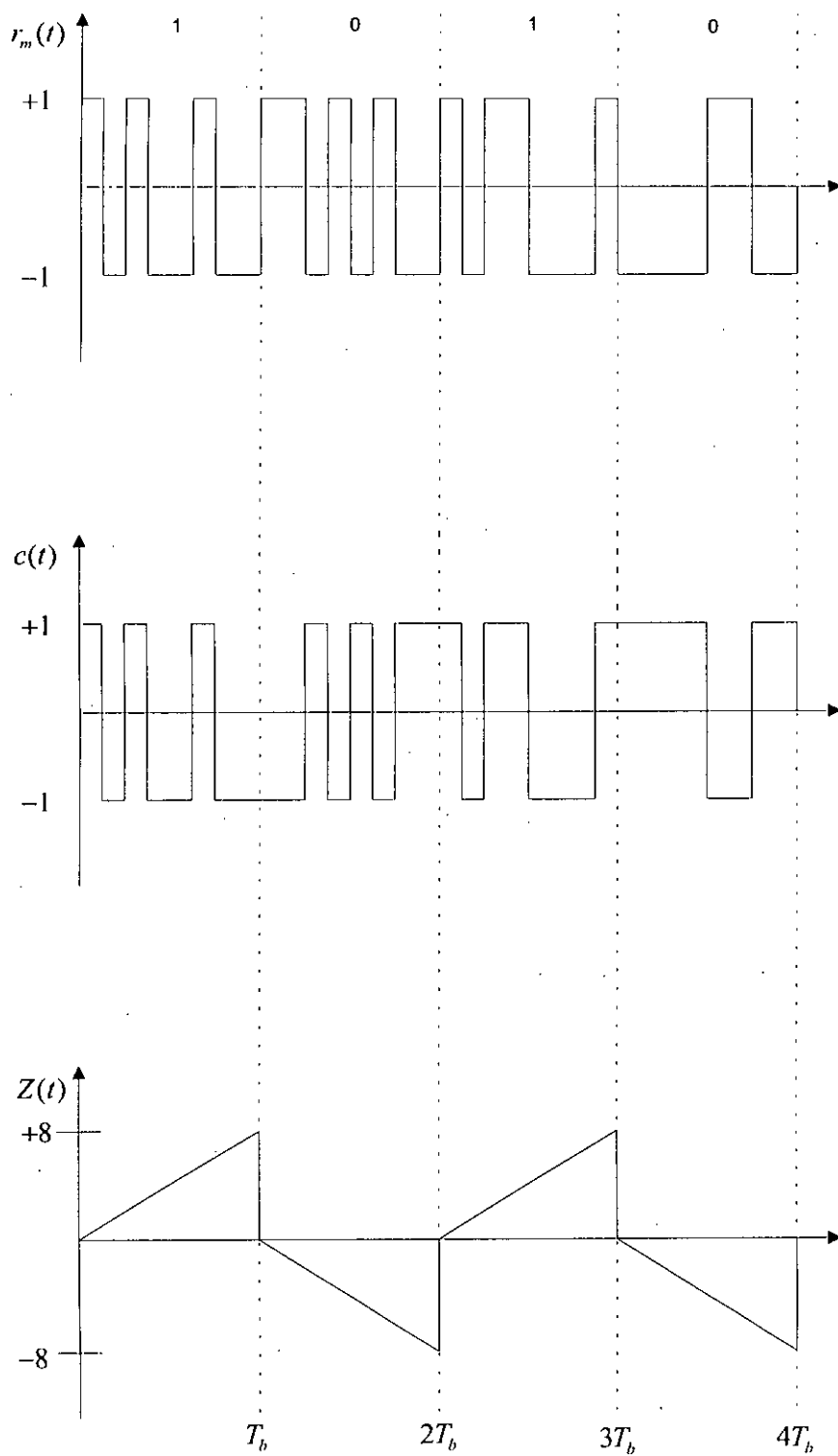
Figure 2.6 Correlator input [$r_m(t)$ and $c(t)$] and output [$C_{cx}(t)$] waveforms for $Fs=8$ and $N=31$.

2.5 Code Division Multiple Access

In DSSS, multiple users can simultaneously transmit and receive over the same frequency spectrum since each user's modulated data looks somewhat like white noise to the other users. Differentiation of each user's data is achieved by using a different PN code to modulate and spread the data. Ideally, if K codes are orthogonal they span a K-dimensional space, which can accommodate K users. Orthogonality in this context means that the cross-correlation of one of the $K-1$ undesired users' DS-modulated signal with the PN code of the desired user is zero. In this sense, the correlator performs a dot product between the desired PN code and the incoming received signal. So only the desired incoming signal will have a non-zero correlation resulting in a recovery of that user's data [20].

The problem with this scenario is that it is difficult to find a set of binary codes that are orthogonal in an asynchronous multi-user transmission environment. To better understand why this is the case, we can look at a simple example of the cross-correlation of two 7-chip PN codes; (1110100) and (1100101) coded as ±1. Figure 2.7 is a plot of the crosscorrelation versus time shifts between the two codes. A correlation value of -1 in this case is essentially zero, there only 3 (-3, -2, and 2) out of 7 possible chip phases (τ) where the two PN codes are "orthogonal". And since two independent users would transmit asynchronously there is no guarantee that the codes would be orthogonal and hence the two transmissions could interfere with one another. In addition to long PN codes, even if two codes were initially orthogonal, over time they could become non-orthogonal due to a slight mismatch in their timing sources. This does not mean that multi-user transmissions cannot be used; on the contrary, as stated previously other users' signals look somewhat like white noise and rejection is via the processing gain mechanism inherent in SS communications. What it does mean is that complete rejection based on orthogonality principles cannot be realized. For this reason asynchronous multi-user transmission is treated as any other interfering source [19].
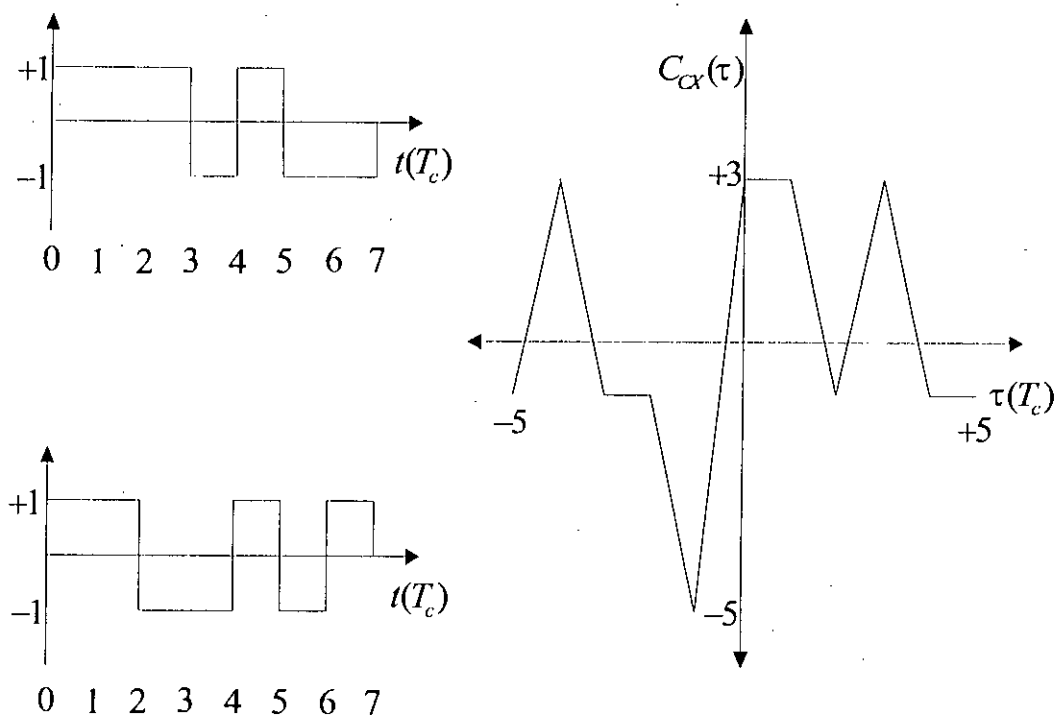
Figure 2.7: CT cross-correlation of two 7-chip PN codes

In the next page, Figure 2.8 is a simplified block diagram of the CDMA transmitter. Normally the orthogonal code rate is the same as the PN code rate so the orthogonal code spreads the spectrum of the user's data. However, in general, these orthogonal codes have a very poor autocorrelation characteristic and therefore cannot be used for synchronization in the receiver. Thus a PN modulation is still needed which will allow the synchronization block to leverage the autocorrelation property to achieve timing lock by peak detection.
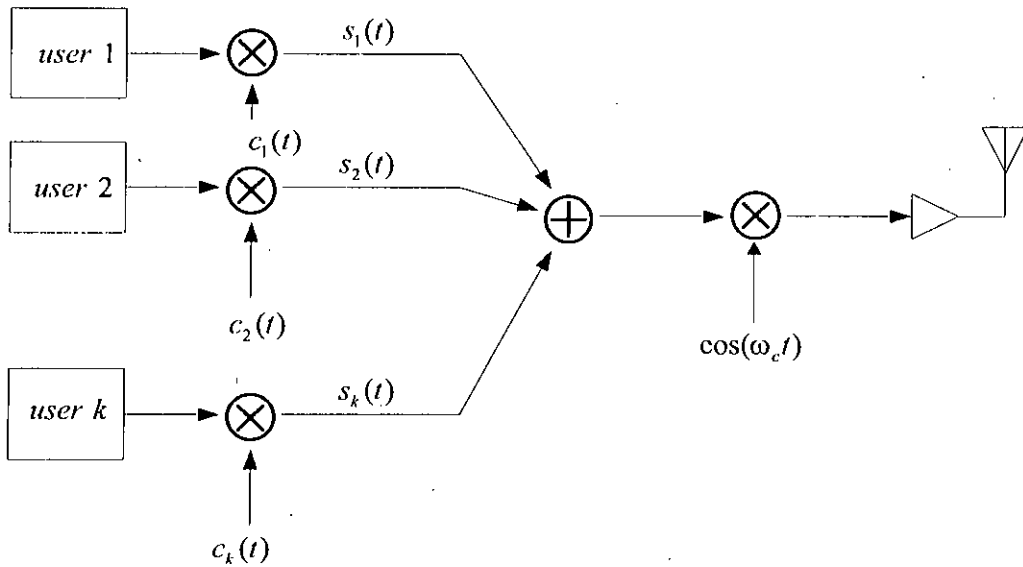
Figure 2.8: An example of a CDMA transmitter.

Demodulation of this doubly-modulated baseband signal can be accomplished by double demodulation as shown in Figure 2.9. Unlike the single-user case, the integration is not a linear ramp but a crooked one due to integrating the other user's signals. However the final value is the same since the other user's signals will integrate to zero. Linearity of the correlator is important for maintaining the orthogonal relationship of the signals, i.e, to ensure that the other users' signals integrate exactly to zero. Second, for the same desired-user signal strength in the single-user case, the dynamic range of the correlator must be larger in the multi-user case to accommodate the larger multilevel signal.
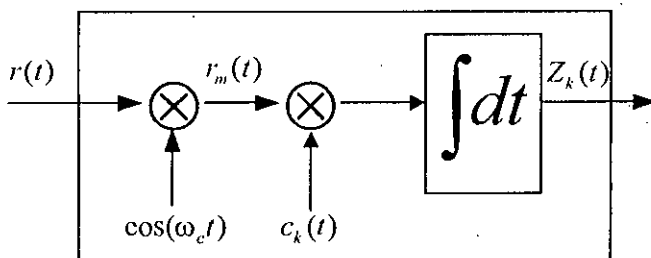
Figure 2.9: Multi-user CDMA receivers: straight-forward implementation.

2.6 RAKE Receiver

A RAKE receiver combines the time-delayed versions of the original signal transmission in order to improve the signal-to-noise ratio at the receiver. It attempts to collect the time-shifted versions of the original signal by providing a separate correlation receiver for each of the multipath signals [16]. Each correlation receiver may be adjusted in time delay, so that a microprocessor controller can cause different correlation receivers to search in different time windows for significant multipath. The range of time delays that a particular correlator can search is called a search window. The RAKE receiver, shown in Figure 2.10, is essentially a diversity receiver designed specially for CDMA, where the diversity is provided by the fact that the multipath components are practically uncorrelated from one another when their relative propagation delays exceed a chip period.
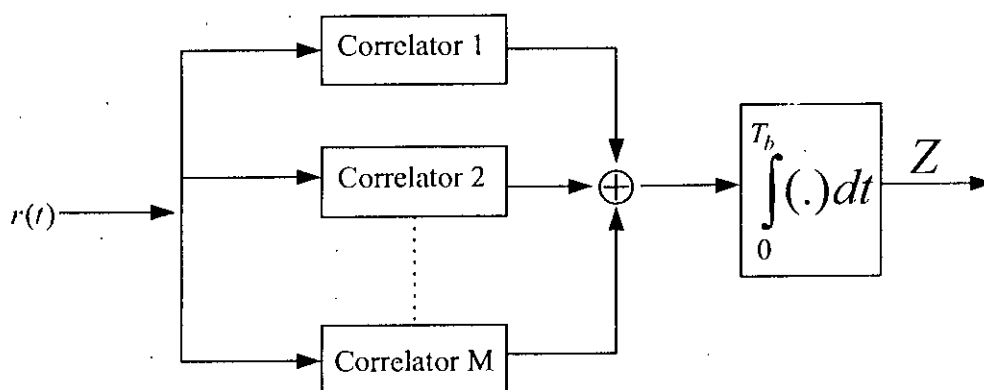
Figure 2.10: An M-finger RAKE receiver implementation.

A RAKE receiver utilizes multiple correlators to separately detect the M strongest multipath components. The output of each correlator (finger) are then weighted to provide a better estimate of the transmitted signal than is provided by a single component. Demodulation and bit decisions are then based on the weighted outputs of the M correlators.

2.7 Processing Gain

The previous two sections (section 2.4 and 2.5) explained how recovery of the desired user's signal and rejection of undesired orthogonal users' signals were accomplished. We now look at all other signals that might be found in the received signal, which we would like to reject. These signals can be divided into two categories; narrowband and wideband interference. Narrowband interference can be simplified to a carrier wave signal as in a broadcast radio transmission or an intentional jamming signal. Wideband interference will encompass white noise sources, multipath SS signals, FHSS signals or asynchronous DS-CDMA signals. For the case of carrier wave (single frequency tone) interference, the correlation process mixes the signal with a PN code and then integrates the result. The PN modulating step of the correlation randomly scrambles the sine wave and spreads its spectrum exactly like the DSSS transmission process, making it look like wideband interference prior to integration. The integrating step then averages or low-pass filters the interference, decreasing its variance or AC signal power. In the second case of wideband interference, the PN modulating step will tend to whiten, or flatten, the spectrum while the integrating step will again lower the AC power of the interfering signal. In either case the averaging effect by the correlator lowers the overall interference power and thus increases the SNR (assuming the desired signal power remains constant) by what is known as the processing gain, G_p. Thus we can define G_p as:

$$G_P = \frac{SNR_o}{SNR_i} \tag{2.7}$$

where SNR_o and SNR_i are the output and input SNR of the correlator, respectively. A somewhat more useful rule-of-thumb definition for G_p is:

$$G_P = \frac{BW_{SS}}{BW_D} \cong \frac{T_b}{T_c} = F_s \tag{2.8}$$

where BW_D and BW_{SS} are the bandwidth of the data before and after SS modulation [22].

2.8 Synchronization

Usually the synchronization process is carried out in two phases. In the first (acquisition) phase a coarse alignment to within one chip time (T_c) is achieved. Once acquisition is attained the second (tracking) phase is begun. The tracking phase performs a fine alignment to within a fraction of T_c and maintains that alignment while the demodulation is in progress.

Acquisition and tracking rely heavily on the autocorrelation characteristic of PN sequences. The tracking correlation length must be equal to the PN sequence length, $N \ Tc$. Whereas the demodulation correlation length needs to be equal to the data bit length, T_b. Acquisition is carried out by monitoring the correlator's output for successive chip (T_c) phase alignments until the peak region is detected signaling an alignment within $\pm T_c$ of peak center. This amounts to tracing the autocorrelation curve of the PN sequence by the correlator. Two difficulties are sometimes encountered in practice; data modulation of the PN sequence and a PN sequence that is longer than a data bit time ($NT_c > T_b$). If the PN sequence length is equal to T_b ($NT_c = T_b$) then acquisition can be attained by including negative as well as positive peak detection. And without data modulation, having a PN sequence longer than T_b

($NT_c > T_b$) implies only performing a longer correlation (beyond that needed for data demodulation) before checking for the peak amplitude. When both conditions occur, which is not infrequent, the peak detection process can be degraded or completely impaired. Acquisition time (τ_{acq}) is the time it takes the receiver to achieve initial coarse PN code alignment lock or reachieve alignment after losing lock [18].

PN code alignment is that maintained by using two tracking correlators in a feedback configuration called a delay-locked loop (DLL). One tracking correlator (Early) samples the input a half chip time ahead of the data demodulator (Data), while the other correlator (Late) samples one half chip time behind the data correlator, as shown in Figure 2.11. The feedback is such that it tries to equalize the output values of the two tracking correlators.
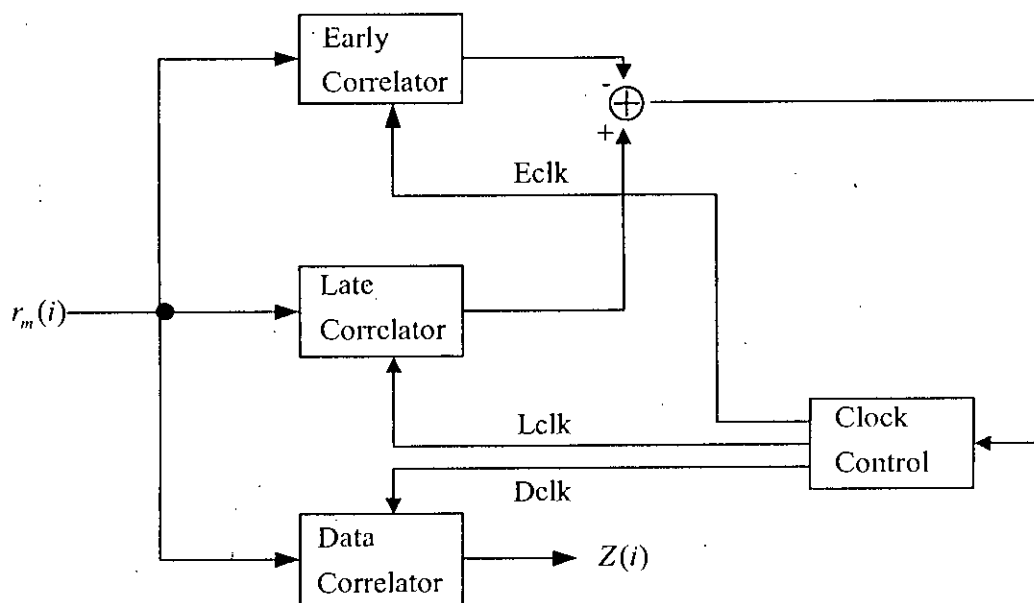
Figure 2.11: Delay-Locked Loop with the data demodulator

This can best be understood by considering the CT $C_{CA}(t)$ function and Early and Late correlator results for three cases; internal PN code ahead of the input signal, aligned to the input signal and behind the input signal, which are shown in Figure 2.12.
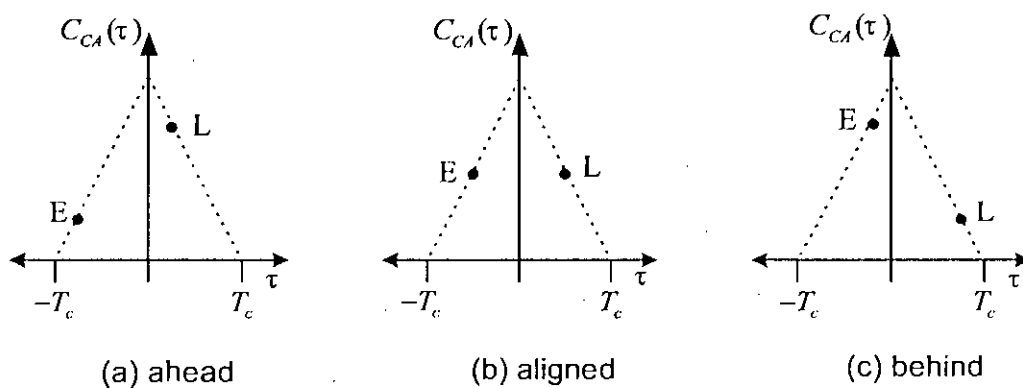
Figure 2.12: Early and Late correlator output values for different timing alignments; (a) internal PN code is ahead of the receive input signal; (b) aligned to input signal; (c) behind input signal.

The Early, Data, and Late correlators perform a correlation on three successive chip phases of the input signal spaced $0.5T_c$ apart, so when the Early and Late output amplitudes are equal, the Data correlator will be perfectly aligned to the input signal and will produce the peak output value [20].

2.9 Summary

This chapter presented a brief description of basic concept of Direct Sequence CDMA system for digital communication. This is a Spread Spectrum Multiple Access (SSMA) technique. In the SS techniques processing gain reduces power of any noise signal at the input of the correlator. Therefore, the benefit of SS modulation is that any finite-energy or narrow-band noise introduced in the channel or by the front-end SS receiver circuitry will be attenuated by the processing gain factor yielding an improvement in the overall SNR. DSSS scheme has the higher degree of jamming resistance than FHSS. For multipath propagation FHSS has a limited immunity. FHSS requires wider bandwidth than DSSS.

CHAPTER 3

POWER LINE CHANNEL

3.1 Introduction

There are many advantages in using a power line network as a communication channel. Firstly, the power network is the most pervasive network compared to any other networks in the world and its availability reaches every socket in our house. Secondly, the installation of the PLC system is very cost effective, since it makes use of existing power lines and no additional wires are required.

However, unlike the other wired communication media such as the unshielded twisted pair (UTP) and coaxial cables, LV Power Lines present an extremely harsh environment for the high frequency communication signals. The three critical channel parameters namely, noise, impedance and attenuation, are found to be highly unpredictable and variable with time, frequency and location [21].

In order to overcome these difficulties, a lot of efforts have been undertaken to characterize and model the LV Power Line channel.

The power line network differs considerably in topology, structure, and physical properties from conventional media such as twisted pair, coaxial cables, or fiber-optic cables. Only in the case of very simple topologies, such as a cable with a single branch, the physical reasons for the observed results (cable loss, reflection, and transmission factors) can be easily identified. In real network topologies - which are always more complicated – a back-tracing of measurement results to physical reasons will generally turn out to be impossible.

Power line channel is treated as a frequency selective fading channel. The channel has multipath phenomena.

3.2 Transmission Line

For lines with losses or for filter-type transmission circuits, we generalize the distributed series element in the circuit model to an impedance Z per unit length, and the distributed shunt element to a general admittance Y per unit length [22].
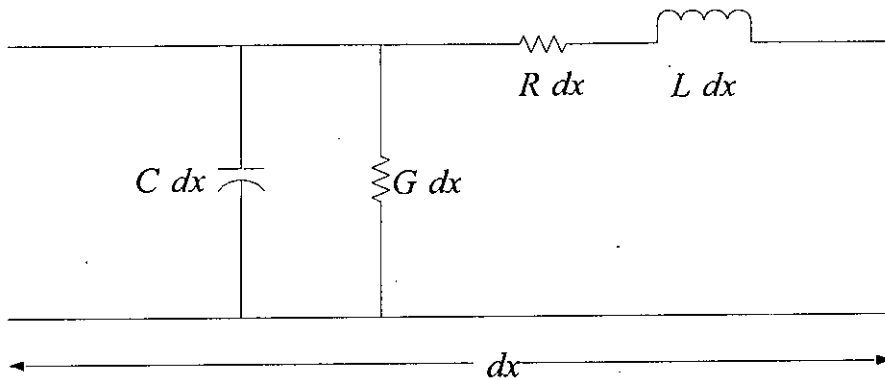
Figure 3.1: Equivalent circuit of a transmission line with distributed parameters

R is the resistance per unit length, G is the conductance per unit length, L includes both external and internal impedance and C is the capacitance per unit length.

Distributed series resistance in the conductors of the line, and distributed shunt conductance because of leakage through the dielectric of the are introduced to consider the losses. Distributed parameters are shown in figure 3.1. Distributed impedance and admittance are then:

$$Z = R + j\omega L \tag{3.1}$$

$$Y = G + j\omega C \tag{3.2}$$

The propagation constant is given by,

$$\gamma = \sqrt{ZY} = \alpha + j\beta \tag{3.3}$$

where α is the attenuation constant and β is the phase constant.

Characteristic impedance of the transmission line is given by,

$$Z_0 = \sqrt{\frac{Z}{Y}} = \sqrt{\frac{(R + j\omega L)}{(G + j\omega C)}} \qquad (3.4)$$

From the equation (3.3) we get,

$$\gamma = \sqrt{(R + j\omega L)(G + j\omega C)}$$

$$= [(RG - \omega^2 LC)^2 + \omega^2 (RC + LG)^2]^{\frac{1}{4}} . e^{j\frac{1}{2}\tan^{-1}[\frac{\omega(RC+LG)}{RG-\omega^2 LC}]} \qquad (3.5)$$

From the equations (3.3) and (3.5) we get, attenuation constant,

$$\alpha = [(RG - \omega^2 LC)^2 + \omega^2 (RC + LG)^2]^{\frac{1}{4}} . \cos[\frac{1}{2}\tan^{-1}\frac{\omega(RC + LG)}{RG - \omega^2 LC}] \qquad (3.6)$$

and the phase constant,

$$\beta = [(RG - \omega^2 LC)^2 + \omega^2 (RC + LG)^2]^{\frac{1}{4}} . \sin[\frac{1}{2}\tan^{-1}\frac{\omega(RC + LG)}{RG - \omega^2 LC}] \qquad (3.7)$$

From the equation (3.4) we get,

$$Z_0 = \left[\frac{R^2 + \omega^2 L^2}{G^2 + \omega^2 C^2} \right]^{\frac{1}{4}} . e^{j\frac{1}{2}\tan^{-1}\left[\frac{G\omega L - R\omega C}{RG + \omega^2 LC}\right]}$$
(3.8)

3.3 Residential Power Line Cable

The low voltage power line cables are generally designed for the frequency of the supplying network (50/60 Hz). The cable manufacturers normally give parameters for the cable, such as inductance, capacitance, and resistance. These values are applicable close to grid frequency. However the high frequency properties of the low voltage power cables have also become important issues.

Radiation effect of residential power lines leaking signal power in the frequency range 0-30 MHz is neglected because the width of a power line is quite small compared with a wavelength in the above so that a transverse electromagnetic (TEM) mode of propagation will occur. That means Poynting power flow can be assumed as axial, so that leakage is negligible from the line [22].

In Bangladesh, most of the indoor cable has two conductors (one live and one neutral conductor) as shown in Figure 3.2.
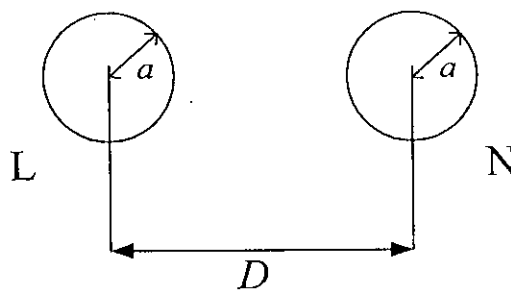
Figure 3.2: Indoor two wire power line cable

PVC (Polyvinyl Chloride) is used as insulation material and phase conductors are made of copper. The relative permittivity for the PVC insulation material at the frequency range 100 KHz-100 MHz is about, $\varepsilon_r \approx 2.9$ [22]. The conductivity of copper is $\rho_{cu} = 1.72 \times 10^{-8} \Omega m$ [21].

The equivalent transmission line parameters can be written as [21]:

Resistance per unit length, $R = \dfrac{R_{scu}}{\pi a}$ Ω $\qquad$ (3.9)

where R_{scu} is the surface resistance of copper and a is the radius of each wire.

Capacitance per unit length, $C = \dfrac{\pi \varepsilon}{\cosh^{-1}(\dfrac{D}{2a})}$ $Farad$ $\qquad$ (3.10)

where, ε is the absolute permittivity of insulating material and D is the distance between the central axis of the conductors.

Absolute permittivity is given by $\varepsilon = \varepsilon_r \varepsilon_0$ $\qquad$ (3.11)

Also, $\varepsilon = \varepsilon' - j\varepsilon''$ $\qquad$ (3.12)

Conductance per unit length, $G = \dfrac{\pi \omega \varepsilon''}{\cosh^{-1}\left(\dfrac{D}{2a}\right)}$ $Siemens$ $\qquad$ (3.13)

Inductance per unit length, $L = 2L_s + \dfrac{\mu}{\pi}\cosh^{-1}\left(\dfrac{D}{2a}\right)$ $Henry$ $\qquad$ (3.14)

where L_s is the self inductance of each conductor and μ is the absolute permeability of copper.

L_s is given by, $L_s = \dfrac{\mu}{8\pi}$ $\qquad$ (3.15)

and, $\mu = \mu_r \mu_0$ $\qquad$ (3.16)

Dielectric losses are usually described by the "loss tangent" or "dissipation factor" $\tan \delta$.

$$\tan \delta = \frac{\varepsilon^{\cdot}}{\varepsilon^{\cdot}} \qquad\qquad (3.17)$$

3.4 Multipath Signal Propagation through Power Line

In the power line channel, signal propagation does not only take place along a direct line-of-sight path between transmitter and receiver, but additional paths (echoes) must also be considered. The result is a multipath scenario with frequency selective fading [23].
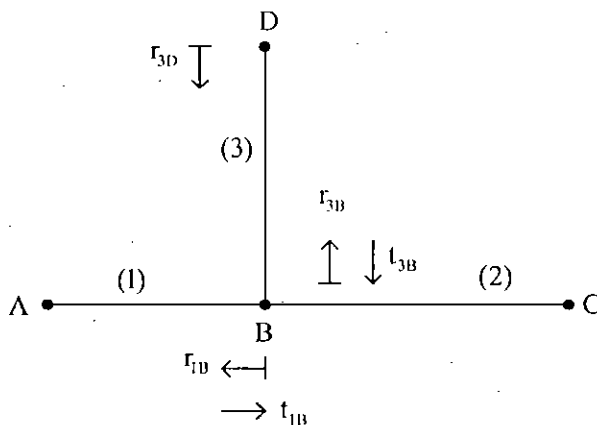
Figure 3.3: Multipath signal propagation; cable with one tape.

Multipath signal propagation is studied by a simple example which can be easily analyzed (Figure 3.3). The link has only one branch and consists of the segments (1), (2), and (3) with the characteristic impedances Z_{L1}, Z_{L2}, and Z_{L3}.

In order to simplify the considerations, A and C are assumed to be matched, which means $Z_A = Z_{L1}$ and $Z_B = Z_{L2}$. The remaining points for reflections are B and D, with the reflection factors denoted as r_{1B}, r_{3D}, r_{3B}, and the transmission factors denoted as t_{1B}, t_{3D}. With these assumptions, an infinite number of propagation paths is possible in principle, due to multiple reflections (i. e., $A \rightarrow B \rightarrow C$, $A \rightarrow B \rightarrow D \rightarrow B \rightarrow C$,

$A \rightarrow B \rightarrow D \rightarrow B \rightarrow D \rightarrow B \rightarrow C$, and so on). Each path i has a weighting factor g_i, representing the product of the reflection and transmission factors at power lines are basically less or equal to one. This is due to the fact that transmission occurs only at joints, where the load of a parallel connection of two or more cables leads to a resulting impedance being lower than the characteristic impedance of the feeding cable. Hence the weighting factor g_i - a product of transmission and reflection factors – is also less or equal to one, i. e.,

$$|g_i| \leq 1 \tag{3.18}$$

The more transmissions and reflections occur along a path, the smaller the weighting factor g_i will be. Furthermore, longer paths exhibit higher attenuation, so that they contribute less to the over all signal at the receiving point. Due to this fact, it is reasonable to approximate the basically infinite number of paths by small number of dominant paths.

3.5 Long Distance Communication through Power Line
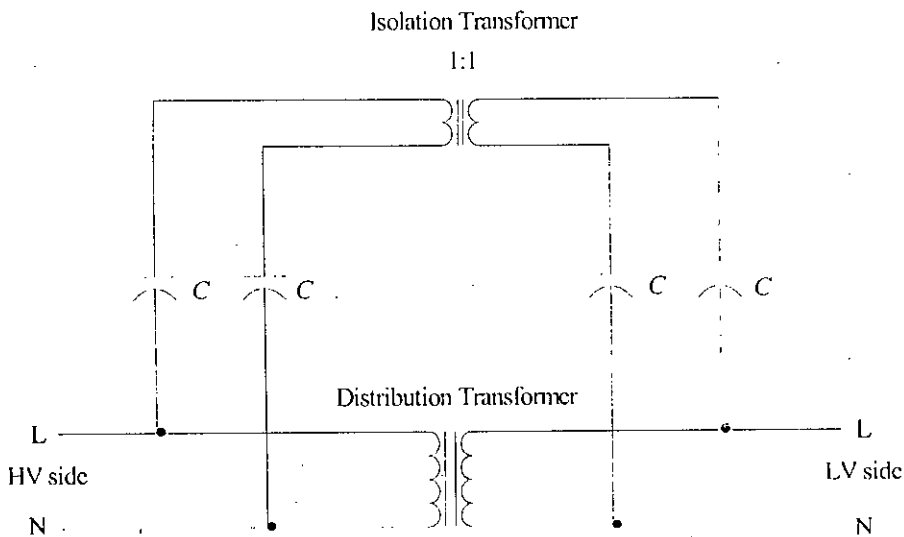
Figure 3.4: Distribution transformer with bypass circuit.

Presence of distribution transformer is a drawback for long distance power line communication. Information signals cannot pass through the distribution transformer because of higher harmonics. Distribution transformers are designed for 50/60 Hz and high voltage. It is required to deploy a bypass circuit to overcome this circumstance.

Figure 3.4 shows one line diagram of a distribution transformer with a bypass circuit based on coupling circuits described in [38], [39]. The capacitors are acted as high-pass filter so that information signal can pass through them. Isolation transformer is used to provide isolation between high voltage side and low voltage side.

3.6 Summary

The channel characteristics of power line are highly dependent on geographical location, network topology, and connected load. High frequency transmission line parameters of a power line cable can be calculated from its physical dimensions. Reflections occur in power line due to impedance mismatching and cause multiple version of information signal. It has been demonstrated that the residential power line cable networks could be modeled as a frequency selective multipath channel.

CHAPTER 4

RESIDENTIAL POWER LINE NOISE CHARACTERISTICS

4.1 Introduction

Noise is omnipresent in all types of communication channels. Residential environment contains a number of complex electronic products and electrical systems. Power line represents a particularly difficult communication environment. Residential power line noises are determined by the responses of home appliances. Figure 4.1 shows the power line noise scenario.
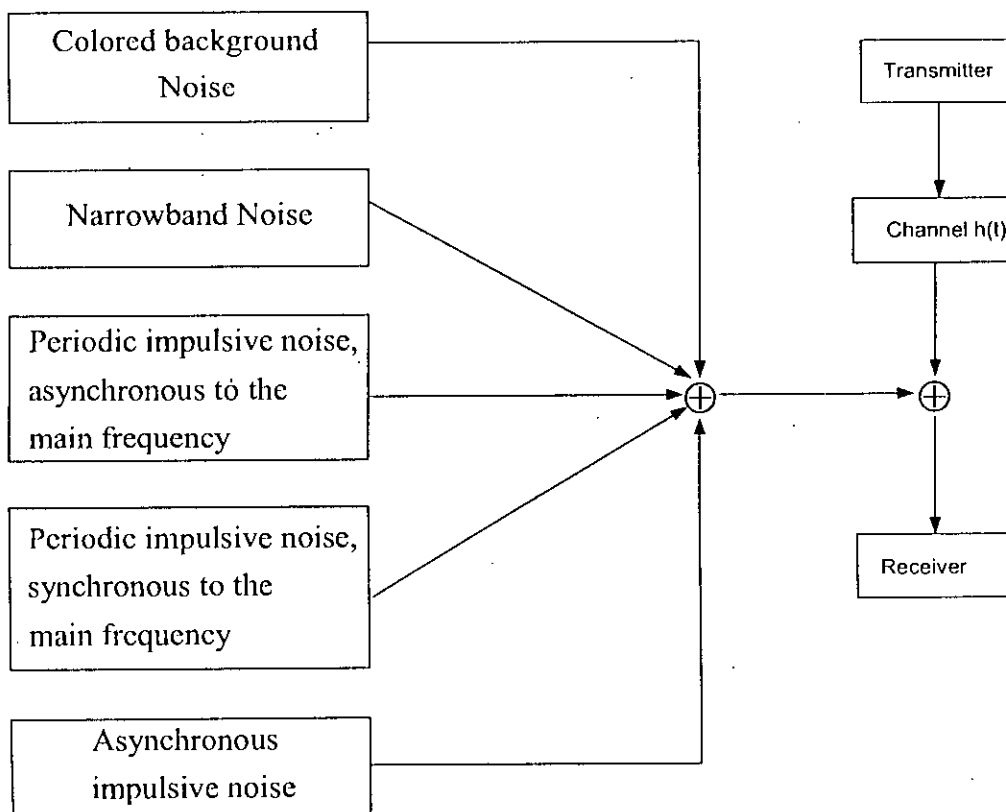
Figure 4.1: Power line noise scenario

Power line noise includes both background and impulsive components. Background noise level decays with increasing frequency. In the case of impulsive noise, however, the time-domain characteristics of the impulses have an important bearing on data communication performance. Important time-domain parameters include impulse amplitude, width, and interarrival time. The amplitude together with the width defines the impulse energy. The interarrival time defines the impulse frequency and, together with the energy, defines impulse noise power [25].

4.2 Classification

The measurement results in reference [26] reveal that the power line noise channel can not be modeled as an Additive White Gaussian Noise (AWGN) channel, which is used to represent noise in the radio communication channel. The radio noise is modeled as a flat spectrum that spans all wireless frequencies with its power equal to $kT/2$, where k denotes the Boltzmann's constant (equal to $1.38 \times 10^{-23} J/K$) and T denotes the temperature in Kelvin.

From the basic approach, five general classes of noise can be defined [27]:

(1) Colored background noise: This type of noise has a relatively low power spectral density (PSD), varying with frequency. This type of noise is mainly caused by summation of numerous noise sources with low power. Its PSD varies over time in terms of minutes or even hours.

(2) Narrow-band noise: Sinusoidal signals, with modulated amplitudes caused by ingress of broadcast stations. The level is varying with daytime.

(3) Periodic impulsive noise asynchronous to the mains frequency: This type of noise has a repetition rate between 50 and 200 KHz, with a discrete line spectrum spaced according to the impulse repetition rate. This type of noise is mostly caused by switched power supplies.

(4) <u>Periodic impulsive noise synchronous to the mains frequency:</u> This type of noise has a repetition rate of 50 or 100 Hz (for 50 Hz mains frequency). The impulses are of short duration (some microseconds) and have a PSD decreasing with frequency. This type of noise is caused by power supplies, mainly by switching of rectifier diodes, which occurs synchronous with the main cycle.

(5) <u>Asynchronous noise:</u> This type of noise is caused switching transients in the network. The impulses have duration of some microseconds up to few milliseconds with random occurrence. The PSD of this type of noise can reach values of more than 50 dB above the background noise.

The properties of noise types (1) - (3) usually remain stationary over periods of seconds and minutes or sometimes even for hours, and may be summarized as background noise [31]. The noise types (4) and (5), however, are time-variant in terms of microseconds to milliseconds. During the occurrence of such impulses, the PSD of the noise rises considerably and may cause bit or burst error in data transmission.

4.3 Background Noise

Available background noise power in watts per hertz is given by [28]:

$$N_{BG} = 10^{-(K + 3.95 \times 10^{-5} f)} [W/Hz] \tag{4.1}$$

where K is a Gaussian random variable with mean (μ) = 5.64, standard deviation (σ) = 0.5 and f is the frequency in hertz.

Equation (4.1) is a statistical approximation of background noise power at any location; this is a frequency dependent relation.

As the background noise is always present in the power line and is mainly caused by the summation of noise sources of low power, it is difficult to predict exactly the level of the background noise or the occurrence of a specific noise disturbance. Background

noise characteristics are shown in Figure 4.2. For frequencies above 1 MHz, background has negligible effects.
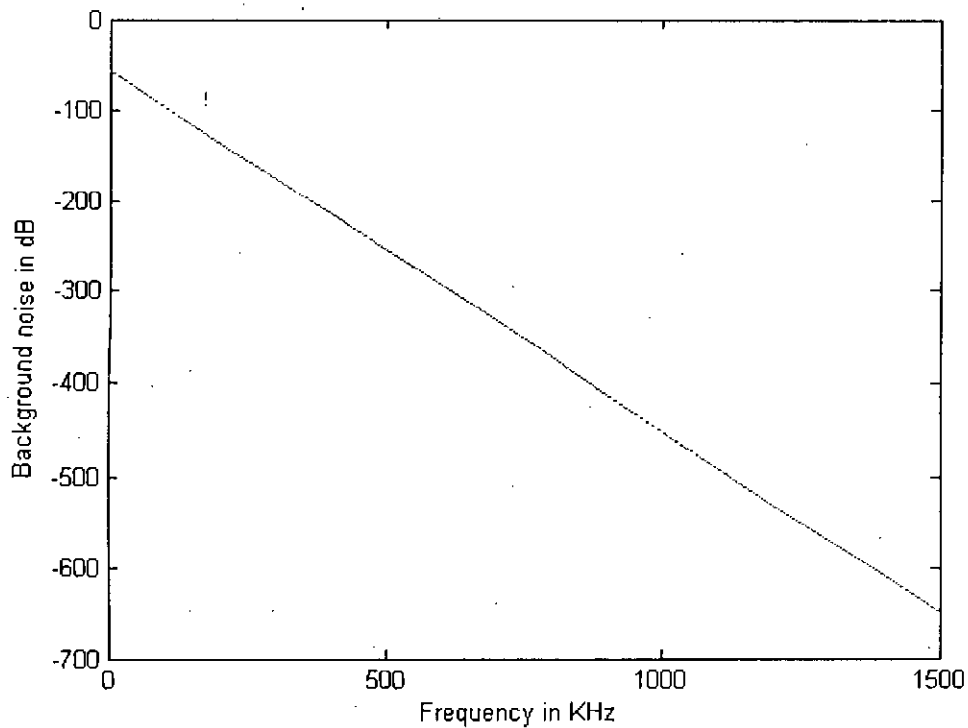
Figure 4.2: Background noise characteristics at frequency range (0-1500 KHz)

4.4 Impulse Noise

Impulse noise is a serious source of impairment for intrabuilding power line communications. Such noise requires approximate description to enable efficient and effective channel utilization. Impulse noise occurs on the line during only a small fraction of time and is characterized by magnitude, duration and interarrival time [25].

There is no accepted model for characterizing the statistics of the impulse noise on power lines because of the lack of sufficient data,. Instead, the models developed for telephone networks are used [29-32].

4.4.1 Impulse Amplitude

Laplace probability density function (PDF) is generally employed to characterize the amplitude of the impulse noise. Unlike in telephone networks, the impulse noise in power lines is expected to be very strong and to destroy the bits when it hits. Figure 4.3 shows Laplace's probability density function.
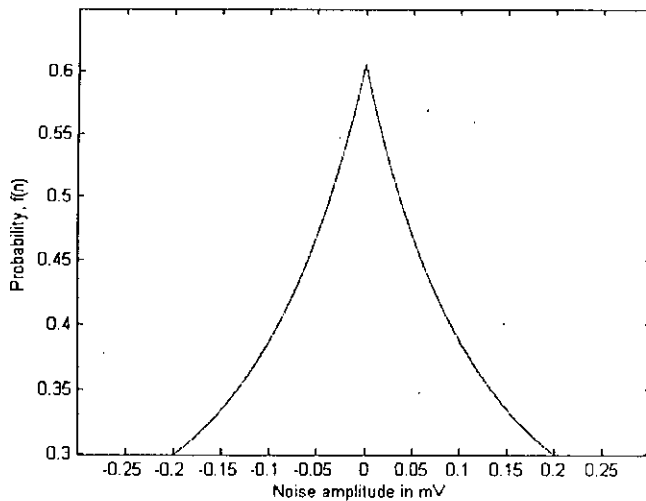
Figure 4.3: Laplace's probability density function

Laplace's probability density function is given by:

$$f(n) = \frac{1}{\sqrt{2}\sigma_n} e^{-\frac{\sqrt{2}|n|}{\sigma_n}}$$

(4.2)

where n is the amplitude of impulsive noise and σ_n is the standard deviation of n. The expected amplitude of impulse noise is given by:

$$A = 2 \int_0^{n_{max}} n f(n) dn = \frac{\sqrt{2}}{\sigma_n} \int_0^{n_{max}} n\, e^{-\frac{\sqrt{2}|n|}{\sigma_n}}\, dn$$

(4.3)

4.4.2 Impulse Width

Time duration (impulse width) is genearally characterized by a log-normal probability density function [31]. The probability density function is given by:

$$f(t) = \frac{1}{\sqrt{2\pi}\sigma_t t} e^{-\frac{[\ln^2(\frac{t}{t_M})]}{2\sigma_t^2}} \qquad (4.4)$$

where, t_M and σ_t are the median and standard deviation of t (sampled impulse width)
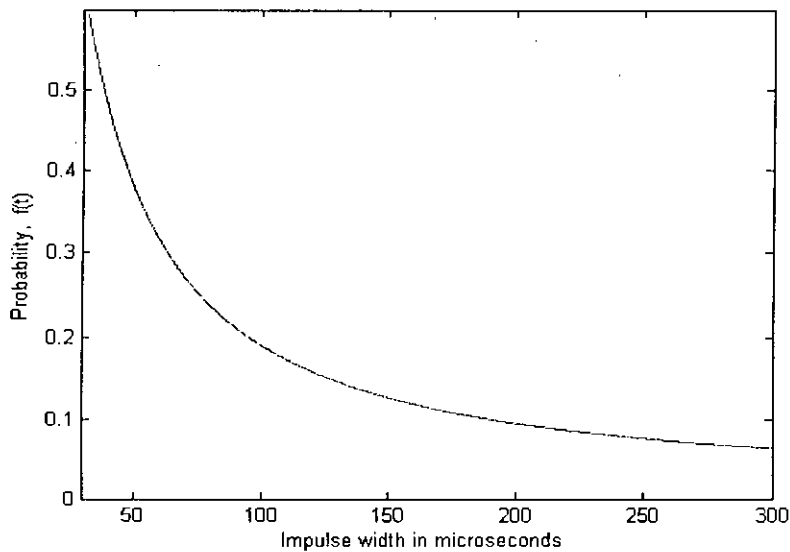
respectively. Figure 4.4 shows the log-normal probability density function.

Figure 4.4: Log-normal probability density function

The expected impulse width is given by:

$$t_w = \int_0^{t_{max}} t f(t) dt = \frac{1}{\sqrt{2\pi}\sigma_t} \int_0^{t_{max}} e^{-\frac{[\ln^2(\frac{t}{t_M})]}{2\sigma_t^2}} dt \qquad (4.5)$$

4.4.3 Interarrival Time

Interarrival time is inversely related to the frequency of occurrence of the impulse noise and is generally described by an exponential PDF,

$$f(t) = \lambda e^{-\lambda t} \tag{4.6}$$

where λ shows the mean frequency of occurrence of the impulse event. The expected interarrival time within an observation window (T_{win}) is given by:

$$t_{IAT} = \int_0^{T_{win}} \lambda t e^{-\lambda t} dt \tag{4.7}$$

4.4.4 Synchronous Impulse Noise

This is the noise caused by switching devices, such as SCR's and certain power supplies. An SCR switches when the power voltage crosses certain value. Since the voltage is cyclic, the SCR switches at 50 Hz or multiple of 50 Hz and thereby causes noise at 50 Hz and multiples thereof. This noise is synchronous with, drifts with, the 50 Hz power frequency. SCR's are a ubiquitous part of every distribution system. This type of noise occurs on both the primary and secondary of the distribution line. The noise has a line spectra with lines at multiples of 50 Hz [33].

Any appliance with SCR causes periodic synchronous impulse noise. The noise is time dependent. A popular residential electrical device which generates high levels of harmonic noise is the solid state light dimmer. The dimmer is wired in series with the incandescent lights and controls lamp brightness by switching ON and OFF rapidly through the use of SCR. The noise produced by the light dimmer is periodic and

synchronous with the 50 Hz power frequency. The light dimmer setting controls the time of light dimmer noise. Figure 4.5 shows the noise caused by a light dimmer.
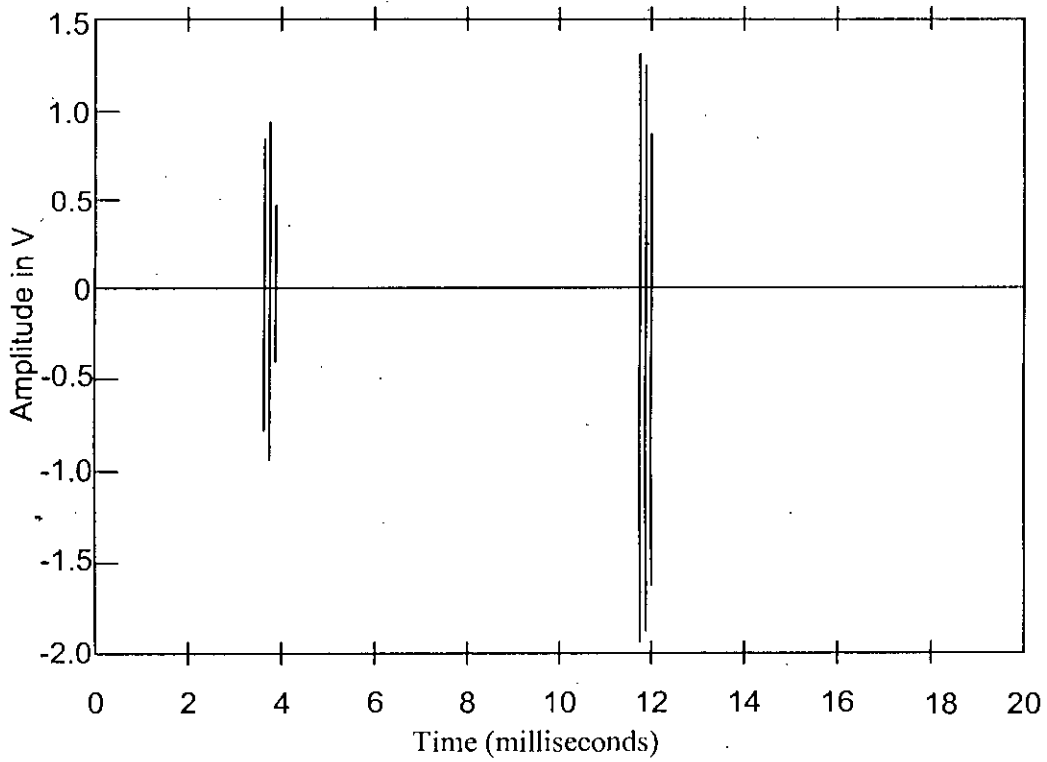
Figure 4.5: Light dimmer noise.

The synchronous impulse noise power can be given by [30]:

$$N_{SI} = \frac{1}{t_{IAT,SI}} \int_{0}^{t_{w,SI}} n_{SI}(t)^2 \, dt \qquad (4.8)$$

4.4.5 Asynchronous Impulse Noise

This type of disturbance is caused by all kinds of switching operations. Switching phenomenon causes asynchronous impulse noise. Sometimes a train of periodic synchronous impulse noise follows an asynchronous impulse in the PLC system. This disturbance affects the whole range of frequency band and its duration is very short. This is the most powerful parameter that affects PLC system performance [27]. This is a random process. Figure 4.6 shows a typical asynchronous impulse noise in power line.
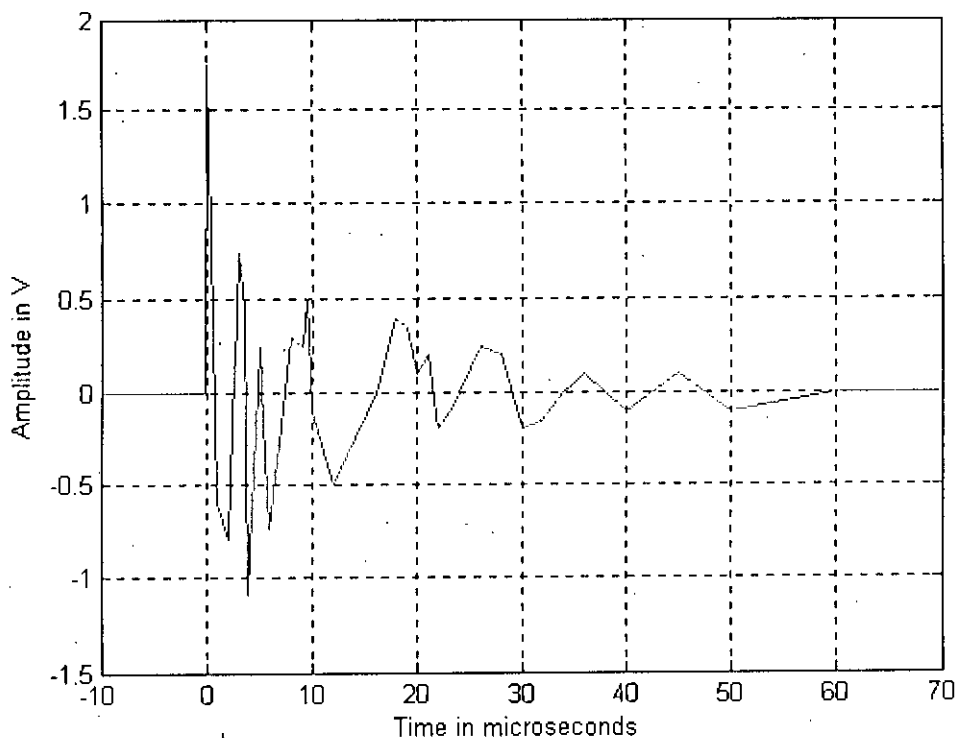
Figure 4.6: Typical asynchronous impulse noise.

Switching transients anywhere in the power line network causes typical asynchronous impulse events. The shape of the impulses is often similar to damped sinusoids or superimposed damped sinusoids. However, there is no general restriction to theses shapes; it depends on switching instance and circuit parameters. The asynchronous impulse noise power can be given by [27]:

$$N_{AI} = \frac{1}{t_{IAT,AI}} \int\limits_{0}^{t_{w,AI}} n_{AI}(t)^2 \, dt \qquad (4.9)$$

4.5 Noise Power in Power Line

In order to account for the contributions of all type of noises, we are introducing a new noise term N_{PL}. From the equation (4.1), (4.8) and (4.9) we get the average power line noise power:

$$N_{PL} = N_{BG} + N_{SI} + N_{AI} \qquad (4.10)$$

We shall use the term of N_{PL} in our performance analysis. If $n(t)$ is the amplitude of total power line noise at any instance then we define N_{PL} as follows:

$$N_{PL}(t) = n^2(t) \qquad (4.11)$$

4.6 Summary

Besides signal distortion due to interference and multipath fading, noise is the most crucial factor degrading high-speed data transmission over power line networks. Due to a considerable rise of the noise power during the occurrence of impulse events, there is a significant probability of bit errors.

In this chapter we have estimated the power line noise level by means of analytical expressions. We need huge statistics about power line noise to get better accuracy in estimating the noise level.

CHAPTER 5

DEVELOPMENT OF AN ANALYTICAL MODEL FOR THE DS-CDMA PLC SYSTEM

5.1 Introduction

In this dissertation we examine the performance of DS-CDMA system over power line channel for high-speed data. The performance of any multiple access technique depends on multiple access interference and channel noise. The indoor power line network is modeled as a multipath propagation environment, where delayed replicas of the transmitted signal reach the receiver with different amplitude and phase characteristics [26]. These multipath signal components are caused by reflections on channel discontinuities, such as termination loads and line junctions. Multipath delay spreads leads to time dispersion and frequency selective fading [16].

The Rayleigh distribution is commonly used to describe the statistical time varying nature of the envelope of an individual multipath component. In reference [15] and [17], it has been seen that the histogram of power line channel transfer function is well approximated by Rayleigh distribution. In our present work, we consider power line as a frequency selective Rayleigh fading channel.

In the previous chapter we have modeled the channel noise. We have introduced a noise term that includes the effect of all type of noises. This noise term will be used in our analytical model.

There are two key aspects for DS-CDMA systems: to combat or suppress the effects of interference due to jamming, interference arising from other users and interference due to multipath propagation, and to achieve message privacy in the presence of other listeners.

In this chapter we provide a mathematical description of an asynchronous DS-CDMA. In our analysis, we consider the BPSK modulation technique. We consider the possible presence of frequency-selective fading and the organization of the system in a power line noise structure.

We estimate system performance in terms of signal to interference ratio (SIR) and bit error rate (BER), based on the statistical description of all the channel impairments. The calculation of SIR and BER is very important for designing a communication system.

The SIR indicates the signal strength against the interference and noise. This information is used to fix the design parameters of a communication system with multiple access. The higher value of SIR ensures the reliable transmission of signal.

The term of BER is the main performance parameter of a digital communication system. This term indicates the reliability of a digital communication system. The optimum values of the design parameters can be calculated from the tolerance limit of BER.

5.2 Analytical model

In our present work, we have designed an analytical model for DS-CDMA power line communication systems. We have taken a system with K_u number of users, L number of multipath and G_p is the processing gain. Bit duration is T_b and chip duration is T_c.

We have considered a channel with frequency-selective fading which obey the Rayleigh distribution. For the calculation of multiple access interference (MAI) we have used the Gaussian approximation [16]. Figure 5.1 shows the DS-CDMA PLC system.
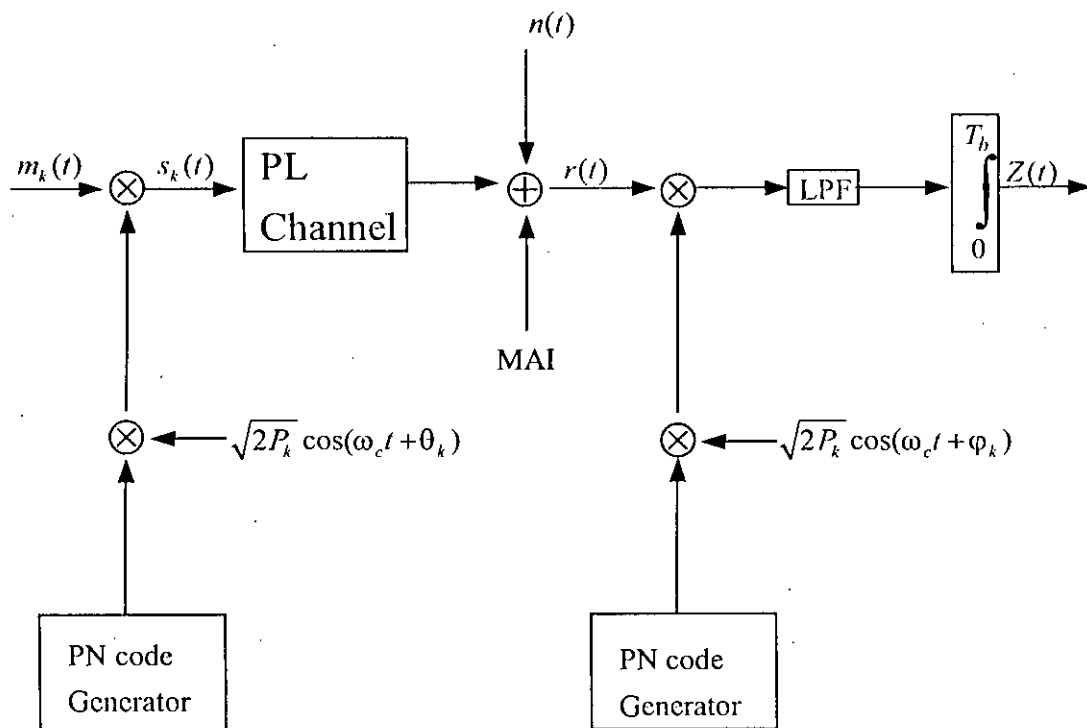
Figure 5.1: DS-CDMA PLC system

5.2.1 Transmitted signal model

Let us assume that there are K_u number of independent users transmitting signals in the DS-CDMA system. Each of them transmits a signal in the form:

$$s_k(t) = \sqrt{2P_k} m_k(t - \tau_k') c_k(t - \tau_k') \cos(\omega_c t + \theta_k) \tag{5.1}$$

where, P_k is the power of the transmitted signal, ω_c is the common carrier frequency, θ_k is a phase shift offset, $m_k(t)$ and $c_k(t)$ are the data and spreading signals respectively and τ_k' is a random transmission delay calculated with respect to

reference transmitted signal, accounting for the lack of synchronization among the users.

The data signal $m_k(t)$ is a sequence of unit amplitude rectangular pulses of duration T_b and phase 0 and π radian with equal probability. Each pulse represents an information bit for user k. The spreading signal $c_k(t)$ is a sequence of unit amplitude rectangular pulses (chips) of duration T_c and phase 0 and π radian with equal probability.

There are G_p chips per bit and thus $G_p = \dfrac{T_b}{T_c}$ is the processing gain for user k.

5.2.2 Channel model

In contrast to many other communication channels, an additive white Gaussian noise (AWGN) model can not describe the noise in a power line environment.

We consider power line channel as a frequency-selective fading channel, which generates the multipath phenomenon, that is a number of replicas of the source signal characterized by their own delays, phase rotations and Rayleigh distributed amplitudes [34].

The kth source signal is transmitted through a channel $h_k(t)$ that can be written in the form [35]:

$$h_k(t) = \sum_{l_k=0}^{L_k} a_{k,l_k} e^{j\phi_{k,l_k}} \delta(t - \tau_{k,l_k}'') \tag{5.2}$$

where ϕ_{k,l_k} and τ_{k,l_k}'' are the phases and time delays introduced by the channel; they can be assumed to be random variables uniformly distributed in $[0, 2\pi)$ and $[0, T_{max}]$ respectively, where T_{max} is the maximum delay at which there can be a multipath ray. L_k is the number of multipaths generated by the frequency selective channel for the kth transmitted signal. a_{k,l_k} is the path gain component with Rayleigh distribution:

$$f_a(a) = \frac{a}{\sigma_a^2} e^{-\frac{a^2}{2\sigma_a^2}} \tag{5.3}$$

5.2.3 Received signal model

In a CDMA system, the signals from many users arrive at the input of the receiver. Thus the received signal contains both the desired users' signals as well as the channel noise. In case of frequency selective fading channels, there are also the multipath components of both the desired interfering users. Thus, the total received signal can be written as:

$$r(t) = \sum_{k=0}^{K_u-1} \sum_{l_k=0}^{l_k-1} \sqrt{2P_k} \, a_{k,l_k} m_k(t - \tau_{k,l_k}) c_k(t - \tau_{k,l_k}) \cos(\omega_c t + \phi_{k,l_k}) + n(t) \qquad (5.4)$$

where $n(t)$ is the power line channel noise with power spectral density N_{pl}. The value of 0_k is included here into the definition of ϕ_{k,l_k}, while the values of τ_k' and τ_{k,l_k}'' are included in τ_{k,l_k}. Without loss of generality, we assume that the signal from user 0 is the signal of interest.

A correlation receiver is typically used to filter the desired user's signal from all others users' signals which share the same bandwidth at the same time. For this purpose the received signal $r(t)$ is mixed down to baseband, multiplied by the spreading sequence associated to the desired user ($c_0(t)$) and integrated over one bit period. This sequence of operations is called despreading. Thus, assuming that the receiver is delay and phase synchronized with the main multipath component of the signal of interest, the bit decision statistics for that user within the bit interval $[lT_b, (l+1)T_b]$ is given by [36]:

$$Z_0(l) = \int_{lT_b}^{(l+1)T_b} r(t) c_0(t - \tau_{0,0}) \cos(\omega_c t) dt$$

$$= m_0(l) a_{0,0} \sqrt{\frac{P_0}{2}} T_b + \sum_{k=0}^{K_u-1} \sum_{[l_k=0,l_0 \neq 0]}^{l_k-1} I_{k,l_k} + \upsilon \qquad (5.5)$$

where $m_0(l)$ is the lth transmitted bit from the source 0.

Useful signal is given by:

$$D_0(l) = m_0(l)a_{0,0}\sqrt{\frac{P_0}{2}}T_b$$

(5.6)

Noise term is given by:

$$\upsilon = \int_{lT_b}^{(l+1)T_b} n(t)c_0(t-\tau_{0,0})\cos(\omega_c t)dt$$

(5.7)

and the summation is given by,

$$I \triangleq \sum_{k=0}^{K_u-1} \sum_{[l_k=0,l_0\neq 0]}^{L_k-1} I_{k,l_k}$$

$$\triangleq \sum_{k=0}^{K_u-1} \sum_{[l_k=0,l_0\neq 0]}^{L_k-1} \int_{lT_b}^{(l+1)T_b} a_{k,l_k}s_k(t-\tau_{k,l_k})e^{j\phi_{k,l_k}}c_0(t-\tau_{0,0})\cos(\omega_c t)dt$$

(5.8)

I Represents the contribution of MAI to the decision statistics. It is worth to notice that the MAI term includes:

-   all the multipath components relative to the desired user: $I_{0,1}$..........I_{0,l_0-1}, while the (0,0) component is the direct ray;

-   all the direct and multipath components relative to the interfering users: $I_{k,0}$..........I_{k,l_k-1} for all $k=1,2,...............K_u-1$.

Thus the decision statistics defined in (5.5) can be re-written as:

$$Z_0(l) = D_0(l)+I+\upsilon$$

(5.9)

where $D_0(l)$ is the desired signal component (first term in (5.5)), I is the MAI (5.7) and υ is the channel noise term (5.6).

5.3 Analysis of signal to interference ratio (SIR) and bit error rate (BER)

In any multiple access system, one of the fundamental design parameter is the signal-to-interference (SIR) at the receiver, which measures the ratio between the useful power and the amount of interference generated by all the other sources sharing the same resource.

Recalling the expression (5.8), it is easy to express the SIR:

$$SIR = \frac{E\{D_0(l)^2\}}{E\{I^2\} + E\{\upsilon^2\}}$$

(5.10)

The statistical averages in equation (5.9) can be calculated as follows for the useful term [17]:

$$E\{D_0(l)^2\} = E\{(m_0(l)\sqrt{\frac{P_0}{2}}a_{0,0}T_b)^2\}$$

$$= \frac{P_0 T_b^2}{2}E\{a_{0,0}^2\}$$

(5.11)

By maintaining the conditioning on the path gain $a_{0,0}$, we get

$$E\{D_0(l)^2 \mid a_{0,0}\} = \frac{P_0 T_b^2}{2}a_{0,0}^2$$

(5.12)

By using Gaussian Approximation, for a frequency-selective Rayleigh fading channel, variance of interference caused by the interfering components can be calculated as follows [35], [16]:

We assume perfect power control and identical L number of paths is available for each user. We want to receive signal from the desired user through a single path. Variance of interference for 0th path is given by:

$$E\{\sum I^2{}_{k0,0}\} = (K_u - 1)\frac{P_0^2 T_b^2}{6G_p} E\{a^2{}_{k0,0}\} \tag{5.13}$$

Variance of interference for the rest of the $L-1$ paths is given by:

$$E\{\sum I^2{}_{k0,lk0}\} = (L-1)K_u \frac{P_0^2 T_b^2}{6G_p} E\{a^2{}_{k0,lk0}\} \tag{5.14}$$

By adding the equation (5.12) and (5.13) we get the variance of interference [26]:

$$E\{I^2\} = E\{a^2{}_{k0,0}\}(K_u - 1)\frac{P_0^2 T_b^2}{6G_p} + E\{a^2{}_{k0,lk0}\}(L-1)K_u \frac{P_0^2 T_b^2}{6G_p}$$

$$\Rightarrow E\{I^2\} = \frac{P_0 T_b^2}{6G_p}[E\{a^2{}_{k0,0}\}(K_u - 1) + K_u(L-1)E\{a^2{}_{k0,lk0}\}] \tag{5.15}$$

where, $a_{k0,lk0}$ are the path gains which are identically Rayleigh distributed, and P_0 is the transmitted signal power.

By applying the properties of Rayleigh distribution we get:

$$E\{a_{k0,0}{}^2\} = E\{a_{k0,lk0}{}^2\} = 2\sigma^2 \tag{5.16}$$

where σ is the variance of path gain components over the power line channel with frequency selective Rayleigh fading.

Hence, we can rewrite the equation (5.15) as:

$$E\{I^2\} = \frac{P_0 T_b^2 \sigma^2}{3G_p}(K_u L - 1) \tag{5.17}$$

The noise term $E\{\upsilon^2\}$ can be expressed as [16]:

$$E\{\upsilon^2\} = \int_0^{T_b} n^2(t) c_0^2(t) \cos^2(\omega_c t) dt$$

$$\approx \frac{N_{PL} T_b}{2} \qquad (5.18)$$

where N_{PL} is the average power line noise power.

Hence we get the equation (5.10) as:

$$SIR\big|_{a_{0,0}} = \frac{\dfrac{P_0 T_b^2}{2} a_{0,0}^2}{\dfrac{P_0 T_b^2 \sigma^2}{3 G_p}(K_u L - 1) + \dfrac{N_{PL} T_b}{2}} \qquad (5.19)$$

Then, averaging over the distribution of $a_{0,0}$, the average signal-to-interference ratio for a power line channel is given by:

$$\Gamma = \frac{1}{\dfrac{(K_u L - 1)}{3 G_p} + \dfrac{N_{PL}}{2\sigma^2 P_0 T_b}} \qquad (5.20a)$$

$$\Rightarrow \Gamma = \frac{1}{\dfrac{K_u L - 1}{3 G_p} + \dfrac{N_{PL}}{2\sigma^2 E_b}} \qquad (5.20b)$$

Equation (5.20b) can be considered as a modified version of the following equation,

$$\Rightarrow \Gamma = \cfrac{1}{\cfrac{K_u L - 1}{3G_p} + \cfrac{N_0}{4\sigma^2 E_b}} \qquad (5.20c)$$

where, energy per bit is given by, $E_b = P_0 T_b$ \qquad (5.21)

Equation (5.20c) is a common expression, which is used for wireless channel with AWGN and frequency selective Rayleigh fading [37]. Where $\frac{N_0}{2}$ is the average power of additive white gaussian noise (AWGN). In chapter 4, it has been shown that power line noise can not be considered as AWGN. We can use a power line noise term N_{PL} instead of $\frac{N_0}{2}$, which has been introduced in chapter 4.

The dissimilarities of SIR expressed by equation (5.20b) and equation (5.21c) are to be noted. The denominators of the two expressions have a common first term $\frac{K_u L - 1}{3G_p}$. But the second terms in the two denominators are different. In the case of wireless transmission, average $\text{AWGN} = \frac{N_0}{2}$ with a flat power spectral density (PSD) is assumed. In the case of power line, N_{PL} is not a noise of the Gaussian type. It is the average value of noise power arising from combined colored background and impulse type of noises, which are actually observed in a power line.

The average bit-error-rate is given by [19],[37]:

$$BER = \frac{1}{2}\left[1 - \sqrt{\frac{\Gamma}{2 + \Gamma}} \right]$$

$$= \frac{1}{2}\left[1 - \sqrt{\cfrac{1}{1 + 2\left(\cfrac{K_u L - 1}{3G_p} + \cfrac{N_{PL} R_b}{2\sigma^2 P_0} \right)}} \right] \qquad (5.22)$$

Equation (5.22) is valid only for correlation receiver with BPSK modulation scheme.

5.4 Performance Analysis for RAKE Receiver

RAKE receiver is used to exploit multipath propagation of information signals. We can consider a RAKE receiver with L fingers for L paths in our system.
The over all signal-to-interference ratio is then [35],

$$SIR_{RAKE} = \frac{\sum_{l_0=0}^{L-1} a_{0,l_0}^2}{\frac{2\sigma^2(K_u L - 1)}{3G_p} + \frac{N_{PL}R_b}{P_0}}$$

$$SIR_{RAKE} = \frac{L}{\frac{K_u L - 1}{3G_p} + \frac{N_{PL}R_b}{2\sigma^2 P_0}} \tag{5.23a}$$

$$SIR_{RAKE} = L\Gamma \tag{5.23b}$$

The average bit-error-rate for RAKE receiver with frequency selective Rayleigh fading channel is given by [38]:

$$BER_{RAKE} = \int_0^\infty Q(\sqrt{x}) f(x) dx \tag{5.24}$$

Where x is a chi-square-distributed random variable with $2L$ degrees of freedom and average Γ, and

$$f(x) = \frac{1}{(L-1)! \Gamma^{-L}} x^{L-1} e^{-\frac{x}{\Gamma}} \tag{5.25}$$

For a RAKE receiver of L fingers for L path, the average bit-error-rate (BER) is given by,

$$BER_{RAKE} = \left[\frac{1}{2}\left(1-\sqrt{\frac{\Gamma}{2+\Gamma}}\right)\right]^L \binom{2L-1}{L}\left[\frac{1}{2}\left(1+\sqrt{\frac{\Gamma}{2+\Gamma}}\right)\right]^L$$

$$= \binom{2L-1}{L}\left[\frac{1}{4}\left(1-\frac{\Gamma}{2+\Gamma}\right)\right]^L$$

$$= \binom{2L-1}{L}\left[\frac{1}{2(2+\Gamma)}\right]^L \tag{5.26a}$$

$$BER_{RAKE} = \binom{2L-1}{L}\left[\cfrac{1}{2\left(2+\cfrac{1}{\cfrac{K_uL-1}{3G_p}+\cfrac{N_{PL}R_b}{2\sigma^2 P_0}}\right)}\right]^L \tag{5.26b}$$

5.5 Summary

In this chapter the analytical model for the PLC channel has been developed and expressed with all the useful terms. The reason for choosing power line as a frequency selective fading channel is also explained. We have derived the expressions for SIR and BER.

CHAPTER 6

PERFORMANCE ANALYSIS AND DISCUSSIONS

6.1 Introduction

The performance issues of any multiple access technique are directly related to the number of users. Thus, the performance of a multiple access technique measures the number of simultaneous users who are facilitated with communication services under an acceptable level of bit error rate (BER).

Following the analytical formulation presented in section 5.3 and 5.4 we evaluate the performance of DS-CDMA PLC system at a chip rate of 10.24 Mchips/sec, using variance of path gain $\sigma^2 = 0.45$. We assume that transmitted signal power is $1V^2$, according to FCC specification for high-speed data transmission over power line channel. We present the impact of power line noise and the impact of multipath propagation with SIR and BER characteristics.

We use equation (5.20b), (5.23a) to calculate SIR and (5.22), (5.26b) to calculate BER. We measure the performance parameters by the number of simultaneous users. These parameters have been calculated by MATLAB 6.5.

The impact of power line noise is evaluated by the SIR and BER curves considering different scenarios: $G_p = 256, R_b = 40 Kbps$ for Correlation receiver; $G_p = 128, R_b = 80 Kbps$ for Correlation receiver; $G_p = 64, R_b = 160 Kbps$ for Correlation receiver; $G_p = 256, R_b = 40 Kbps$ for RAKE receiver; $G_p = 128, R_b = 80 Kbps$ for RAKE receiver; and $G_p = 64, R_b = 160 Kbps$ for RAKE receiver. We also compare SIR and BER performance of Correlation and RAKE receiver under same noise level.

The impact of multipath propagation is evaluated by the SIR and BER curves considering different scenarios: $G_p = 256, R_b = 40 Kbps$ for Correlation receiver; $G_p = 128, R_b = 80 Kbps$ for Correlation receiver; $G_p = 64. R_b = 160 Kbps$ for Correlation receiver; $G_p = 256, R_b = 40 Kbps$ for RAKE receiver; $G_p = 128, R_b = 80 Kbps$ for RAKE receiver; and $G_p = 64, R_b = 160 Kbps$ for RAKE receiver. We also compare SIR and BER performance of Correlation and RAKE receiver under same number of multipath.

6.2. Impact of Power Line Noise

From the residential power line noise survey results in [40], we observe that average power line noise power can vary from −170 dB to −26 dB. In previous references [8-14], power line noise were considered between −85 dB and −35 dB. In our case a noise level below −90 dB has no significant impact on the system performance.

Figure 6.1 to Figure 6.6 depict the plots of SIR versus number of simultaneous users (K_u) under different combinations of R_b, G_p and receiver with the values of noise power N_{PL} as -50 dB, -60 dB, -70 dB and -90 dB. For all the cases we consider the number of available path $L = 2$.

Figure 6.7 depicts the comparative SIR performance of Correlation and RAKE receiver.

Figure 6.8 to Figure 6.13 depict the plots of BER versus number of simultaneous users (K_u) under different combinations of R_b, G_p and receiver with the values of N_{PL} as -50 dB, -60 dB, -70 dB and -90 dB. For all the cases we consider the number of available path $L = 2$.

Figure 6.14 depicts the comparative BER performance of Correlation and RAKE receiver.

Figure 6.1 depicts the various plots of signal to interference ratio (SIR) as a function of power line noise, N_{PL}, for the bit rate, $R_b = 40 Kbps$ and the processing gain $G_p = 256$ with Correlation receiver. The SIR increases exponentially with the decrease of power line noise. The system shows good signal strength between noise levels −90 dB and −70 dB.

Figure 6.1: Plots of signal to interference ratio (SIR) versus various number of users in a direct sequence CDMA PLC system for different values of power line noise, N_{PL}, in case of Correlation receiver with bit rate $R_b = 40 Kbps$ and processing gain $G_p = 256$, at a chip rate 10.24 Mchips/sec with transmitted signal power $P_0 = 1 \text{ V}^2$ and $\sigma^2 = 0.45$.

Figure 6.2 depicts the various plots of signal to interference ratio (SIR) as a function of power line noise, N_{PL}, for the bit rate, $R_b = 80 Kbps$ and the processing gain $G_p = 128$ with Correlation receiver. The SIR increases exponentially with the decrease of power line noise. The system shows good signal strength between noise levels –90 dB and –70 dB.

Figure 6.2: Plots of signal to interference ratio (SIR) versus various number of users in a direct sequence CDMA PLC system for different values of power line noise, N_{PL}, in case of <u>Correlation receiver</u> with bit rate $R_b = 80 Kbps$ and processing gain $G_p = 128$, at a chip rate 10.24 Mchips/sec with transmitted signal power $P_0 = 1 \text{ V}^2$ and $\sigma^2 = 0.45$.

Figure 6.3 depicts the various plots of signal to interference ratio (SIR) as a function of power line noise, N_{PL}, for the bit rate, $R_b = 160 Kbps$ and the processing gain $G_p = 64$ with Correlation receiver. The SIR increases exponentially with the decrease of power line noise. The system shows poor signal strength between noise levels −70 dB and above.
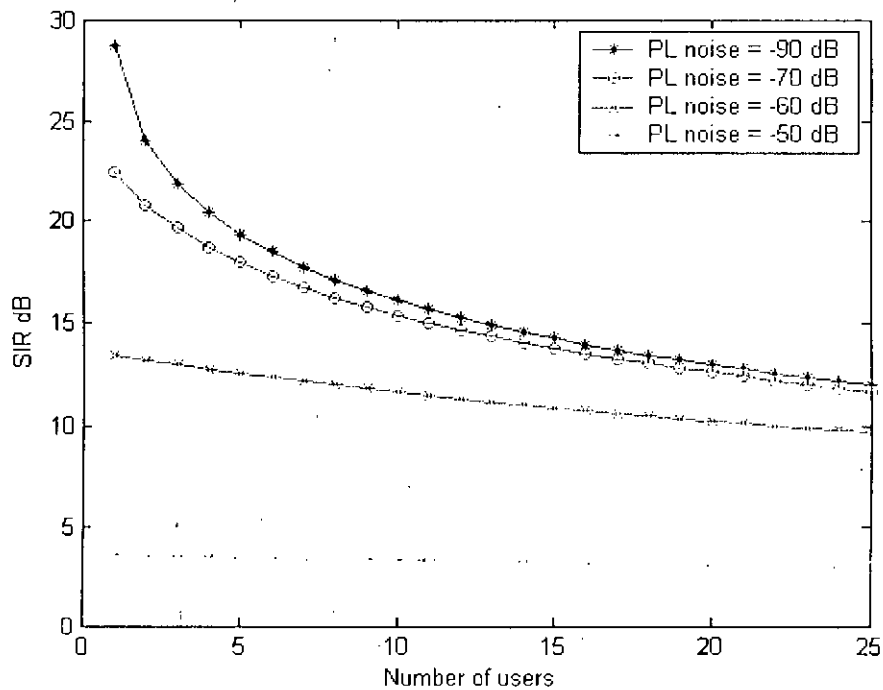

Figure 6.3: Plots of signal to interference ratio (SIR) versus various number of users in a direct sequence CDMA PLC system for different values of power line noise, N_{PL}, in case of <u>Correlation receiver</u> with bit rate $R_b = 160 Kbps$ and processing gain $G_p = 64$, at a chip rate 10.24 Mchips/sec with transmitted signal power $P_0 = 1 \ V^2$ and $\sigma^2 = 0.45$.

Figure 6.4 depicts the various plots of signal to interference ratio (SIR) as a function of power line noise, N_{PL}, for the bit rate, $R_b = 40 Kbps$ and the processing gain $G_p = 256$ with RAKE receiver. The SIR increases exponentially with the decrease of power line noise. The system shows good signal strength below levels –60 dB.
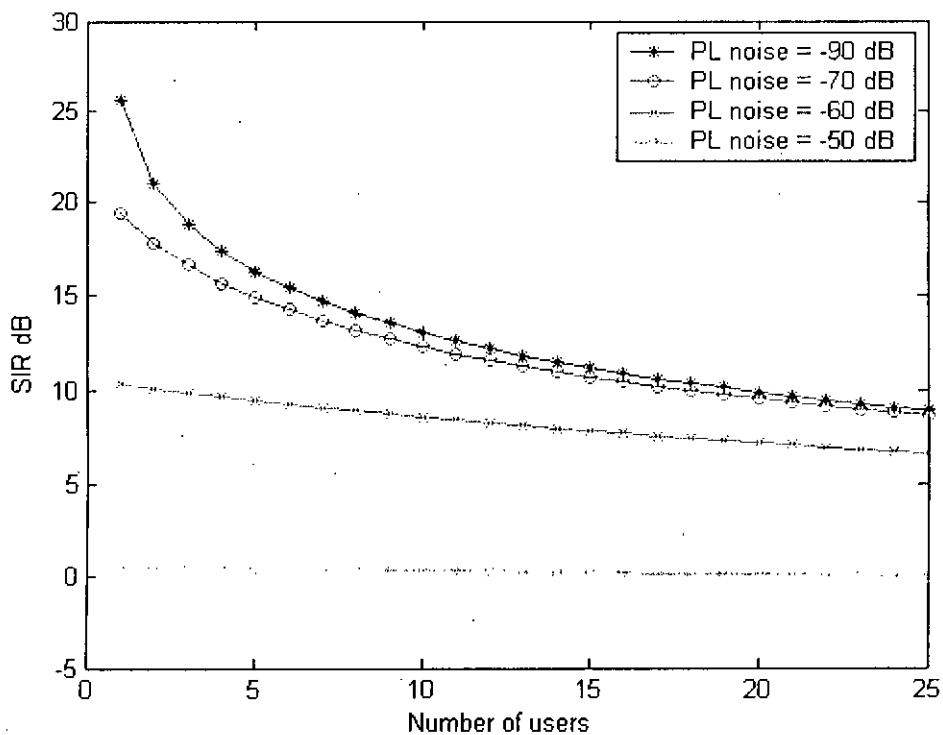

Figure 6.4: Plots of signal to interference ratio (SIR) versus various number of users in a direct sequence CDMA PLC system for different values of power line noise, N_{PL}, in case of RAKE receiver with bit rate $R_b = 40 Kbps$ and processing gain $G_p = 256$, at a chip rate 10.24 Mchips/sec with transmitted signal power $P_0 = 1\ V^2$ and $\sigma^2 = 0.45$.

Figure 6.5 depicts the various plots of signal to interference ratio (SIR) as a function of power line noise, N_{PL}, for the bit rate, $R_b = 80Kbps$ and the processing gain $G_p = 128$ with RAKE receiver. The SIR increases exponentially with the decrease of power line noise. The system shows good signal strength between noise levels -90 dB and -70 dB.
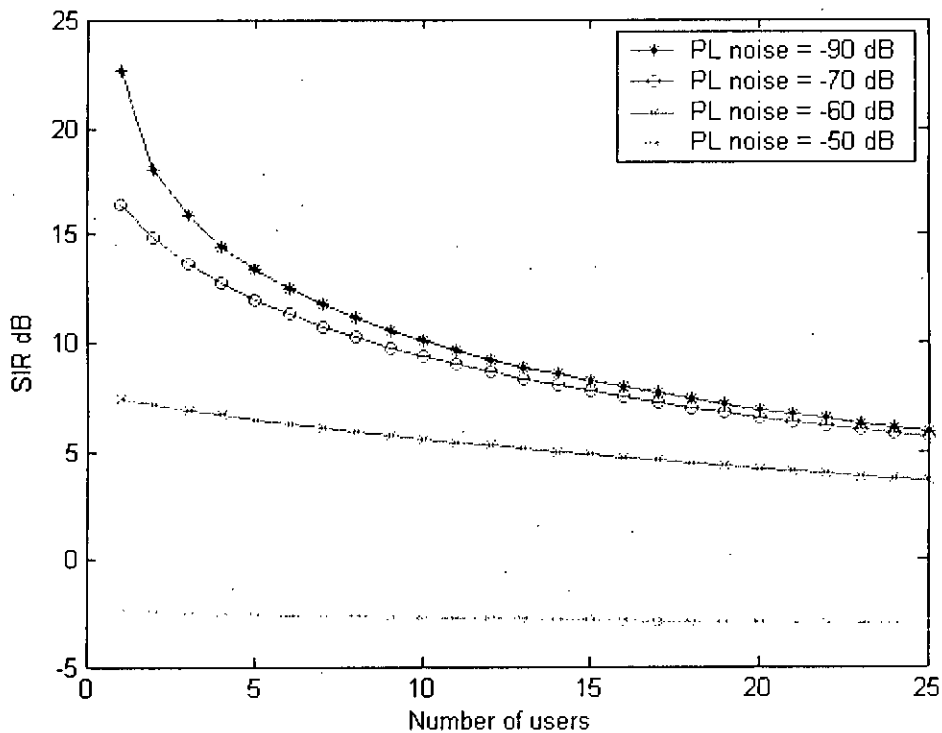

Figure 6.5: Plots of signal to interference ratio (SIR) versus various number of users in a direct sequence CDMA PLC system for different values of power line noise, N_{PL}, in case of RAKE receiver with bit rate $R_b = 80Kbps$ and processing gain $G_p = 128$, at a chip rate 10.24 Mchips/sec with transmitted signal power $P_0 = 1$ V^2 and $\sigma^2 = 0.45$.

Figure 6.6 depicts the various plots of signal to interference ratio (SIR) as a function of power line noise, N_{PL}, for the bit rate, $R_b = 160 Kbps$ and the processing gain $G_p = 64$ with RAKE receiver. The SIR increases exponentially with the decrease of power line noise. The system shows poor signal strength between noise levels −60 dB and above.
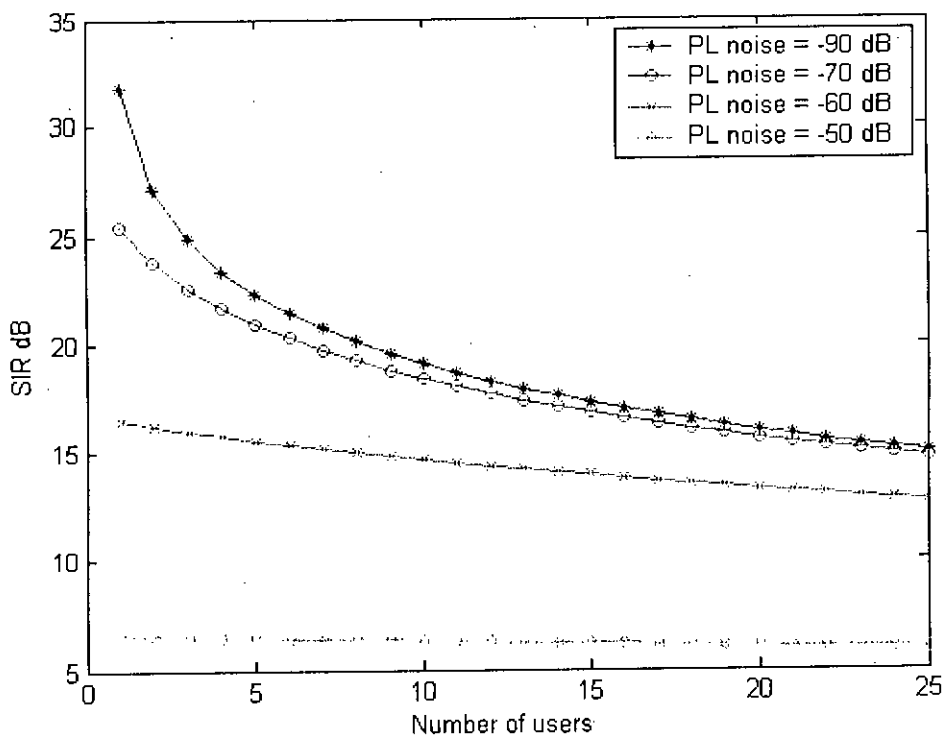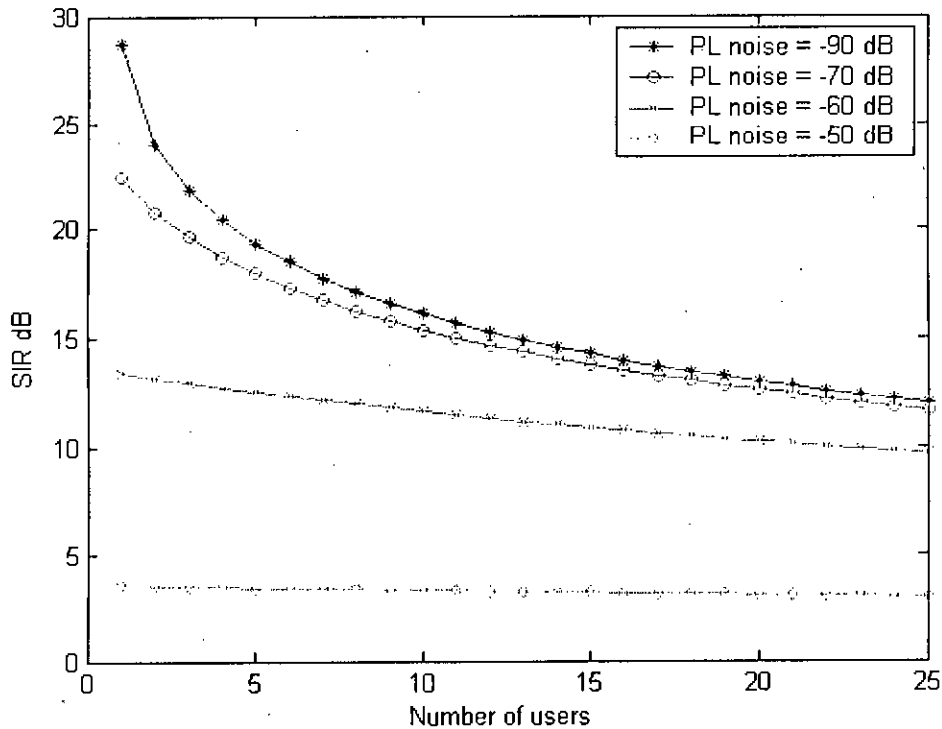

Figure 6.6: Plots of signal to interference ratio (SIR) versus various number of users in a direct sequence CDMA PLC system for different values of power line noise, N_{PL}, in case of RAKE receiver with bit rate $R_b = 160 Kbps$ and processing gain $G_p = 64$, at a chip rate 10.24 Mchips/sec with transmitted signal power $P_0 = 1$ V^2 and $\sigma^2 = 0.45$.

Figure 6.7 depicts the comparative signal to interference ratio (SIR) plots for Correlation and RAKE receiver as a function of power line noise, N_{PL}, for the bit rate, $R_b = 40 Kbps$ and the processing gain $G_p = 256$. We observe that using a RAKE receiver the SIR of the system are better than a Correlation receiver.
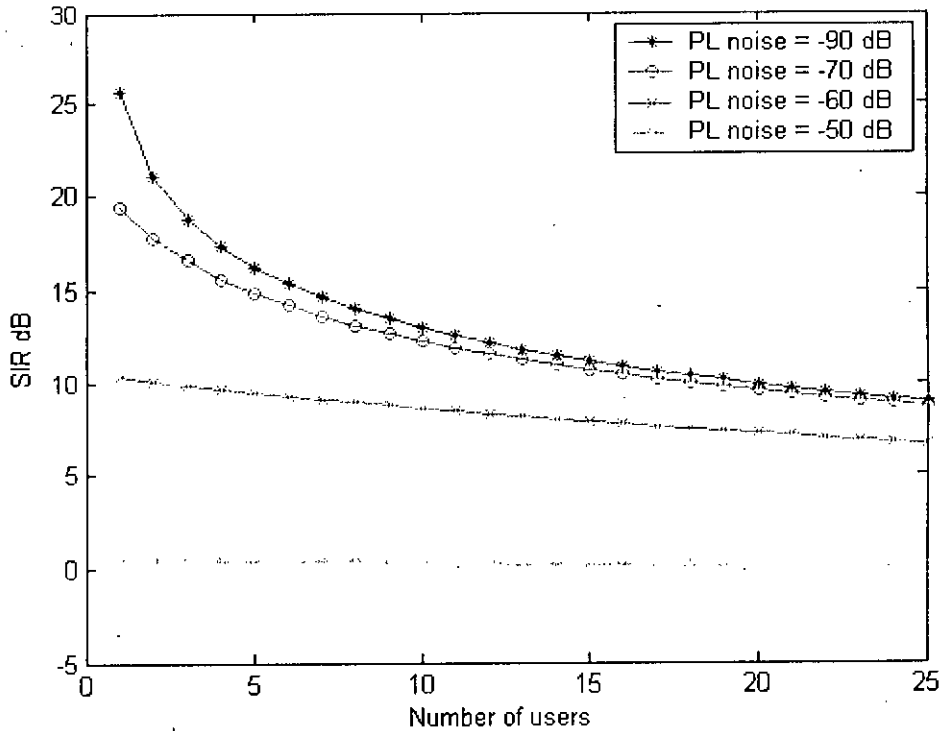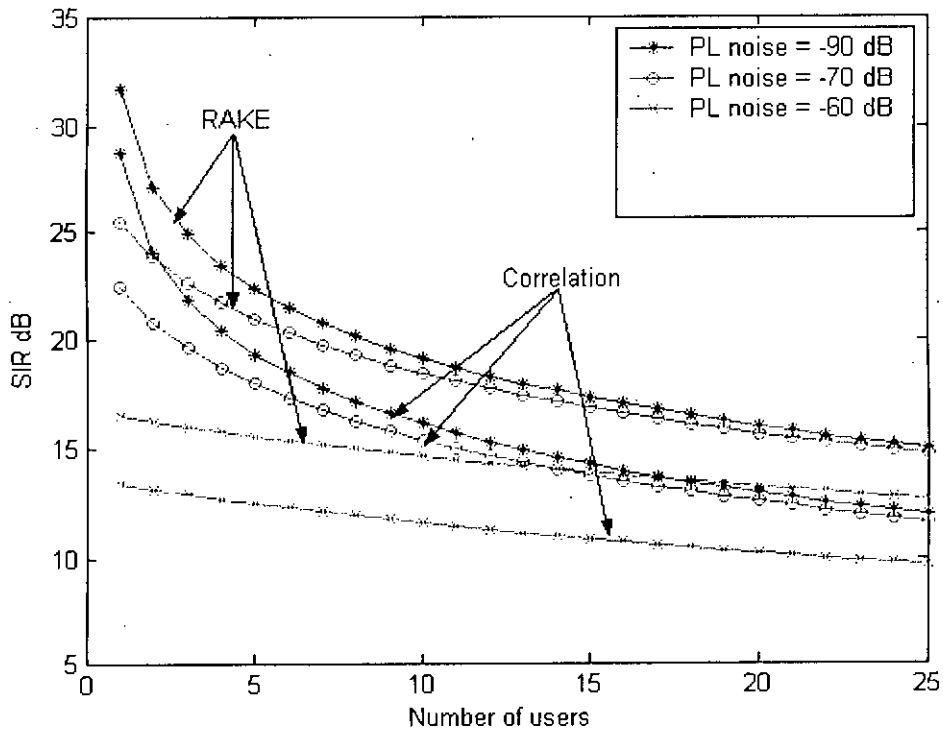

Figure 6.7: Plots of comparative signal to interference ratio (SIR) versus various number of users in a direct sequence CDMA PLC system for different values of power line noise, N_{PL}, in case of RAKE receiver with bit rate $R_b = 40 Kbps$ and processing gain $G_p = 256$, at a chip rate 10.24 Mchips/sec with transmitted signal power $P_0 = 1$ V^2 and $\sigma^2 = 0.45$.

Figure 6.8 depicts the various plots of bit error rate (BER) as a function of power line noise, N_{PL}, for the bit rate, $R_b = 40 Kbps$ and the processing gain $G_p = 256$ with Correlation receiver. The BER decreases exponentially with the decrease of power line noise. The system shows poor performance for noise level above –70 dB.

Figure 6.8: The bit error rate (BER) performance against number of users of a direct sequence CDMA PLC system for different values of power line noise, N_{PL}, in case of Correlation receiver with bit rate $R_b = 40 Kbps$ and processing gain $G_p = 256$, at a chip rate 10.24 Mchips/sec with transmitted signal power $P_0 = 1 \ V^2$, and $\sigma^2 = 0.45$.

Figure 6.9 depicts the various plots of bit error rate (BER) as a function of power line noise, N_{PL}, for the bit rate, $R_b = 80Kbps$ and the processing gain $G_p = 128$ with Correlation receiver. The BER decreases exponentially with the decrease of power line noise. The system shows poor performance for noise level above –90 dB.

Figure 6.9: The bit error rate (BER) performance against number of users of a direct sequence CDMA PLC system for different values of power line noise, N_{PL}, in case of Correlation receiver with bit rate $R_b = 80Kbps$ and processing gain $G_p = 128$, at a chip rate 10.24 Mchips/sec with transmitted signal power $P_0 = 1 \text{ V}^2$, and $\sigma^2 = 0.45$.

Figure 6.10 depicts the various plots of bit error rate (BER) as a function of power line noise, N_{PL}, for the bit rate, $R_b = 160 Kbps$ and the processing gain $G_p = 64$ with Correlation receiver. The BER decreases exponentially with the decrease of power line noise. The system shows very poor performance for noise level above -90 dB.
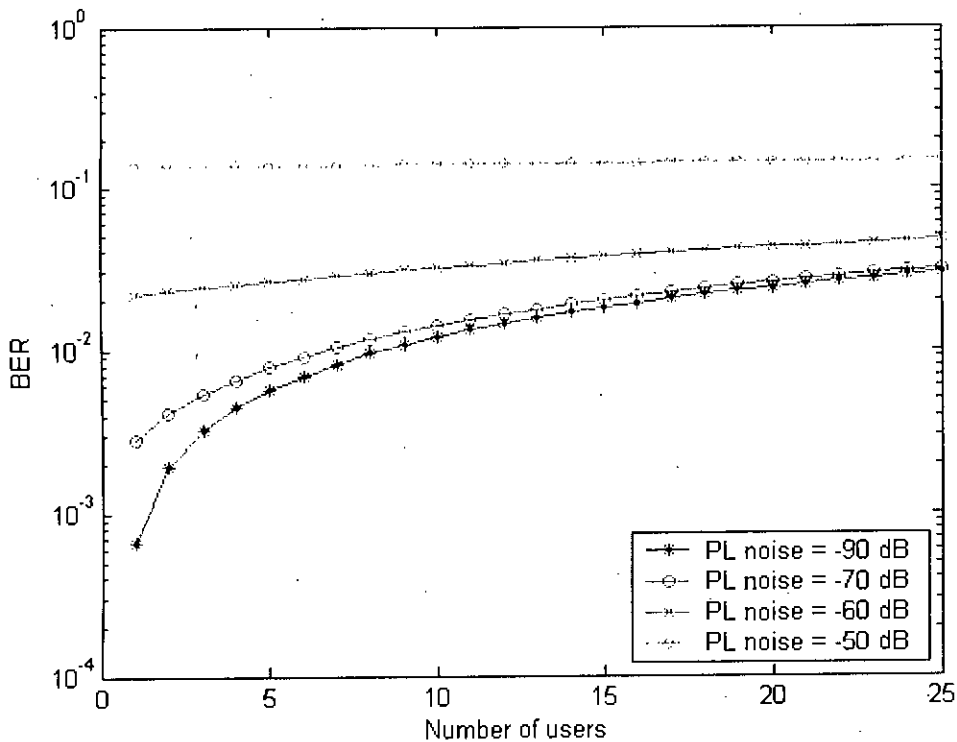

Figure 6.10: The bit error rate (BER) performance against number of users of a direct sequence CDMA PLC system for different values of power line noise, N_{PL}, in case of Correlation receiver with bit rate $R_b = 160 Kbps$ and processing gain $G_p = 64$, at a chip rate 10.24 Mchips/sec with transmitted signal power $P_0 = 1$ V^2, and $\sigma^2 = 0.45$.

Figure 6.11 depicts the various plots of bit error rate (BER) as a function of power line noise, N_{PL}, for the bit rate, $R_b = 40Kbps$ and the processing gain $G_p = 256$ with RAKE receiver. The BER decreases exponentially with the decrease of power line noise. The system shows good performance for noise level below −60 dB.
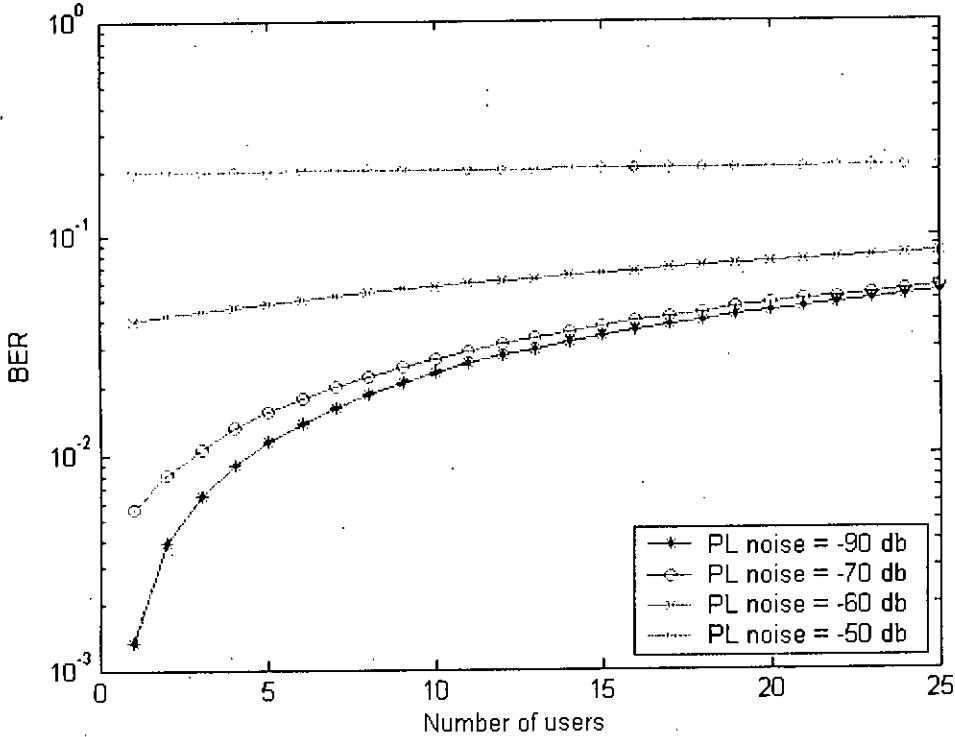

Figure 6.11: The bit error rate (BER) performance against number of users of a direct sequence CDMA PLC system for different values of power line noise, N_{PL}, in case of RAKE receiver with bit rate $R_b = 40Kbps$ and processing gain $G_p = 256$, at a chip rate 10.24 Mchips/sec with transmitted signal power $P_0 = 1$ V^2, and $\sigma^2 = 0.45$.

Figure 6.12 depicts the various plots of bit error rate (BER) as a function of power line noise, N_{PL}, for the bit rate, $R_b = 80Kbps$ and the processing gain $G_p = 128$ with RAKE receiver. The BER decreases exponentially with the decrease of power line noise. The system shows good performance for noise level below −70 dB.

Figure 6.12: The bit error rate (BER) performance against number of users of a direct sequence CDMA PLC system for different values of power line noise, N_{PL}, in case of RAKE receiver with bit rate $R_b = 80Kbps$ and processing gain $G_p = 128$, at a chip rate 10.24 Mchips/sec with transmitted signal power $P_0 = 1 \text{ V}^2$, and $\sigma^2 = 0.45$.

Figure 6.13 depicts the various plots of bit error rate (BER) as a function of power line noise, N_{PL}, for the bit rate, $R_b = 160 Kbps$ and the processing gain $G_p = 64$ with RAKE receiver. The BER decreases exponentially with the decrease of power line noise. The system shows good performance for noise level below -90 dB.
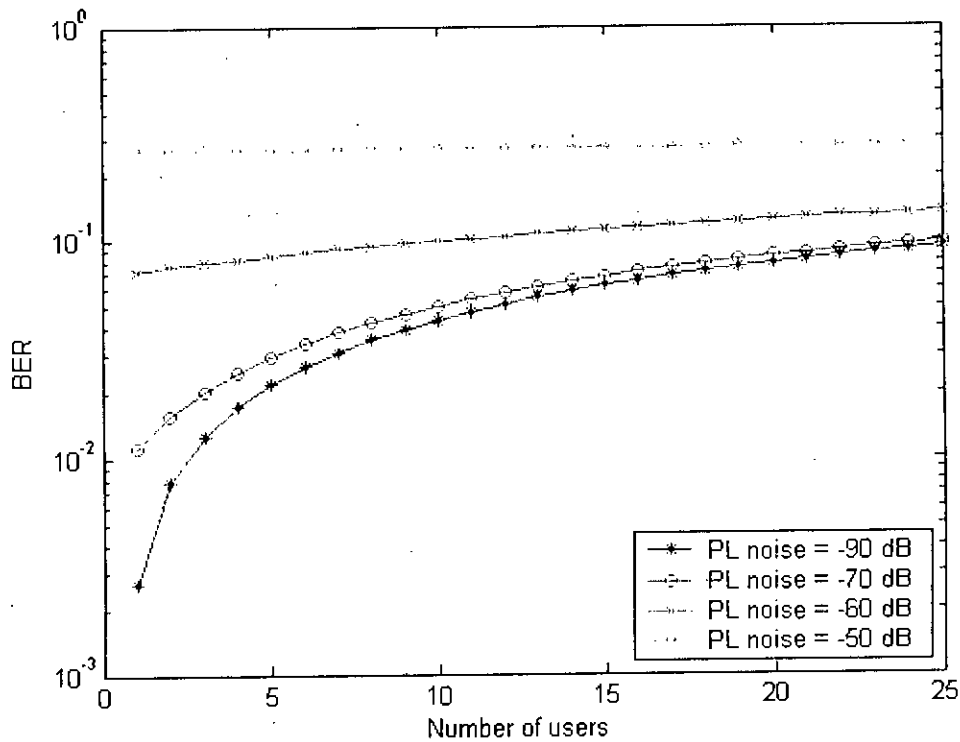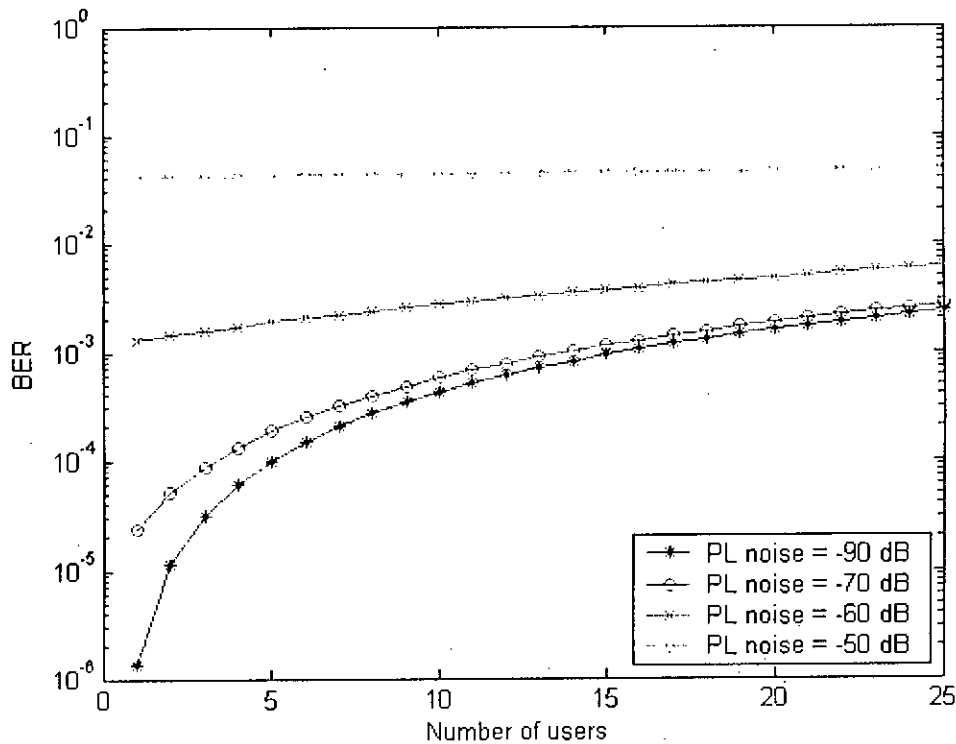

Figure 6.13: The bit error rate (BER) performance against number of users of a direct sequence CDMA PLC system for different values of power line noise, N_{PL}, in case of RAKE receiver with bit rate $R_b = 160 Kbps$ and processing gain $G_p = 64$, at a chip rate 10.24 Mchips/sec with transmitted signal power $P_0 = 1\ \text{V}^2$, and $\sigma^2 = 0.45$.

Figure 6.14 depicts the comparative bit error rate (BER) plots for Correlation and RAKE receiver as a function of power line noise, N_{PL}, for the bit rate, $R_b = 40Kbps$ and the processing gain $G_p = 256$. We observe that using a RAKE receiver the performance of the system are better than a Correlation receiver.

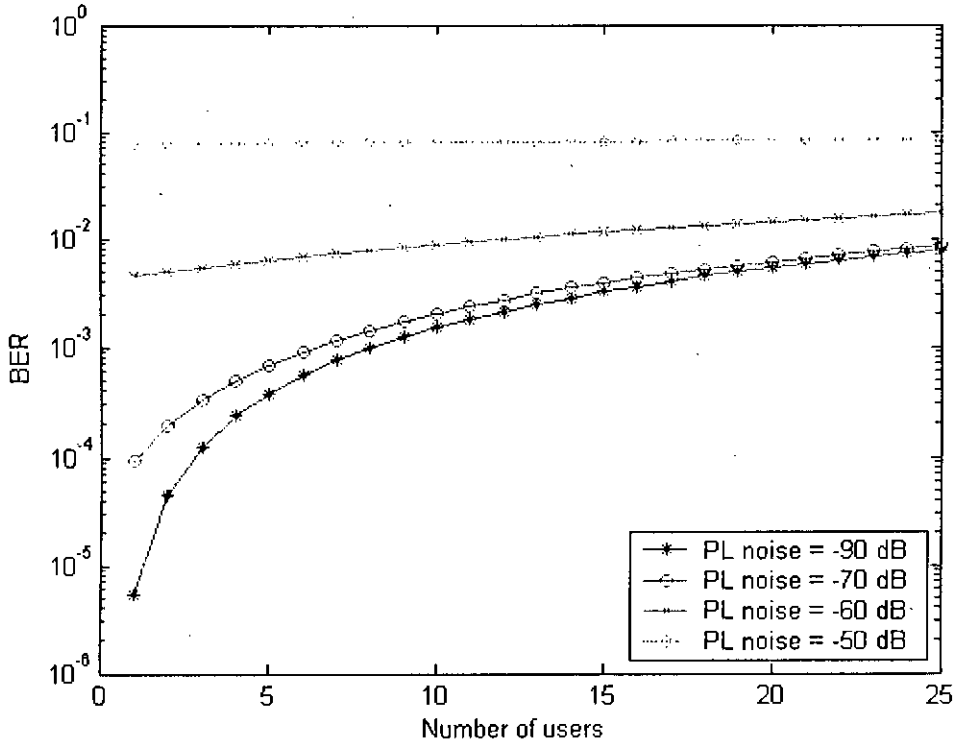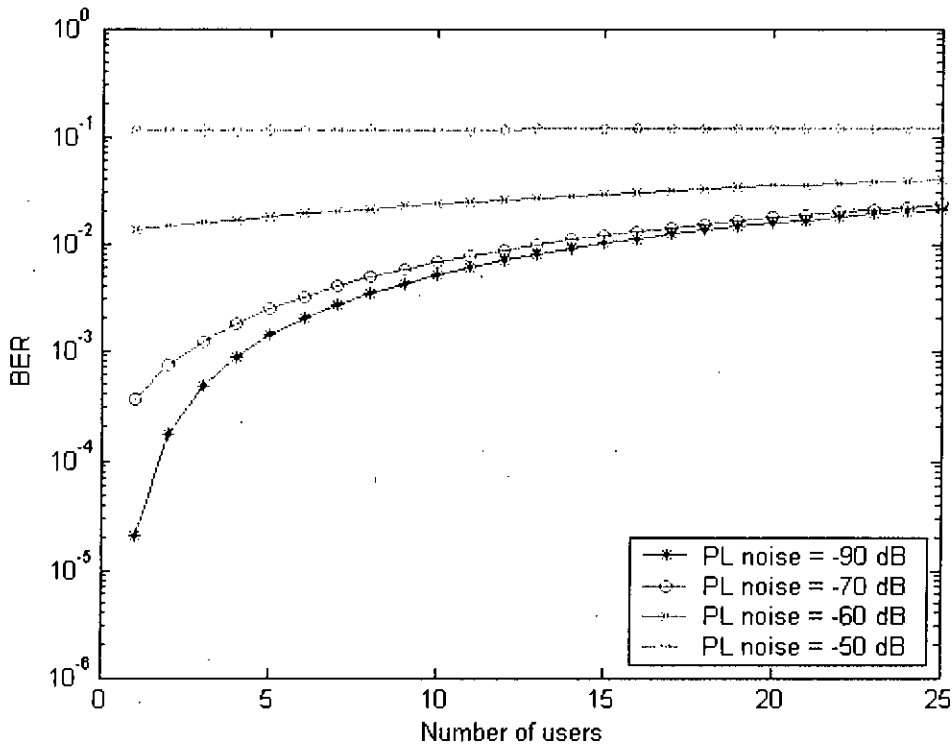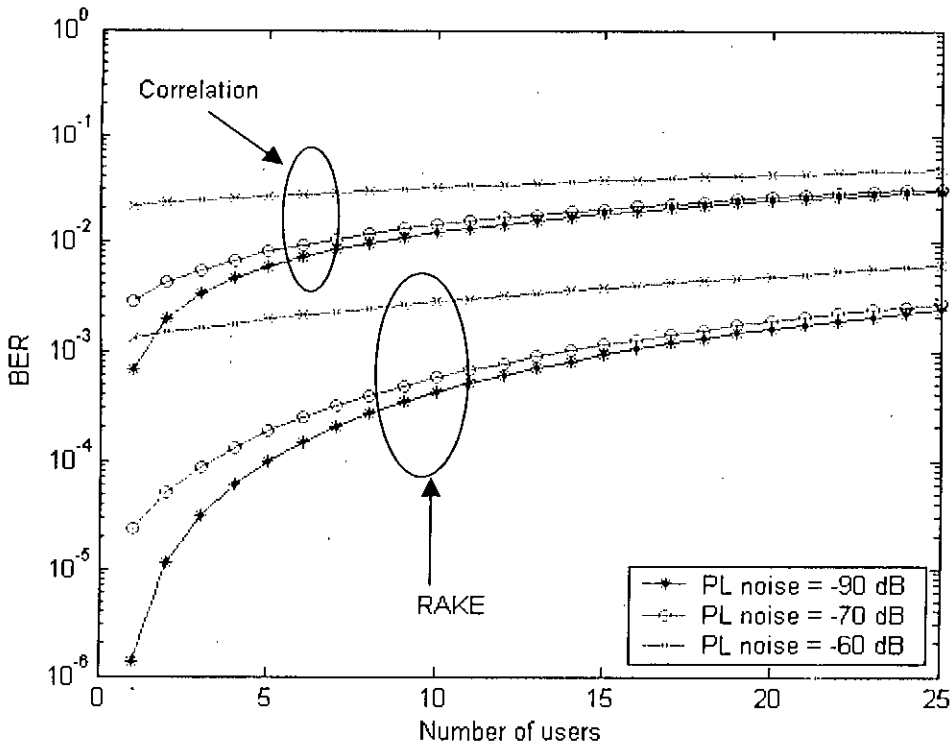Figure 6.14: Plots of comparative bit error rate (BER) versus various number of users in a direct sequence CDMA PLC system for different values of power line noise, N_{PL}, in case of RAKE receiver with bit rate $R_b = 40Kbps$ and processing gain $G_p = 256$, at a chip rate 10.24 Mchips/sec with transmitted signal power $P_0 = 1$ V^2 and $\sigma^2 = 0.45$.

6.3 Impact of Multipath

Theoretically infinite number of path is possible in power line but dominant paths are limited. In CDMA wireless communication standard IS-95, only three paths are considered. In current research, we consider maximum four paths in our analysis.

Figure 6.15 to Figure 6.20 depict the plots of SIR versus number of simultaneous users (K_u) under different combinations of R_b, G_p and receiver with the values of L as 1, 2, 3 and 4. For all the cases we consider the power line noise level −90dB.

Figure 6.21 depicts the comparative SIR performance of Correlation and RAKE receiver.

Figure 6.22 to Figure 6.27 depict the plots of BER versus number of simultaneous users (K_u) under different combinations of R_b, G_p and receiver with the values of L as 1, 2, 3 and 4. For all the cases we consider the power line noise level −90dB.

Figure 6.28 depicts the comparative BER performance of Correlation and RAKE receiver.

Figure 6.15 depicts the various plots of signal to interference ratio (SIR) as a function of number of available path, L, for the bit rate, $R_b = 40Kbps$ and the processing gain $G_p = 256$ with Correlation receiver. The SIR decreases exponentially with the increase of number of available path. The system shows good signal strength up to $L = 3$.

Figure 6.15: Plots of signal to interference ratio (SIR) versus various number of users in a direct sequence CDMA PLC system for different number of available path, L, in case of <u>Correlation receiver</u> with bit rate $R_b = 40Kbps$ and processing gain $G_p = 256$, at a chip rate 10.24 Mchips/sec with transmitted signal power $P_0 = 1$ V^2 and $\sigma^2 = 0.45$.

Figure 6.16 depicts the various plots of signal to interference ratio (SIR) as a function of number of available path, L, for the bit rate, $R_b = 80 Kbps$ and the processing gain $G_p = 128$ with Correlation receiver. The SIR decreases exponentially with the increase of number of available path. The system shows good signal strength up to $L = 3$.

Figure 6.16: Plots of signal to interference ratio (SIR) versus various number of users in a direct sequence CDMA PLC system for different number of available path, L, in case of <u>Correlation receiver</u> with bit rate $R_b = 80 Kbps$ and processing gain $G_p = 128$, at a chip rate 10.24 Mchips/sec with transmitted signal power $P_0 = 1 \text{ V}^2$ and $\sigma^2 = 0.45$.

Figure 6.17 depicts the various plots of signal to interference ratio (SIR) as a function of number of available path, L, for the bit rate, $R_b = 160Kbps$ and the processing gain $G_p = 64$ with Correlation receiver. The SIR decreases exponentially with the increase of number of available path. The system shows good signal strength up to $L \leq 2$.
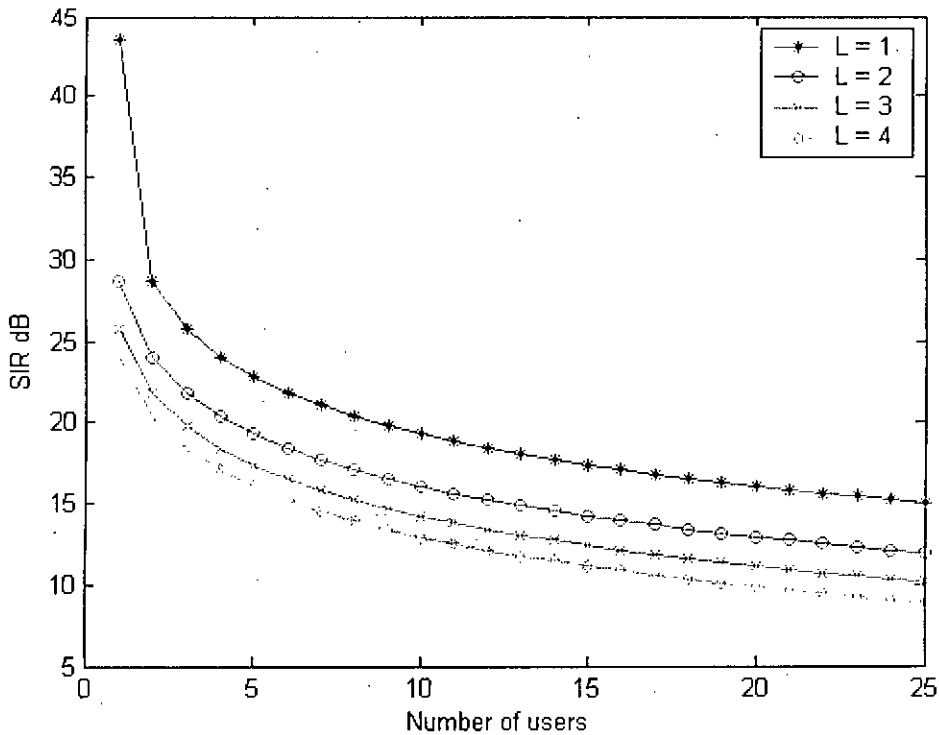

Figure 6.17: Plots of signal to interference ratio (SIR) versus various number of users in a direct sequence CDMA PLC system for different number of available path, L, in case of <u>Correlation receiver</u> with bit rate $R_b = 160Kbps$ and processing gain $G_p = 64$, at a chip rate 10.24 Mchips/sec with transmitted signal power $P_0 = 1$ V^2 and $\sigma^2 = 0.45$.

Figure 6.18 depicts the various plots of signal to interference ratio (SIR) as a function of number of available path, L, for the bit rate, $R_b = 40Kbps$ and the processing gain $G_p = 256$ with RAKE receiver. The SIR decreases exponentially with the increase of number of available path. The system shows excellent signal strength (above 15 dB) in all the cases.
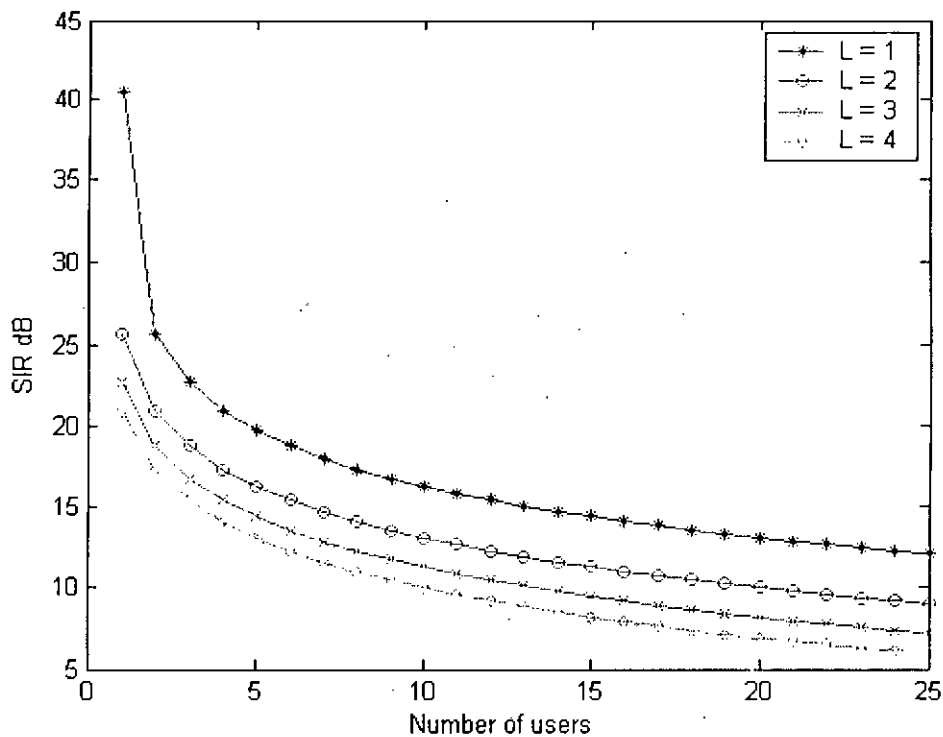

Figure 6.18: Plots of signal to interference ratio (SIR) versus various number of users in a direct sequence CDMA PLC system for different number of available path, L, in case of RAKE receiver with bit rate $R_b = 40Kbps$ and processing gain $G_p = 256$, at a chip rate 10.24 Mchips/sec with transmitted signal power $P_0 = 1$ V^2 and $\sigma^2 = 0.45$.

Figure 6.19 depicts the various plots of signal to interference ratio (SIR) as a function of number of available path, L, for the bit rate, $R_b = 80Kbps$ and the processing gain $G_p = 128$ with RAKE receiver. The SIR decreases exponentially with the increase of number of available path. The system shows signal strength above 15 dB up to 15 simultaneous users in all the cases.
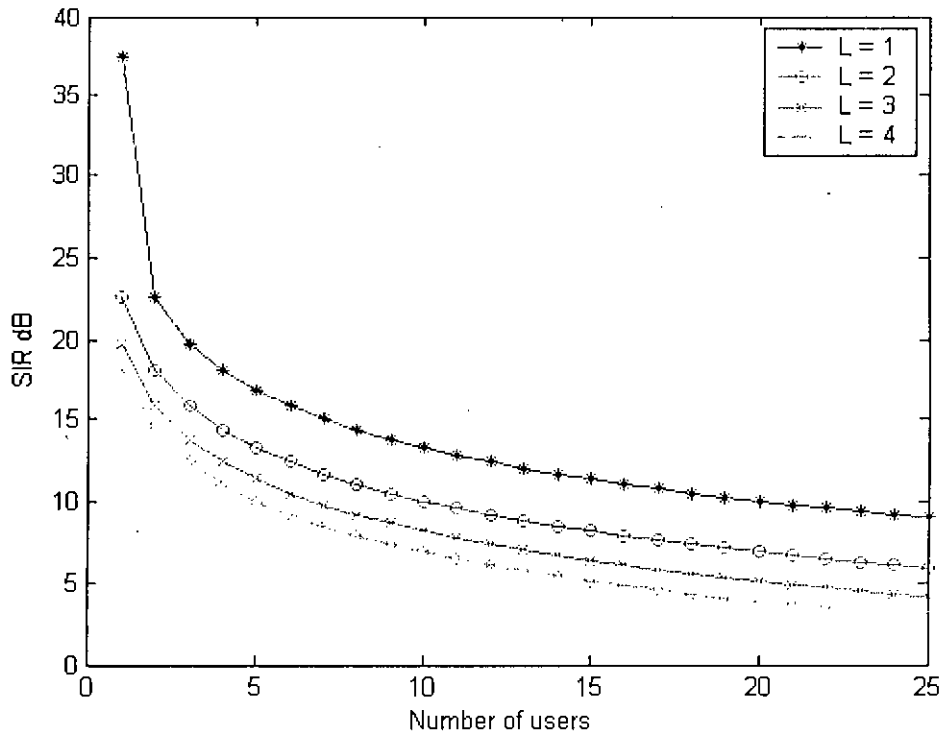

Figure 6.19: Plots of signal to interference ratio (SIR) versus various number of users in a direct sequence CDMA PLC system for different number of available path, L, in case of RAKE receiver with bit rate $R_b = 80Kbps$ and processing gain $G_p = 128$, at a chip rate 10.24 Mchips/sec with transmitted signal power $P_0 = 1$ V^2 and $\sigma^2 = 0.45$.

Figure 6.20 depicts the various plots of signal to interference ratio (SIR) as a function of number of available path, L, for the bit rate, $R_b = 160 Kbps$ and the processing gain $G_p = 64$ with RAKE receiver. The SIR decreases exponentially with the increase of number of available path. The system shows signal strength above 10 dB up to 15 simultaneous users in all the cases.
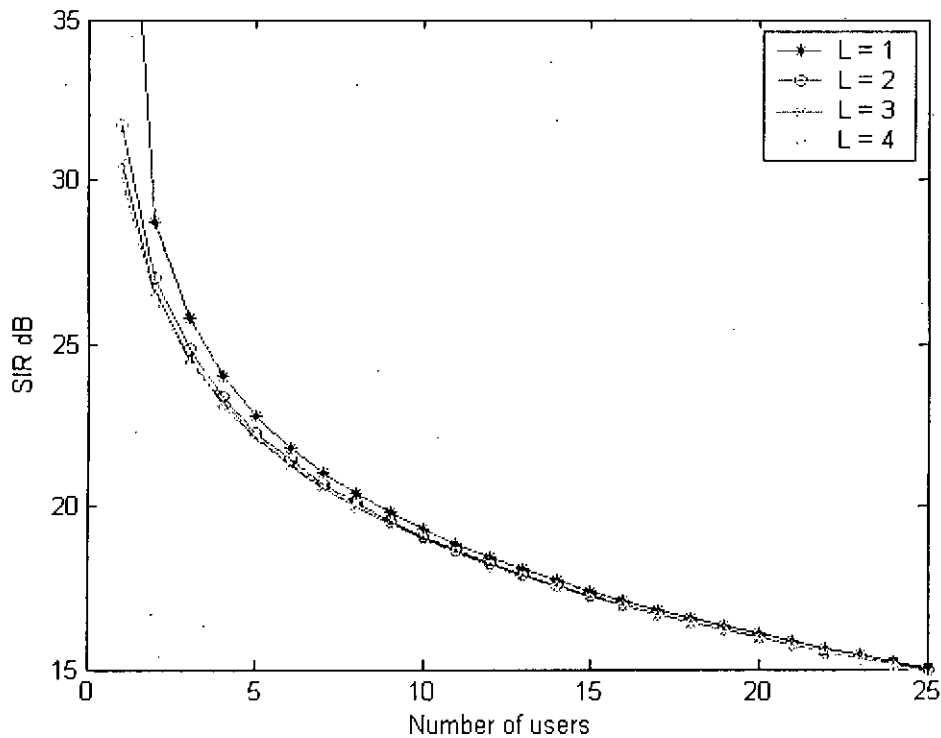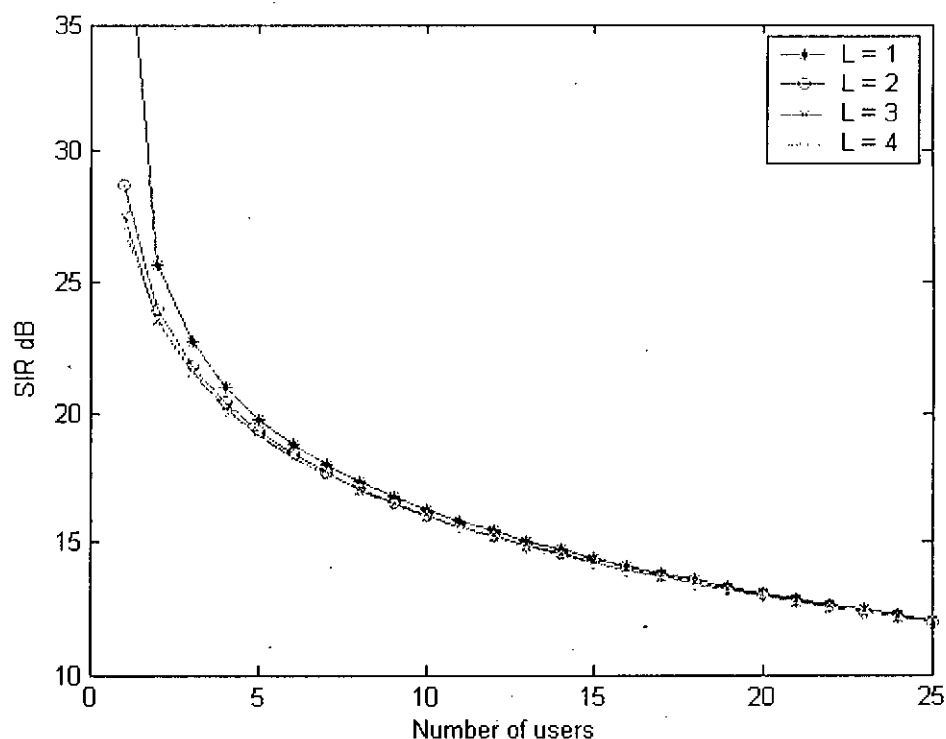

Figure 6.20: Plots of signal to interference ratio (SIR) versus various number of users in a direct sequence CDMA PLC system for different number of available path, L, in case of RAKE receiver with bit rate $R_b = 160 Kbps$ and processing gain $G_p = 64$, at a chip rate 10.24 Mchips/sec with transmitted signal power $P_0 = 1$ V^2 and $\sigma^2 = 0.45$.

Figure 6.21 depicts the comparative signal to interference ratio (SIR) plots for Correlation and RAKE receiver as a function of number of available path, L, for the bit rate, $R_b = 40Kbps$ and the processing gain $G_p = 256$. We observe that using a RAKE receiver the SIR of the system are better than a Correlation receiver. The number of available path affects the SIR of a Correlation receiver severely. The SIR of a RAKE receiver shows a robust characteristic against multipath propagation.

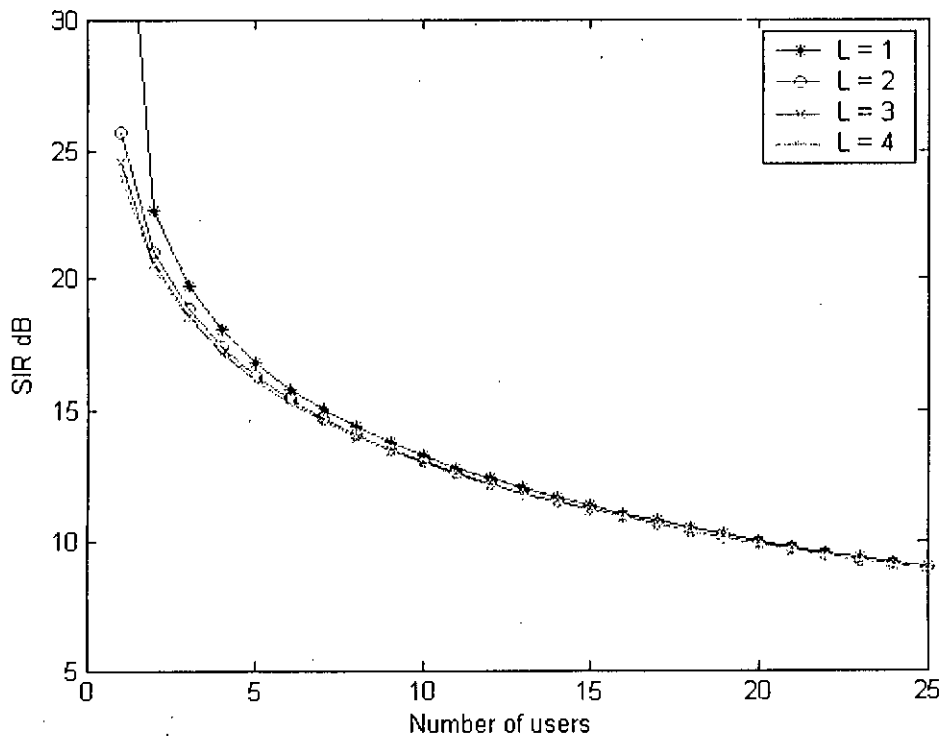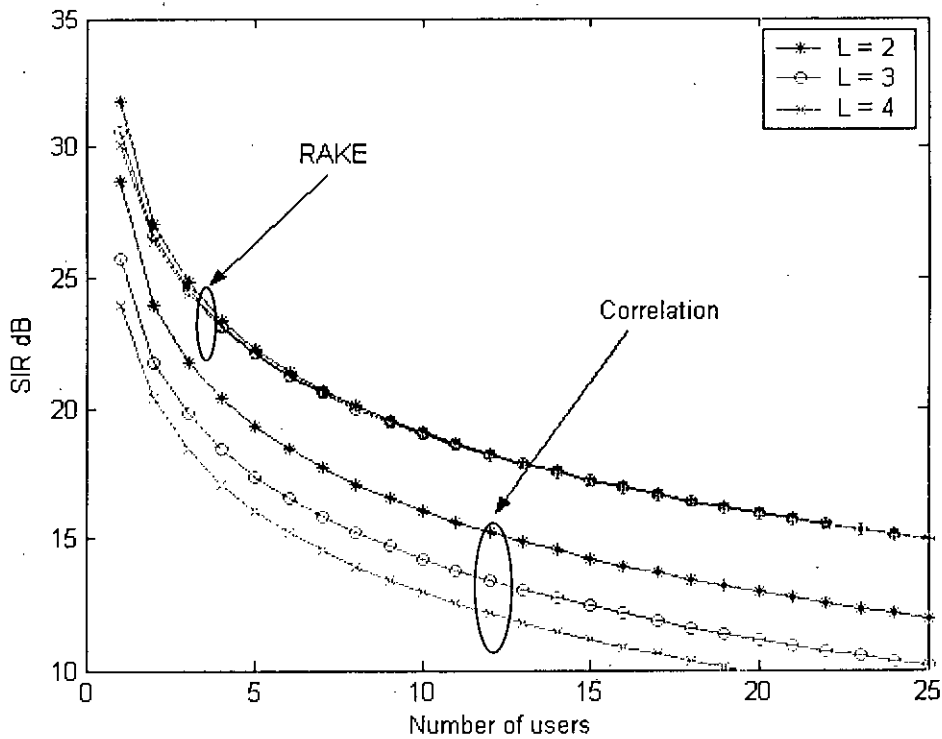Figure 6.21: Plots of comparative signal to interference ratio (SIR) versus various number of users in a direct sequence CDMA PLC system for different number of available path, L, in case of RAKE receiver with bit rate $R_b = 40Kbps$ and processing gain $G_p = 256$, at a chip rate 10.24 Mchips/sec with transmitted signal power $P_0 = 1$ V^2 and $\sigma^2 = 0.45$.

Figure 6.22 depicts the various plots of bit error rate (BER) as a function of number of available path, L, for the bit rate, $R_b = 40Kbps$ and the processing gain $G_p = 256$ with Correlation receiver. The BER increases exponentially with the increase of number of available path. The system shows good performance for number of available path ≤ 2.

Figure 6.22: The bit error rate (BER) performance against number of users of a direct sequence CDMA PLC system for different number of available path, L, in case of Correlation receiver with bit rate $R_b = 40Kbps$ and processing gain $G_p = 256$, at a chip rate 10.24 Mchips/sec with transmitted signal power $P_0 = 1$ V^2, and $\sigma^2 = 0.45$.

Figure 6.23 depicts the various plots of bit error rate (BER) as a function of number of available path, L, for the bit rate, $R_b = 80Kbps$ and the processing gain $G_p = 128$ with Correlation receiver. The BER increases exponentially with the increase of number of available path. The system shows very poor performance for number of available path > 2.

Figure 6.23: The bit error rate (BER) performance against number of users of a direct sequence CDMA PLC system for different number of available path, L, in case of Correlation receiver with bit rate $R_b = 80Kbps$ and processing gain $G_p = 128$, at a chip rate 10.24 Mchips/sec with transmitted signal power $P_0 = 1$ V^2, and $\sigma^2 = 0.45$.

Figure 6.24 depicts the various plots of bit error rate (BER) as a function of number of available path, L, for the bit rate, $R_b = 160 Kbps$ and the processing gain $G_p = 64$ with Correlation receiver. The BER increases exponentially with the increase of number of available path. The system shows very poor performance for number of available path > 1.

Figure 6.24: The bit error rate (BER) performance against number of users of a direct sequence CDMA PLC system for different number of available path, L, in case of Correlation receiver with bit rate $R_b = 160 Kbps$ and processing gain $G_p = 64$, at a chip rate 10.24 Mchips/sec with transmitted signal power $P_0 = 1$ V^2, and $\sigma^2 = 0.45$.

Figure 6.25 depicts the various plots of bit error rate (BER) as a function of number of available path, L, for the bit rate, $R_b = 40 Kbps$ and the processing gain $G_p = 256$ with RAKE receiver. The BER decreases exponentially with the increase of number of available path. The system shows very good performance for number of available path > 1.
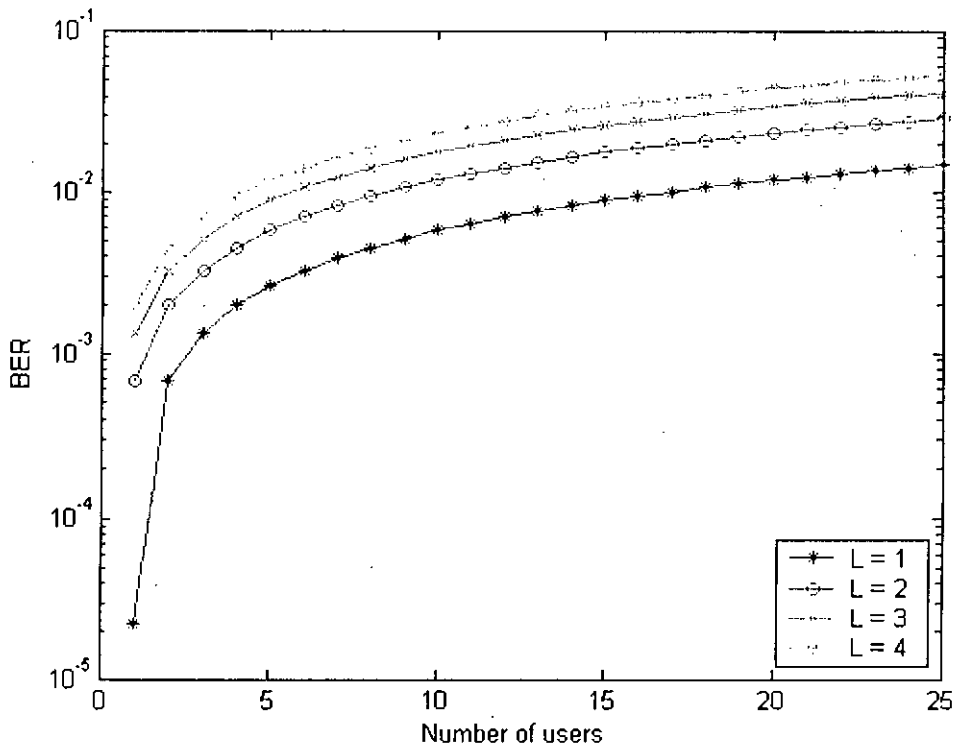

Figure 6.25: The bit error rate (BER) performance against number of users of a direct sequence CDMA PLC system for different number of available path, L, in case of RAKE receiver with bit rate $R_b = 40 Kbps$ and processing gain $G_p = 256$, at a chip rate 10.24 Mchips/sec with transmitted signal power $P_0 = 1 V^2$, and $\sigma^2 = 0.45$.

Figure 6.26 depicts the various plots of bit error rate (BER) as a function of number of available path, L, for the bit rate, $R_b = 80Kbps$ and the processing gain $G_p = 128$ with RAKE receiver. The BER decreases exponentially with the increase of number of available path. The system shows good performance for number of available path ≥ 2.
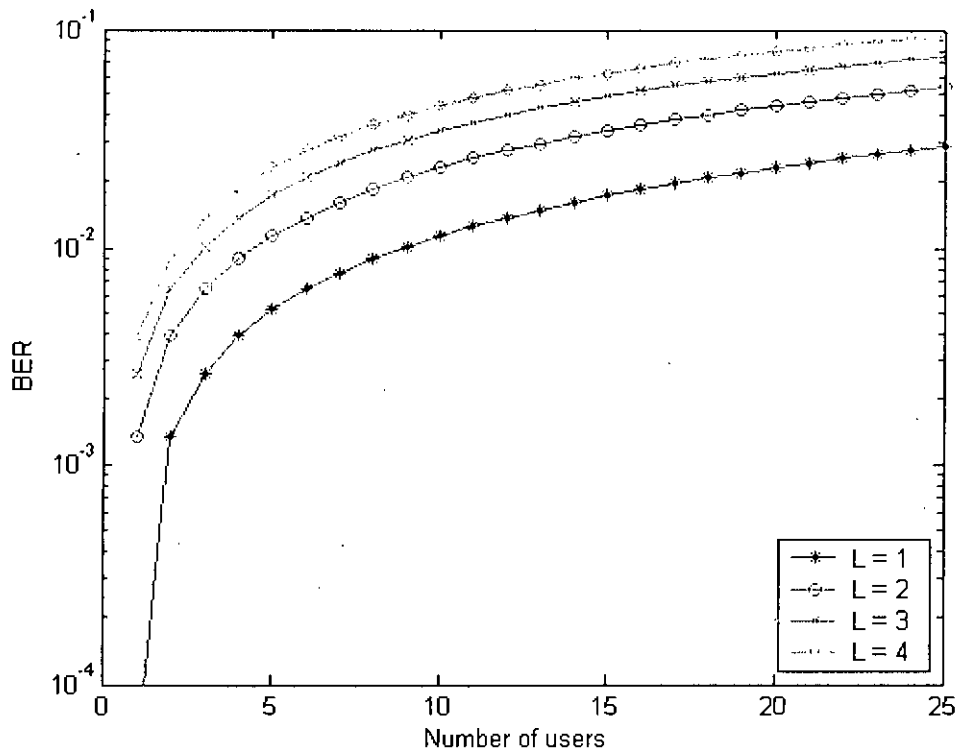

Figure 6.26: The bit error rate (BER) performance against number of users of a direct sequence CDMA PLC system for different number of available path, L, in case of RAKE receiver with bit rate $R_b = 80Kbps$ and processing gain $G_p = 128$, at a chip rate 10.24 Mchips/sec with transmitted signal power $P_0 = 1$ V^2, and $\sigma^2 = 0.45$.

Figure 6.27 depicts the various plots of bit error rate (BER) as a function of number of available path, L, for the bit rate, $R_b = 160 Kbps$ and the processing gain $G_p = 64$ with RAKE receiver. The BER decreases exponentially with the increase of number of available path. The system shows good performance for number of available path > 2 with 5 simultaneous user.
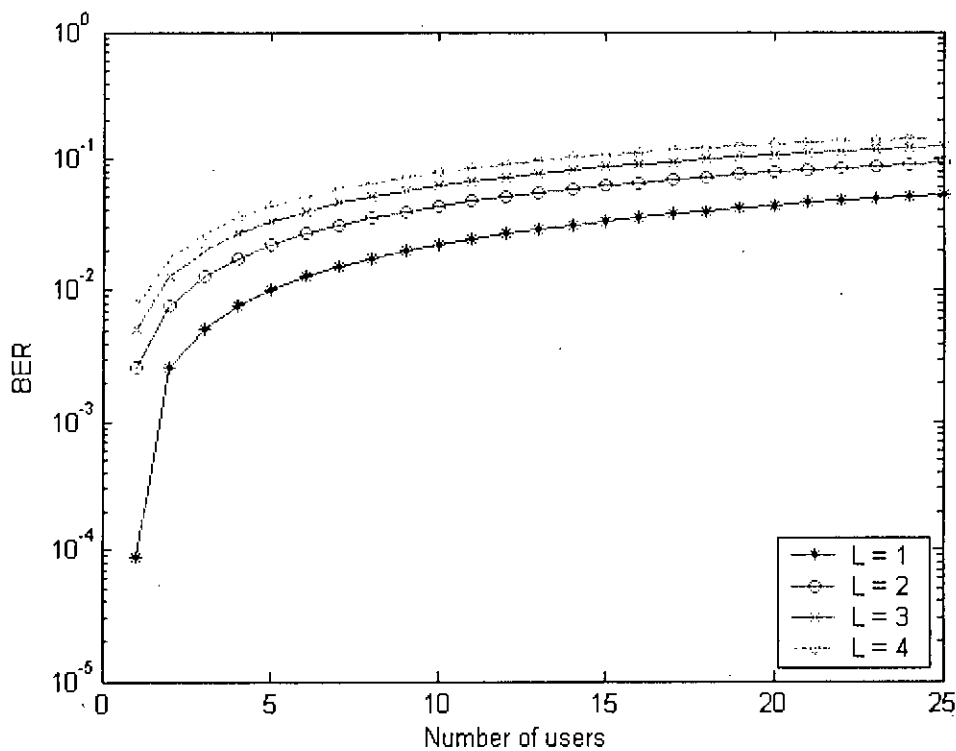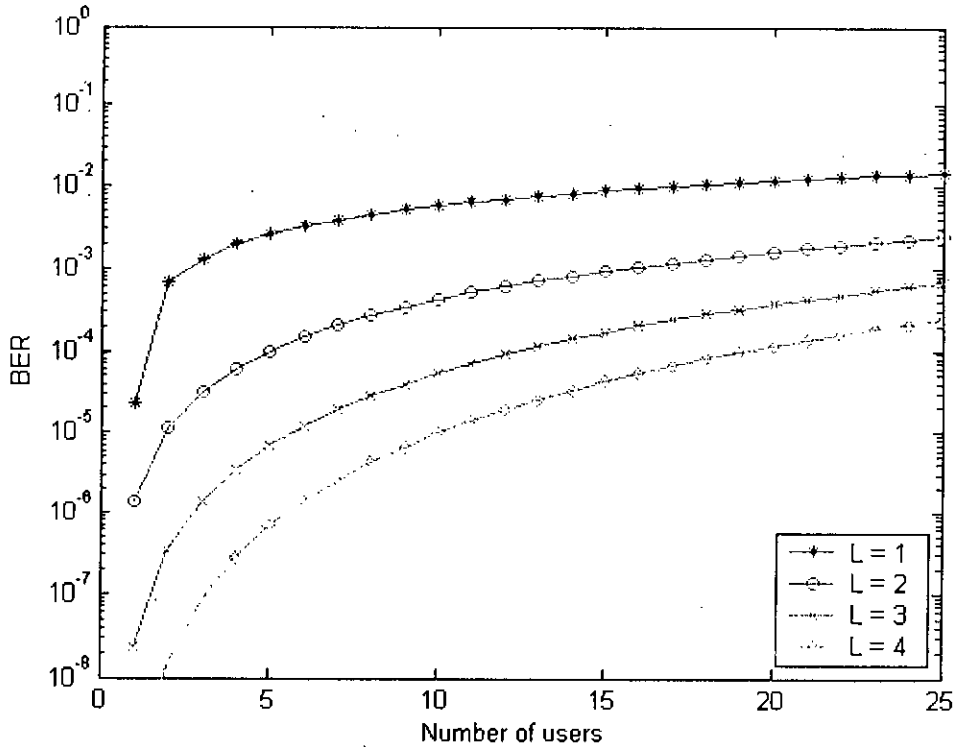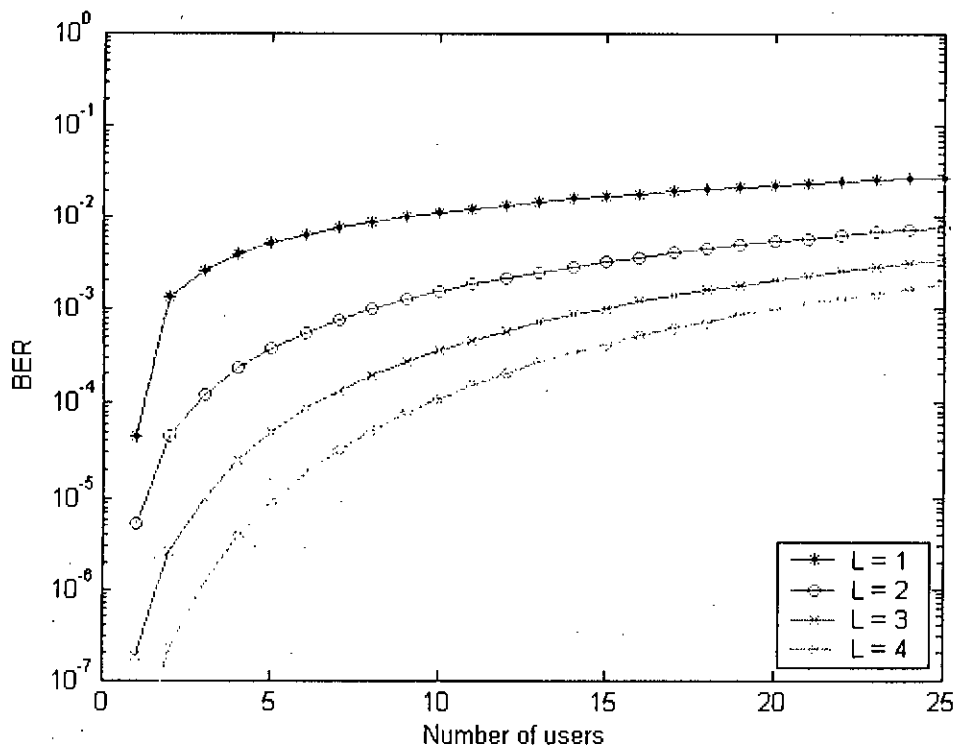

Figure 6.27: The bit error rate (BER) performance against number of users of a direct sequence CDMA PLC system for different number of available path, L, in case of RAKE receiver with bit rate $R_b = 160 Kbps$ and processing gain $G_p = 64$, at a chip rate 10.24 Mchips/sec with transmitted signal power $P_0 = 1$ V^2, and $\sigma^2 = 0.45$.

Figure 6.28 depicts the comparative bit error rate (BER) plots for Correlation and RAKE receiver as a function of number of available path, L, for the bit rate, $R_b = 40Kbps$ and the processing gain $G_p = 256$. We observe that using a RAKE receiver the performance of the system are better than a Correlation receiver. The performance of a Correlation receiver degrades with number of available path. For RAKE receiver we see that performance improves as the number of available path increases (assuming that number of RAKE finger ≥ number of available path).
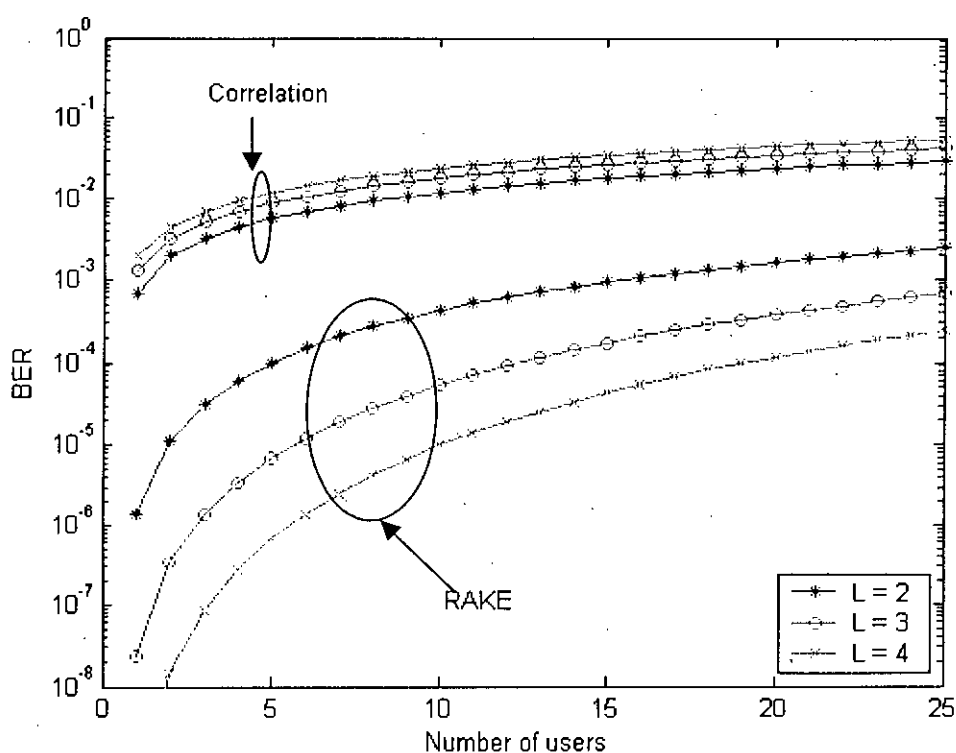
Figure 6.28: Plots of comparative bit error rate (BER) versus various number of users in a direct sequence CDMA PLC system for different number of available path, L, in case of RAKE receiver with bit rate $R_b = 40Kbps$ and processing gain $G_p = 256$, at a chip rate 10.24 Mchips/sec with transmitted signal power $P_0 = 1$ V^2 and $\sigma^2 = 0.45$.

6.4 Performance Analysis for other Frequencies

To examine performance of our system for other carrier frequencies, we choose three different carrier frequencies: 6.144 MHz, 15.36 MHz, and 25.6 MHz.

Figure 6.29 depicts the various plots of bit error rate (BER) under different conditions, for the carrier frequency 6.144 MHz and the number of available path, $L = 2$ with RAKE receiver. The system shows better noise performance for higher processing gain with lower bit rate.
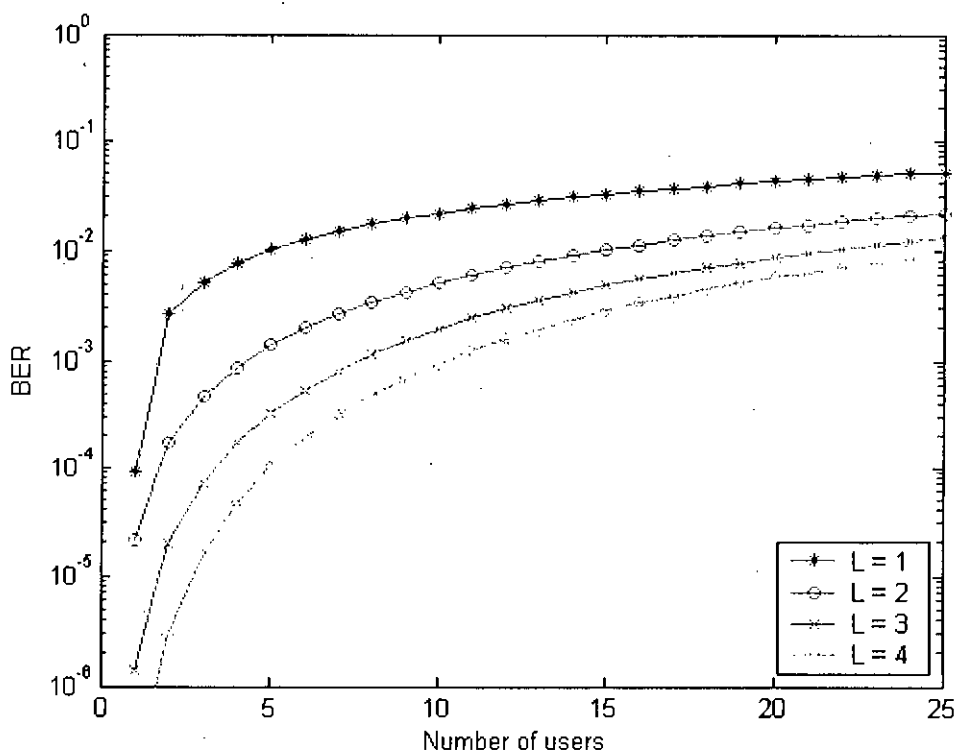

Figure 6.29: The bit error rate (BER) performance against number of users of a direct sequence CDMA PLC system for different conditions, in case of RAKE receiver with carrier frequency, $f_c = 6.144$ MHz and number of available path $L = 2$, at a chip rate 3.072 Mchips/sec with transmitted signal power $P_0 = 1$ V^2, and $\sigma^2 = 0.45$.

Figure 6.30 depicts the various plots of bit error rate (BER) under different conditions, for the carrier frequency 6.144 MHz and the power line noise, $N_{PL} = -90$ dB with RAKE receiver. The system shows better multipath performance for higher processing gain with lower bit rate. RAKE receiver performs better with increment of number of available path, even with lower processing gain and higher bit rate.

Figure 6.30: The bit error rate (BER) performance against number of users of a direct sequence CDMA PLC system for different conditions, in case of RAKE receiver with carrier frequency, $f_c = 6.144$ MHz and power line noise, $N_{PL} = -90$ dB, at a chip rate 3.072 Mchips/sec with transmitted signal power $P_0 = 1$ V^2, and $\sigma^2 = 0.45$.

Figure 6.31 depicts the various plots of bit error rate (BER) under different conditions, for the carrier frequency 15.36 MHz and the number of available path, $L = 2$ with RAKE receiver. The system shows better noise performance for higher processing gain with lower bit rate.

Figure 6.31: The bit error rate (BER) performance against number of users of a direct sequence CDMA PLC system for different conditions, in case of RAKE receiver with carrier frequency, $f_c = 15.36$ MHz and number of available path $L = 2$, at a chip rate 7.68 Mchips/sec with transmitted signal power $P_0 = 1$ V^2, and $\sigma^2 = 0.45$.

Figure 6.32 depicts the various plots of bit error rate (BER) under different conditions, for the carrier frequency 15.36 MHz and the power line noise, $N_{PL} = -90$ dB with RAKE receiver. The system shows better multipath performance for higher processing gain with lower bit rate. RAKE receiver performs better with increment of number of available path, even with lower processing gain and higher bit rate.

Figure 6.32: The bit error rate (BER) performance against number of users of a direct sequence CDMA PLC system for different conditions, in case of RAKE receiver with carrier frequency, $f_c = 15.36$ MHz and power line noise, $N_{PL} = -90$ dB, at a chip rate 7.68 Mchips/sec with transmitted signal power $P_0 = 1$ V^2, and $\sigma^2 = 0.45$.

Figure 6.33 depicts the various plots of bit error rate (BER) under different conditions, for the carrier frequency 25.6 MHz and the number of available path, $L = 2$ with RAKE receiver. The system shows better noise performance for higher processing gain with lower bit rate.
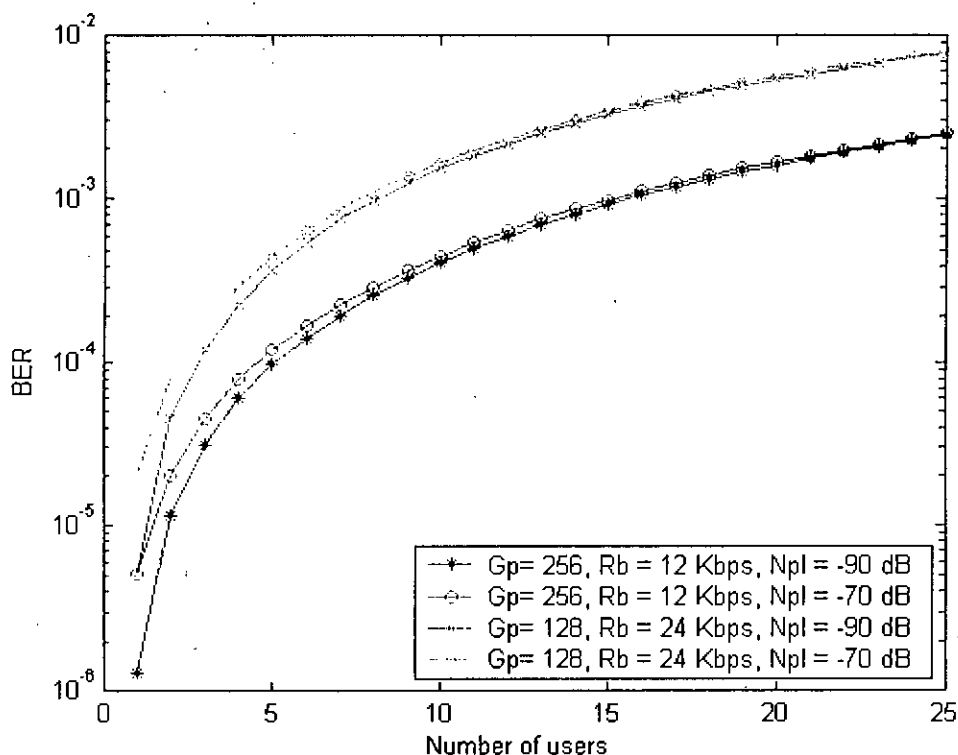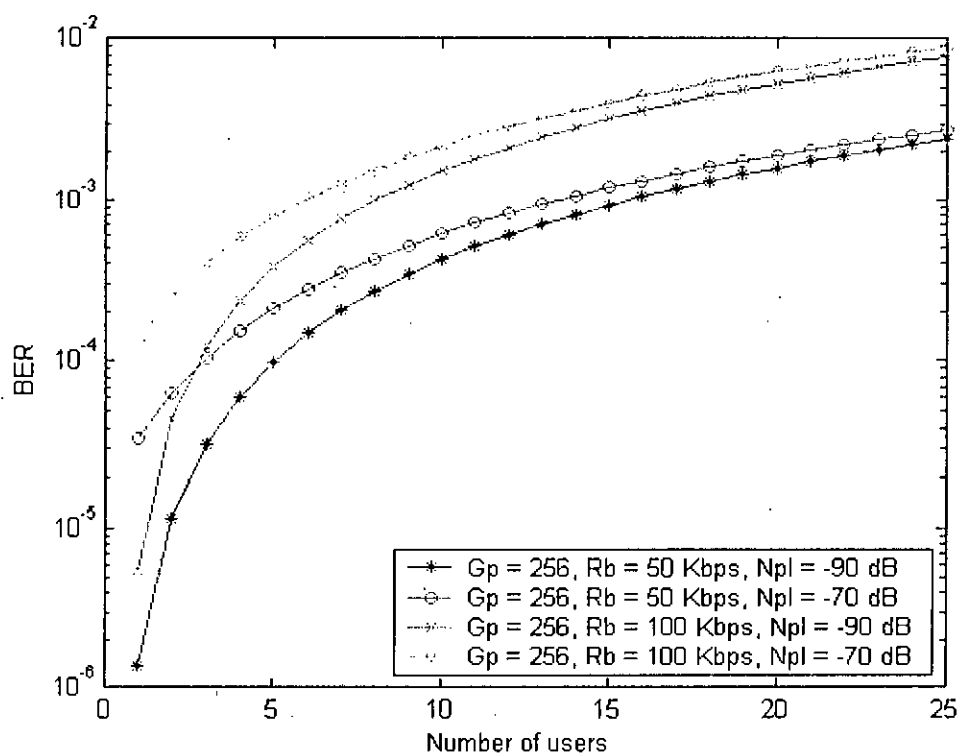

Figure 6.33: The bit error rate (BER) performance against number of users of a direct sequence CDMA PLC system for different conditions, in case of RAKE receiver with carrier frequency, $f_c = 25.6 \text{MHz}$ and number of available path $L = 2$, at a chip rate 12.8 Mchips/sec with transmitted signal power $P_0 = 1 \text{ V}^2$, and $\sigma^2 = 0.45$.

Figure 6.34 depicts the various plots of bit error rate (BER) under different conditions, for the carrier frequency 25.6 MHz and the power line noise, $N_{PL} = -90$ dB with RAKE receiver. The system shows better multipath performance for higher processing gain with lower bit rate. RAKE receiver performs better with increment of number of available path, even with lower processing gain and higher bit rate.
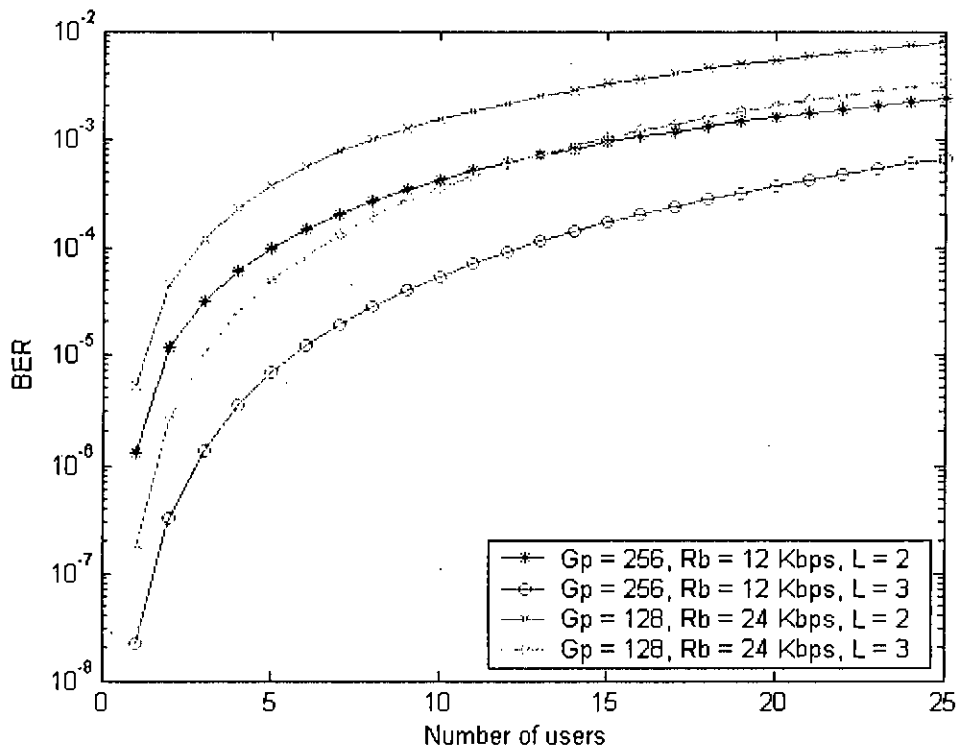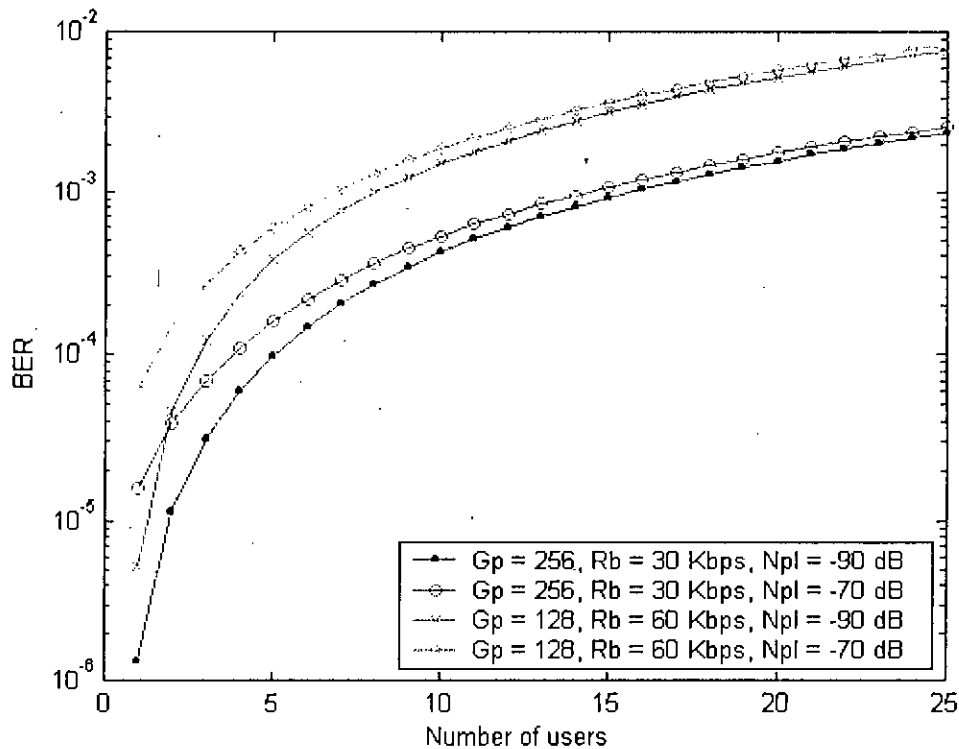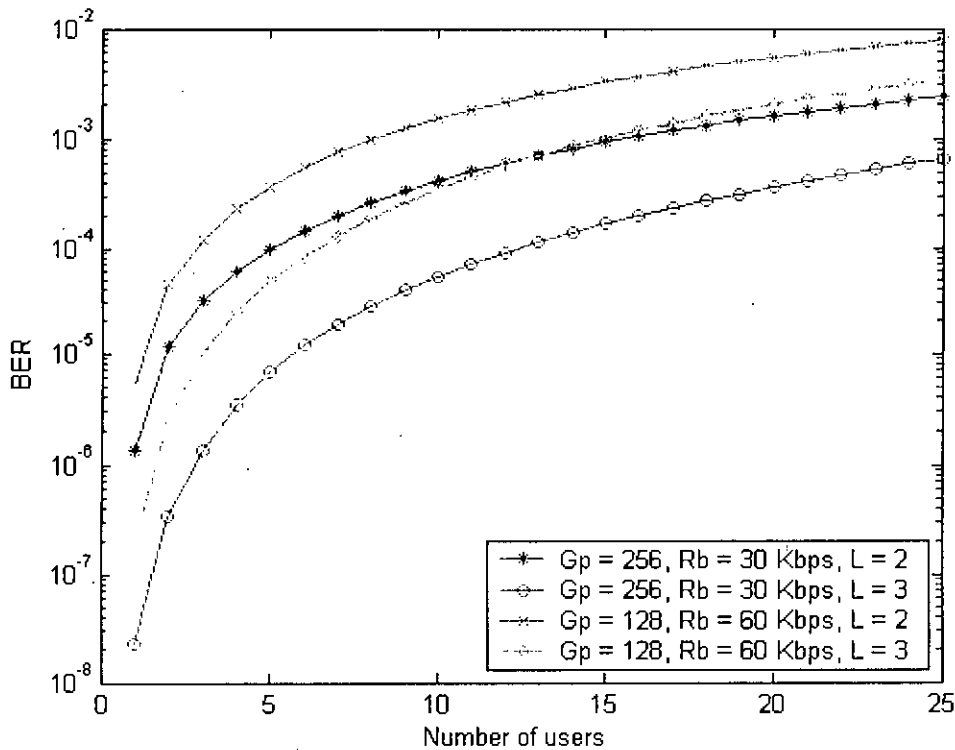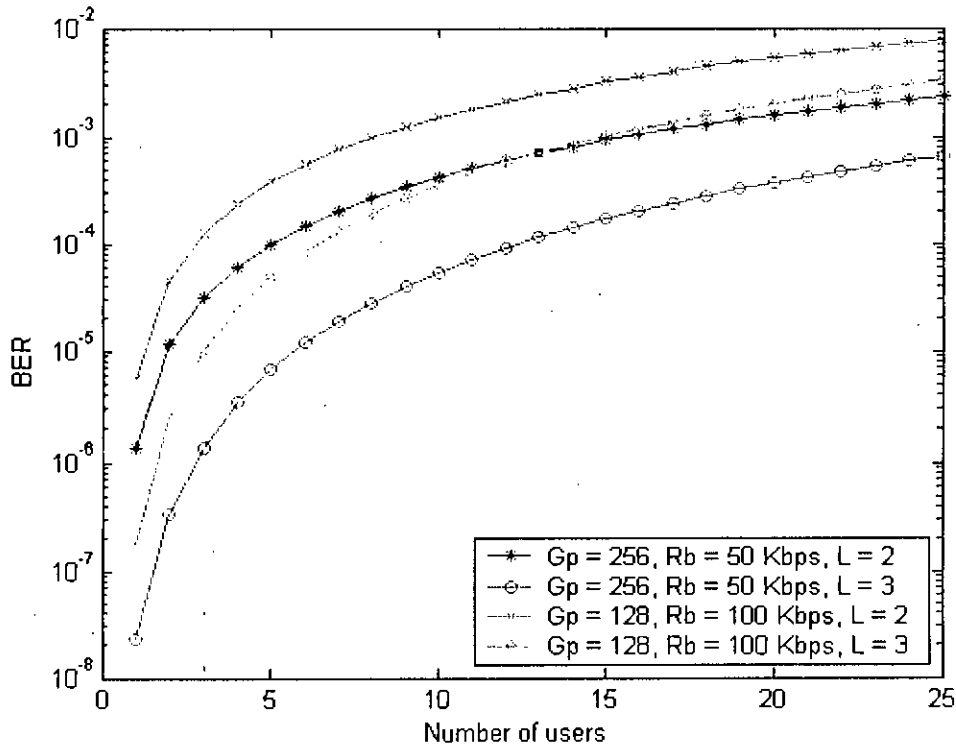

Figure 6.34: The bit error rate (BER) performance against number of users of a direct sequence CDMA PLC system for different conditions, in case of RAKE receiver with carrier frequency, $f_c = 25.6$ MHz and power line noise, $N_{PL} = -90$ dB, at a chip rate 12.8 Mchips/sec with transmitted signal power $P_0 = 1$ V^2, and $\sigma^2 = 0.45$.

6.5 Validity / Comparison

The BER for a single path power line with AWGN was simulated in reference [42]. The BER was evaluated by using the equation described in [42] for bit rate $R_b = 9.6$ Kbps and chip rate 14 Kchips/sec. The validity of our derived equation 5.20b has been checked for bit rate $R_b = 9.6$ Kbps and chip rate 14 Kchips/sec. Signal to noise ratio has been taken 20 dB for both cases. Figure 6.35 shows the comparative plots of BER versus number of simultaneous users.
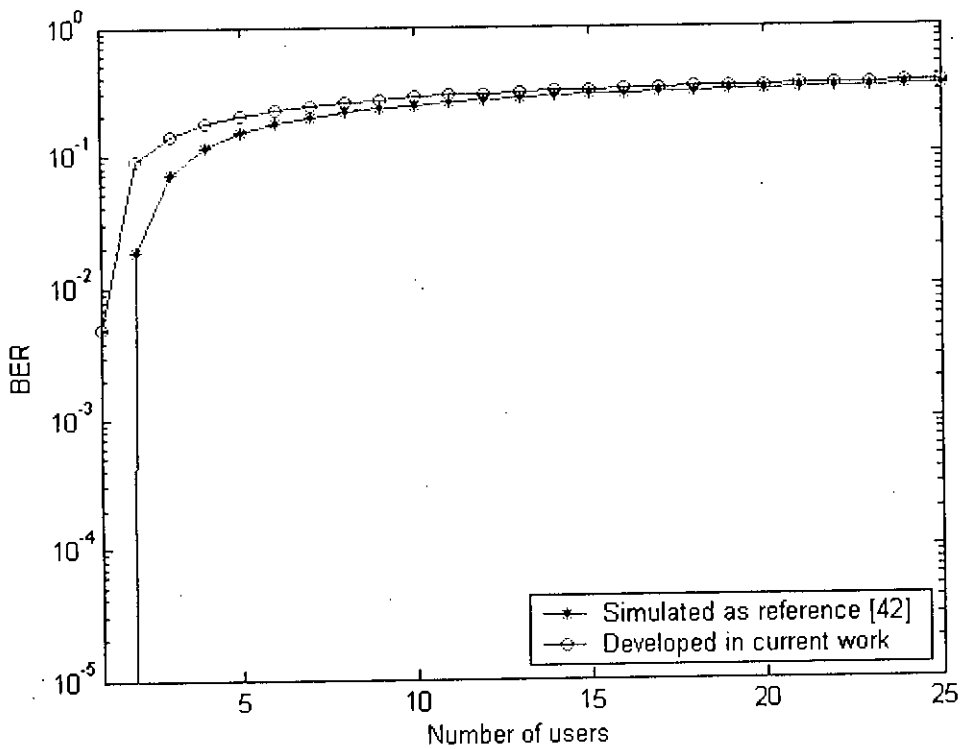
Figure 6.35 Comparison between previously simulated results in [42] and developed model in current work.

It has been seen that developed model shows higher BER than that of previously simulated results for same number of users. Higher BER is observed for developed model due to fading criteria and the nature of power line noise, which is more realistic.

6.6 Summary

The impacts of various parameters on direct sequence CDMA PLC system performance are analyzed. All the performance issues are presented graphically. We also compare the performance of Correlation receiver and RAKE receiver.

Noise power is an important factor for system design. More statistical data are required to estimate power line noise level accurately. We see that a RAKE receiver provides better noise performance.

System performance is severely affected by the number of available path for signal propagation. The performance of Correlation degrades with number of available path increases. Though the SIR of a RAKE receiver degrades with number of available path increases, BER improves with it.

We also see that higher processing gain with lower bit rate can provide us better system performance.

For a small number of users, a RAKE receiver can provide better performance with comparatively lower processing gain and higher bit rate for more number of available paths.

CHAPTER 7

CONCLUSIONS AND SUGGESTIONS

7.1 Conclusions of this study

A theoretical analysis is provided for a Direct Sequence Code Division Multiple Access (DS-CDMA) Power Line Communication (PLC) system with Binary Phase Shift Keying (BPSK) modulation scheme. We consider Correlation receiver and RAKE receiver separately. The analysis is carried out to evaluate the effect of frequency-selective Rayleigh fading on the PLC system performance and then the expressions for Signal to Interference Ratio (SIR) and Bit Error Rate (BER) are developed.

SIR and BER are evaluated at a chip rate of 10.24 Mchip/sec with a transmitted signal power $1V^2$, for different sets of values of number of paths, power line noise, processing gain, bit rate and the number of users. The results show that the performance of a direct sequence CDMA PLC system degrades due to power line noise which is evident from both the SIR and BER analysis. In case of a Correlation receiver noise level above −90 dB degrades system performance severely. We observe better noise performance for a RAKE receiver with power line noise level below −70 dB. The noise level above −70 dB our system gives poor performance in all the cases. So, we should fix an average power line noise by means of statistical analysis from sufficient data. Noise rather than lower bit rate affect higher bit rate.

It is also evident that number of available path seriously degrades the SIR and BER performance of our system with Correlation receiver. We can observe these effects from both the SIR and BER curves. Multipath exists due to impedance mismatch within transmission medium. Correlation receiver performance degrades severely, if there exists more than 2 path for signal propagation. RAKE receiver can exploit multipath phenomena of wave propagation. In our system with RAKE receiver, we

see SIR degrades with number of available path but BER decreases with that. Direct sequence CDMA is capable of overcoming multipath impairments by increasing the processing gain. When we try to increase processing gain, bit rate decrease by the same factor because of band limitation of power line channel. So, our system has to compromise with high-speed issue.

The main objective of any multiple access technique is to integrate more simultaneous user with the system. When we try to involve more users, system performance degrades with the number of simultaneous user. More users cause more interference. According to the plots, our system shows the best performance with a RAKE receiver at bit rate, $R_b = 40 Kbps$ and processing gain, $G_p = 256$.

Most of the previous researches plotted the BER versus SNR curves for power lines ignoring EMC effects. However, we have considered in our calculation the EMC effect. They considered some arbitrary values of SNR in their plot. But the signal power in PLC system can not be increased arbitrarily due to EMC (electromagnetic compatibility) problem. We fixed signal power according to FCC regulations for current carrier systems and assume the noise level separately in our analysis. This approach is more realistic. We have plotted curves of SIR versus number of simultaneous users and BER versus number of simultaneous user in order to focus multiple accessibility of the system. We considered the Correlation and RAKE receiver to point out the effect of frequency selective fading criteria of power line channel. Moreover, we considered all types of power line noises in our analysis. Thus, we can say that a full-featured analysis of DS-CDMA PLC system has been presented here. The analytical model developed here can be used for software simulation and system design of DS-CDMA based power line communication systems, such as automatic meter reading, home automation, industrial control, power line carrier telephony, etc.

We also observe the comparison between the performance of Correlation and RAKE receiver over power line channel. A RAKE receiver provides better performance than a Correlation receiver.

At the last portion of our analysis, three different carrier frequencies are considered. It has been observed that system performance has no direct relationship with carrier frequency. System performance varies with combination of processing gain and bit rate. Bit rate depends on carrier frequency.

A RAKE receiver performs well with more number of available paths. In some cases, it shows better performance under comparatively lower processing gain and higher bit rate due to more number of available paths.

PLC with DS-CDMA is found to be a promising option for future telecommunication in a LAN and MAN.

7.2 Suggestions for future work

Future research in this area can be carried out to deploy the spread spectrum techniques with higher spectral efficiency so that we can meet the challenge of high-speed data communication.

Further research in this area can also be carried out to investigate the system performance for FH CDMA on PLC.

Further research related work can be carried out to reduce the effect of multiple access interference (MAI), which will increase the number of simultaneous users by deploying Gold sequence and Goley sequence.

Further works of importance are to determine the impact of modulation schemes for DS-CDMA over power line channel such as DPSK, DQPSK etc.

Leakage of signal power for extremely short duration or PCM pulses may be a subject of considerable research in future.

REFERENCES

[1] S. P. Serbin, N. G. Pommereau, "Power Line Communications: An Innovative Solution to the "Broadband Divide"," NEMCOG Board Meeting April 25, 2003.

[2] Md. Mahmud Hasan, Md. Abdul Matin, and Md. Saifur Rahman, "Group Velocity Characteristics of PVC Insulated Cable in a PLC System," scheduled to be presented in ICCIT 2005, Dec. 28-30, IUT, Dhaka, Bangladesh.

[3] Wei-Jung Guan, "Broadband Powerline Communication," Final report 2002, Germany.

[4] Australian Communication Authority, "Broadband PLC systems A Background Brief," September 2003.

[5] K. H. Zubery, "Powerline Carrier (PLC) Communication Systems," M.Sc. Thesis, KTH, Sweden, September 2003.

[6] K. Dostert, "Telecommunications Over the Power Distribution Grid, Possibilities and limitations," ISPLC 1997, Essen, Germany.

[7] H. Phillips, "Modeling of Powerline Communication Channels," ISPLC 1999, Lancaster, UK.

[8] S. -J. Lee, et. al., "On the digital design with FPGA for power line voice-modem using the MC DS-CDMA," ISPLC, 2001. Modem Aspects.

[9] P. K. Van Der Gracht, R. W. Donaldson, "Communication Using Pseudonoise Modulation on Electric Power Distribution Circuits," IEEE Trans. on Communications, vol.33, No. 9, Sep. 1985.

[10] M. Ferreiro et al., "A Low Complexity All-Digital DS-SS Transceiver for Powerline Communication," ISPLC, Spain.

[11] G. Zsoldos et al., "Performance Comparison of Different Powerline Telecommunication Architectures," 6th International OFDM-Workshop (INOWO) 2001, Humburg.

[12] H. Dai, V. Poor, "Advance Signal Processing for Powerline Communications," Invited paper National Science Foundation 2003, USA.

[13] E. Del Re et al, "Comparision of CDMA and OFDM Techniques for Downstream Power-Line Communications on Low Voltage Grid," IEEE Trans. on Power Delivery, Vol. 18, No. 4, October 2003.

[14] C. L. Giovaneli, P. Farrel, and B. Honary, "Space-Time Block Codes with Rate ≥ 1 for Power Line Channel," ISPLC 1999, Lancaster, UK.

[15] L. Lampe, and J. B. Huber, "Bandwidth Efficient Power Line Communications Based on OFDM," AEU International Journal on Electrical Communications, vol. 54, issue 1, 2000, Germany.

[16] T. S. Rappaport, "Wireless Communications: Principles & Practice," Prentice Hall PTR, New Jersey, 1996.

[17] Simon Haykin, "Communication Systems," 3rd edition, 1996, John Wiley & Sons, Singapore.

[18] K. Onodera, "Low Power Techniques for High Speed Wireless Systems," Ph.D. dissertation, University of California, Berkeley, 1995.

[19] B. P. Lathi, "Modern Digital and Analog Communication Systems," Oxford University Press Inc., New York, 1998.

[20] Amol Shah, "Code Division Multiple Access: A Tutorial," Fall 1999, Rowan University.

[21] L. T. Tang, P. L. So, E. Gunawan, S. Chen, T. T. Lie, and Y. L. Guan, "Characteristics of in-house power distribution lines for high-speed data transmission," in Proc. 5th Int. Power Engineering Conf. (IPEC 2001), May 2001.

[22] S. Ramo, J. R. Whinnery, T. V. Duzer, "Field and Waves in Communication Electronics,"3rd edition 2002, John Wiley & Sons, Delhi.

[23] J. Ahola, T. Lindh, J. Partanen, "Determination of properties of low voltage power cables at frequency Band 100KHz-100MHz," ICEM 2002, Bruges, Belgium, 2002.

[24] M. Zimmermann, K. Dostert, "A Multipath Model for the Power Line Channel," IEEE Transactions on Communications, vol. 50, No. 4, April 2002.

[25] M. H. L. Chan, "Amplitude, Width, and Interarrival Distributions for Noise Impulses on Intrabuilding Power Line Communication Networks," IEEE Trans. on EMC, vol.31, No.3, August 1989.

[26] L. T. Tang, P. L. So, E. Gunawan, S. Chen, T. T. Lie, and Y. L. Guan, "Characterization of In-house Power Distribution Lines for High-speed data transmission," in Proc. Int Power Eng. Conf., vol.1, Singapore, 2001.

[27] K. Dostert et al, "Analysis and Modelling of Impulsive Noise in Broad-Band Powerline Communications," IEEE Trans. on EMC, vol.44, No.1, Feb. 2002.

[28] O. G. Hooijen, "A robust system for digital data transmission over the low-voltage network using spread spectrum techniques," in Proc. IEEE, ISSS TA, vol.2, 1996.

[29] E. Yavuz et al, "Modelling of Power Lines for Digital Communication," ISPLC 2000.

[30] W. Hankel, T. Kessler, and H. Y. Chang, "Coded 64-CAP ADSL in an Impulse-Noise Environment- Modelling of Impulse Noise and First Simulation Results," IEEE Journal on Selected Areas in Communications, vol.13, No.9, December 1995.

[31] W. Hankel, T. Kessler, "A Simplified Impulse-Noise Model for the XDSL Test Environment," 1999 BAC, Finland.

[32] L.F. Lind, N. A. Mufti, Efficient method for modelling impulse noise in a communication system, Electronics Letters, vol.32, no.16, pp.1440-1441, 1st August 1996.

[33] R. M. Vines, H. J. Trussell, L. J. Gale, and J. B. O'Neal, "Noise on Residential Power Distribution Circuits," IEEE Trans. on EMC, Vol. 26, No. 4, November 1984.

[34] L. Salender, " Power Line Communications Channel Properties and Communication Strategies," Ph.D. dissertation, Lund University, Sweden, pp. 92-94, 1999.

[35] E. Falletti, F. Vipiana, R. Lo Cigno, " On SIR & BER Approximations in DS-CDMA System," Department of Electronics, Polytechnic of Turin, Italy 2000.

[36] M. Oguz Sunay, Peter J. McLane, "Calculating Error Probabilities for DS-CDMA Systems: when not to use the Gaussian Approximation," IEEE Global Telecommunication Conference, 1996. Proceedings of GLOBECOM," vol.3, pp. 1744-49

[37] J. Cheng, N. C. Beaulieu, "Accurate DS-CDMA Bit-Error Probability Calculation in Rayleigh Fading," IEEE Transactions on Wireless Communication Vol.1, No.1, January 2002.

[38] J. G. Prokais, " Digital Communication," Fourth Edition, McGraw-Hill International Editions 2001, Singapore.

[39] M. H. L. Chan and R. W. Donaldson, "Attenuation of Communication Signals on Residential and Commercial Intrabuilding Power-Distribution Circuits," IEEE Trans. on EMC, Vol. EMC-28, No.4, November 1986.

[40] C. J. Kim and M. F. Chouika, "Attenuation Characteristics of High Rate Home-Networking PLC Signals," IEEE Trans. on Power Delivery, Vol. 17, No.4, October 2002.

[41] Albert A. Smith, "Power Line Noise Survey," IEEE Trans. on EMC, February 1972.

[42] P. K. Van Der Gracht, R. W. Donaldson, "Pseudonoise Signaling for Power Line Carrier Applications," IEEE Trans. on Power Delivery, vol.1, No. 1, Jan. 1986.